SYNTHESIS OF TRIFLUORONITROMETHANE, CF_3NO_2: PHOTOCHEMICAL SCALE-UP AND A NEW THERMOGENERATION METHOD WITH A REFINED PURIFICATION TECHNIQUE

by

JOHN O. HAUPTFLEISCH

A DISSERTATION

Submitted in partial fulfillment of the requirements
for the degree of Doctor of Philosophy in
the Department of Chemistry
in the Graduate School of
The University of Alabama

TUSCALOOSA, ALABAMA

2009

ABSTRACT

The research herein investigates two primary methods to synthesize trifluoronitromethane, CF_3NO_2. The first method, a photochemical synthesis, was discovered by the Thrasher group and published in 2002. This photochemical method was the first one-step method for generating CF_3NO_2 and uses trifluoroiodomethane, CF_3I, and nitrogen dioxide, $\cdot NO_2$, as the reactants. This process is initiated by a 420 nm blue light apparatus that splits the C-I bond. The optimization and scale-up of this reaction had not been previously investigated. The production of multiple grams of CF_3NO_2 in a single reaction turned out to be impractical due to the equilibrium of $2\ \cdot NO_2 \rightleftharpoons N_2O_4$. However, the ideal conditions for the maximum generation of CF_3NO_2 were found to be a total pressure of 0.3 atm, a stoichiometric ratio of 1.1 : 1 of $\cdot NO_2$: CF_3I, a temperature of at least 55 °C, and a reaction time of 18 hours. Even though this method could not be scaled-up, it still represents the fastest and least expensive method for generating lab quantities of 1-3 grams of CF_3NO_2 via multiple reactions.

Because of the aforementioned limitations of the photochemical method, a new method for generating larger quantities of CF_3NO_2 had to be discovered. This new method involves the homolysis of the C-I bond in CF_3I at approximately 200 °C in the presence of $\cdot NO_2$ in a pressure vessel. The increase in reaction temperature allows for the previous limitations due to the $2\ \cdot NO_2 \rightleftharpoons N_2O_4$ equilibrium to be overcome, allowing for larger quantities, 10-100 grams, of CF_3NO_2 to be produced in a single reaction. This method can be carried out over a large pressure range, 10-60 atm; similar reaction times, 18-24 hours; and with a modest increase in the yield to 35-50%. A detailed kinetics study of this new preparative route was carried out by

following both the disappearance of CF_3I and the appearance of CF_3NO_2. The results yielded a C-I bond energy for CF_3I that is in agreement with literature values. A new purification method was also developed for the larger quantities of CF_3NO_2, and the thermal properties of CF_3NO_2 were investigated using an accelerating rate calorimetry (ARC). The molecule CF_3NO_2 was found to be stable to almost 300 °C.

DEDICATION

This dissertation is dedicated to everybody who helped me get through my research and writing, especially my parents who have stood by me, and supported me, my entire life in whatever goals I decided to tackle.

LIST OF ABBREVIATIONS AND SYMBOLS

ARC	Accelerating Rate Calorimeter
°C	Degree Celsius
DMSO	Dimethyl sulfoxide
g	Grams
L	Liters
mL	Milliliters
nm	Nanometers
cm	Centimeters
GWP	Global warming potential
ODP	Ozone depletion potential
RF	Radiative Forcing
IRF	Instantaneous radiative forcing
CFC	Chlorofluorocarbons
HCFC	Hydrochlorofluorocarbons
HFC	Hydrofluorocarbons
ppb	Parts per billion
h	Hours
δ	Chemical shift
$K_{(eq)}$	Equilibrium constant
atm	Atmospheres

FT/IR	Fourier transform infrared spectroscopy
Eq.	Equation
·	Radical
EDAX	Energy-dispersive X-ray spectroscopy
TFA	Trifluoroacetic acid
psi	Pound per square inch
GC/MS	Gas chromatography-mass spectroscopy
GC/FID	Gas chromatography-flame ionization detector
EI	Electron impact ionization
NMR	Nuclear magnetic resonance
M	Molarity (mol/L)
s	Seconds
BDE	Bond dissociation energy
ms	Milliseconds
E_a	Activation energy
Kg	Kilograms
O.D.	Outer diameter

ACKNOWLEDGEMENTS

I would like to thank all my colleagues, friends, faculty, and family who have helped me with my research project over the years. I am most indebted to Professor Thrasher, my advisor, for all his help over the years in my research, classes, writing, and for his advice as well as introducing me to the wonderful world of fluorine chemistry. I would also like to thank my committee members Professors Arduengo, Shaughnessy, Vincent, and O'Brien who answered my questions and gave insight into my research when necessary. An extra thanks to Professor O'Brien who taught me how to use a vacuum line in my first year. I would like to thank Dr. Waterfeld for his help in refining my experimental techniques and helping me out in the lab. I would like to thank Dr. Belmore for all his help with the NMR spectroscopy, including experimental ideas, interpretation of spectra, and setting up the ^{19}F probe when I needed to run a sample. A special thanks to Matt Hennek. He was always around to bounce ideas around with, challenge my conclusions, or to pass time with in the lab while we worked. Finally, I would like to thank Dr. Fernandez who has been a second advisor for my time at Alabama, helping me with research and planning my future, his ideas and guidance were invaluable.

Thank you again everybody I mentioned and thank you to the many people I have not mentioned; without everybody's help this would not have been possible.

TABLE OF CONTENTS

LIST OF TABLES

LIST OF FIGURES

LIST OF SCHEMES

CHAPTER ONE

INTRODUCTION

1.1 Background: Uses of CF_3NO_2

Trifluoronitromethane, CF_3NO_2, has been a characterized compound for at least 50 years. It was discovered soon after trifluoronitrosomethane, CF_3NO, by oxidizing CF_3NO with a variety of different oxidizing agents.[1.1,1.2] Trifluoronitromethane existed in relative anonymity for almost half a century with the occasional paper or proposed use, but very little chemistry was performed on CF_3NO_2 due to the absence of a simple and scalable synthesis. Over the years several uses have been proposed for CF_3NO_2, which include: (1) a solvent for optical recording,[1.3] (2) a heat transfer fluid,[1.4] (3) a gaseous ultrasound contrast media,[1.5] (4) a gas and gaseous precursor-filled microspheres as topical and subcutaneous deliver vehicles,[1.6] (5) a solid porous matrix for pharmaceutical uses,[1.7] (6) an acoustically active drug deliver system,[1.8] and the two most promising uses, (7) a refrigerant,[i] and (8) a dielectric gas or mixture gas for the replacement of sulfur hexafluoride, SF_6.[1.9,1.10]

The research presented in this dissertation will investigate the scalability of the photochemical synthesis of CF_3NO_2 discovered in the Thrasher group,[1.11] a new high temperature/high pressure method developed for the preparation of CF_3NO_2 and how to scale

[i] No references were found for this proposal, but the physical properties are similar to many refrigerants.

this synthesis as well as a new purification method. Larger amounts of pure CF_3NO_2 are needed to study some of its physical properties, such as the compound's thermal stability and its atmospheric lifetime with respect to reaction with hydroxide radicals. We studied the thermal decay of CF_3NO_2 using an accelerating rate calorimeter (ARC).

1.2 Preparative Methods for Generating Trifluoronitromethane

Trifluoronitromethane, CF_3NO_2, is a difficult compound to synthesize. Very few effective ways to generate CF_3NO_2 have been reported over the past 50 years. Generally, when synthesizing a compound, the number of steps, availability of starting materials, conversion factors and ease of purification need to be optimized in order to have a potentially cost effective preparative method. Several methods for generating CF_3NO_2 have been reported, but most of them fall short of an ideal synthesis in one way or another. The synthetic methods include the following: (1) oxidation of trifluoronitrosomethane, CF_3NO, (2) thermal generation using trifluoroacetic acid, (3) thermal decomposition of $CF_3N(O)NCF_3$, acyl nitrates and molecules formed from reactions with fluorine nitrate, (4) electrophilic trifluoromethylation of sodium nitrite, $NaNO_2$, using Umemoto's reagent, (5) random methods that are not easily categorized, (6) photochemical generation using trifluoriodomethane, CF_3I and nitrogen dioxide, $\cdot NO_2$ and (7) thermal generation using CF_3I and $\cdot NO_2$, which will be discussed in detail in Chapter 3.

1.2.1 Method 1. Oxidation of Trifluoronitrosomethane

Trifluoronitrosomethane, CF_3NO, is a royal blue gas with a boiling point of -84 °C and a melting point below -196 °C and is most commonly synthesized by irradiating CF_3I and ·NO in the presence of mercury.[1.1] Many different oxidizing agents were reacted with CF_3NO with varying degrees of success, producing a trace to ~90% yields of CF_3NO_2 and the results are summarized in Table 1. Often during these oxidation reactions, byproducts are formed complicating the purification.

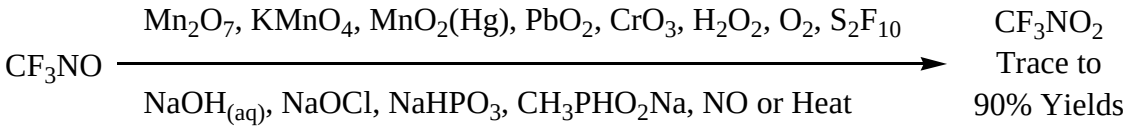

Most of the reactions require multiple purification steps in order to isolate the CF_3NO_2. In most cases, temperatures above 100 °C are required for the reaction to proceed. Since trifluoronitrosomethane, CF_3NO, is expensive and not readily available, a better synthetic procedure is desirable.

Table 1.1. Successful Oxidizers of CF_3NO

Oxidizer	% Yield	Listed Byproducts	References
Mn_2O_7	49%	NA	1.12, 1.13
CrO_3	38%	NA	1.12, 1.13
PbO_2	37%	CO_2, SiF_4, COF_2	1.12, 1.13
PbO_2	trace	NA	1.13, 1.14
S_2F_{10}	NA	$CF_3N(SF_5)OSF_2$, SOF_2, SF_6, CF_3NNCF_3	1.15
O_2	80%		1.1, 1.13
H_2O_2	80%		1.1
NaOH	80%	$CF_3NN(O)CF_3$	1.16
NaOH	NA	CF_3NNOCF_3	1.1, 1.19
Heat/Carbon 100 °C	NA	COF_2, $CF_3NN(O)CF_3$	1.1
Heat 250-300 °C, 1-2 min	NA	NO, $(CF_3)_2NOCF_3$, $(CF_2NF)_n$, COF_2	1.17
·NO	NA	$(CF3)_2NONO$, $\cdot NO_2$, N_2O	1.13, 1.18
NaOCl	90%	NA	1.19

1.2.2 Method 2. Thermal Generation Using Trifluoroacetic Acid or Trifluoroacetic Anhydride

Two similar thermal methods for generating CF_3NO_2 were reported by Boschan[1.20] and Scribner.[1.21,1.22] Their synthetic pathways exploited the thermal decay of a trifluoroacetyl nitrate, CF_3COONO_2, an intermediate formed from either trifluoroacetic anhydride (Boschan) or trifluoroacetic acid (Scribner) and $\cdot NO_2$ as the starting materials. Both reactions proceed through a very similar mechanism as shown in Schemes 1.1 and 1.2.[1.20]

The Scribner reaction was carried out at 200 °C for ~6 hours; no isolated yields were given, but analysis of the product mixture by GC/MS, gas chromatography-mass spectroscopy, gave a conversion of ~30%. Attempts to reproduce Scribner's results will be discussed in Chapter 3. This reaction was also applied to longer perfluoroalkylcarboxylic acids, i.e., adding

the nitro group to the end of perfluorocarbon radical chains, and the results indicate that the mechanism is probably the same as for the thermal reaction of perfluoroalkyl iodides with $\cdot NO_2$.

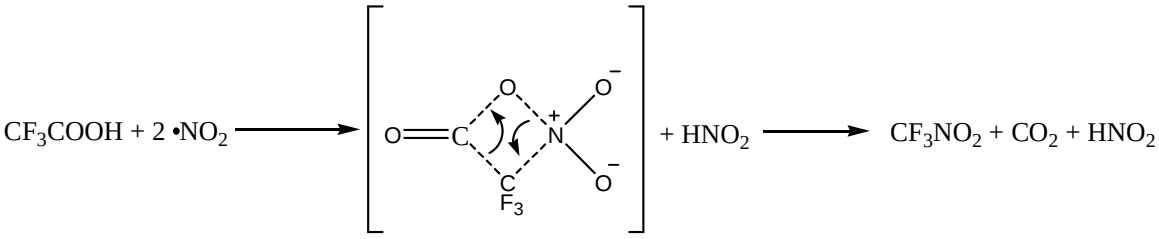

Scheme 1.1. Proposed Mechanism for the Generation of CF_3NO_2 Using Trifluoroacetic Acid and $\cdot NO_2$

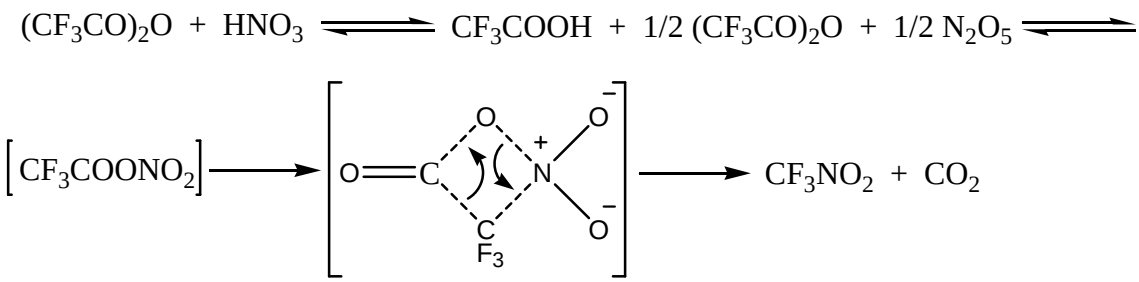

Scheme 1.2. Mechanism for CF_3NO_2 Generation Using Trifluoroacetic Anhydride

The Boschan method follows a similar mechanism to the Scribner reaction with a few notable exceptions. The reaction is performed in nitric acid at 100 °C, and both reactions progress through the same trifluoroacetyl nitrate intermediate once the trifluoroacetic anhydride has been split and protonated by the nitric acid forming trifluoroacetic acid. Boschan's method, Scheme 1.2, produces very little CF_3NO_2, 7% yield, due to formation of N_2O_5, which decays at 100 °C. The formation of N_2O_5 reduces the amount of trifluoroacetyl nitrate formed, and the nitrate intermediate must be formed in order for decarboxylation to CF_3NO_2 to take place.

Scribner's synthesis is proof that CF_3NO_2 is stable at 200 °C, and the Scribner reaction allows for a broader application to perfluoronitroalkanes.

1.2.3 Method 3. Thermal Decomposition of Molecules

Another method used to synthesize CF_3NO_2 is the pyrolysis of large molecules into smaller components including the desired CF_3NO_2 molecule. Examples of this method include (1) the decay of the product from the reaction between fluorine nitrate and tetrafluoroethylene and (2) the pyrolysis of $CF_3N(O)NCF_3$.

The decay of perfluoroalkyl nitrates into CF_3NO_2 was demonstrated by Cady *et al.*[1.23] They found that small quantities of fluorine nitrate, $FONO_2$, react almost quantitatively at room temperature with tetrafluoroethylene, C_2F_4, forming CF_3NO_2 and COF_2 from the decay of the intermediate $C_2F_5ONO_2$.

The pyrolysis of $CF_3N(O)NCF_3$ occurs slowly at 300 °C, cleaving the N=N bond ultimately forming CF_3NO_2, $(CF_3N)_2$ and CF_3NCF_2 among other products.[1.24] The temperature at which the pyrolysis occurs may be problematic for the formation of CF_3NO_2, which begins to decompose at temperatures between 275-290 °C (see Chapter 5). Any preparative method involving elevated temperature must avoid temperatures where the desired product itself decays; however, more detailed information on the thermal stability of CF_3NO_2 had not been reported prior to this dissertation.

The thermal reaction described in Method 2 can also be described as a thermal decomposition reaction where the trifluoroacetyl nitrate intermediate decays into CF_3NO_2.

1.2.4 Method 4. Electrophilic Trifluoromethylation Using Umemoto's Reagent

This referenced method developed by Shreeve *et al.* is the latest published procedure for preparing CF_3NO_2. This method is a one-step reaction that utilizes the "CF_3^+" transfer ability of Umemoto's reagent, S-(trifluoromethyl) dibenzothiophenium tetrafluoroborate, in an electrophilic trifluoromethylation transfer to sodium nitrite, $NaNO_2$, in DMSO at 80 °C.[1.25] This reaction gives excellent yields, 90%, and has a very simple purification method involving vacuum removal of the gaseous CF_3NO_2 from the DMSO solution (Scheme 1.3).

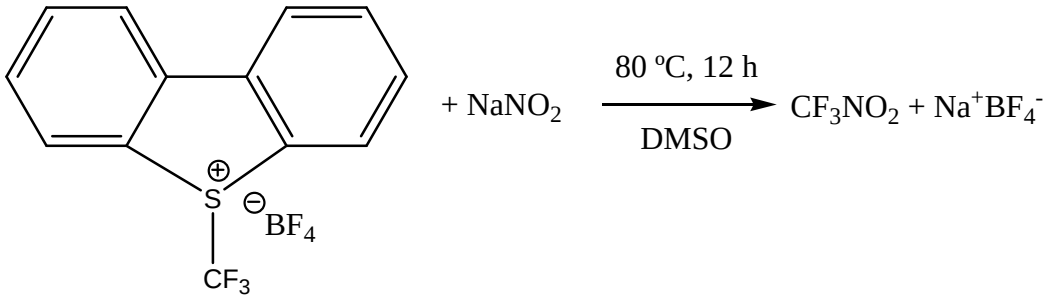

Scheme 1.3. Generation of CF_3NO_2 Using Umemoto's Reagent

The main downside to this method is the very high cost of Umemoto's reagent; at ca. $50 per gram (SynQuest Laboratories, Inc. 2007/08 catalogue) the cost of a large-scale synthesis would be prohibitive.

1.2.5 Method 5. Random Methods for Generating CF_3NO_2

In several published procedures, CF_3NO_2 was produced only as a byproduct. The yields are typically low, and no attempts were made to optimize the reaction conditions for making CF_3NO_2.

An early example involved condensing NOCl into a flask containing liquid oxygen and slowly adding CF_3CO_2Ag. This mixture was then warmed to -10 °C, shaken, and any unreacted NOCl was removed by distillation. After several trap-to-trap distillations, a 13% isolated yield of CF_3NO_2 was recovered.[1.26]

A second example was performed in an autoclave at 160 °C and involved the mixing of $BrCF_2NO_2$ and ClF_3, which produced only trace amounts of CF_3NO_2. This finding was not investigated further.[1.14]

A third example involves reacting trifluoronitrosomethane, CF_3NO and ammonia, NH_3, in ether at -115 °C. In this reaction, the CF_3NO is acting as the oxidizing reagent. Trace amounts of CF_3NO_2 are formed. The major products are hexafluoroazoxomethane, $CF_3(NO)NCF_3$, NH_4F and $(CF_3)_2NOH{\cdot}Et_2O$.[1.27]

A fourth example involves the conversion of 4 $R_fNO \rightarrow 2R_fNO_2 + R_fN{=}NR_f$ ($R_f = CF_3$ or *n*-C_3F_7) by decomposition of the free-radical copolymer generated from reacting hexafluoropropylene (HFPO) with an excess of perfluoro-2,5-diazahexane 2,5-dioxyl producing the polymer shown in Scheme 1.4.[1.28] Pyrolysis of this polymer gives a 62% yield of CF_3NO_2, but it is obviously problematic due to both the cost and the huge amount of byproducts formed during the reaction. The exact decay mechanism was not confirmed, but three possible mechanisms were proposed, and they are summarized in Scheme 1.4. The major difference

between mechanisms is the number of CF_3NO molecules that add across the polymer. In this reaction, heat is also required to propagate the decay of the polymer, and the only other major decay product is $(CF_3)_2NON(CF_3)_2$, which can be easily separated from CF_3NO_2 by distillation.

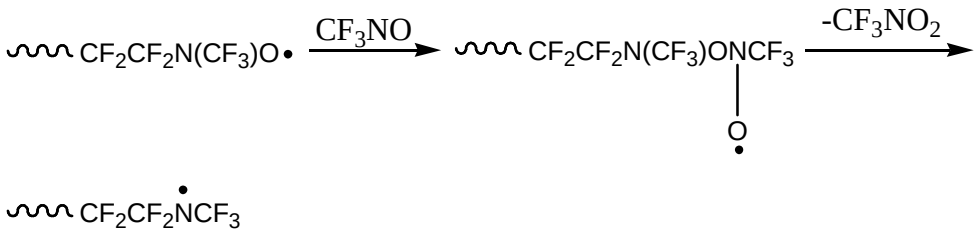

Scheme 1.4. Proposed Mechanism for the Formation of CF_3NO_2 from Free Radical Polymer

1.2.6 Method 6. Photochemical Generation of CF_3NO_2

In 2002, Lu and Thrasher introduced a one-step method for generating CF_3NO_2 from commercially available CF_3I and $\cdot NO_2$.[1.11] The activation energy for this reaction was provided by a diazo blue light. The diazo blue light's λ_{max} is centered at 420 nm and is sufficient to break the C-I bond forming the trifluoromethyl radical, $\cdot CF_3$, which reacts with the nitrogen dioxide radical, $\cdot NO_2$. The single electron of the $\cdot NO_2$ radical is delocalized over all three atoms and forms both (1) the O-bonded and (2) the N-bonded molecule.

The N-bonded molecule is the stable CF_3NO_2 product, while the O-bonded molecule, F_3CONO, is not stable at reaction conditions and will quickly and irreversibly decay into COF_2 and FNO. (Scheme 1.5)[1.11] This reaction was discovered to not be scalable beyond 3 g of product in a 16-L reaction vessel due to the temperature and pressure dependent equilibrium between $2\ \cdot NO_2 \rightleftharpoons N_2O_4$, which will be discussed in detail in Chapter 2.

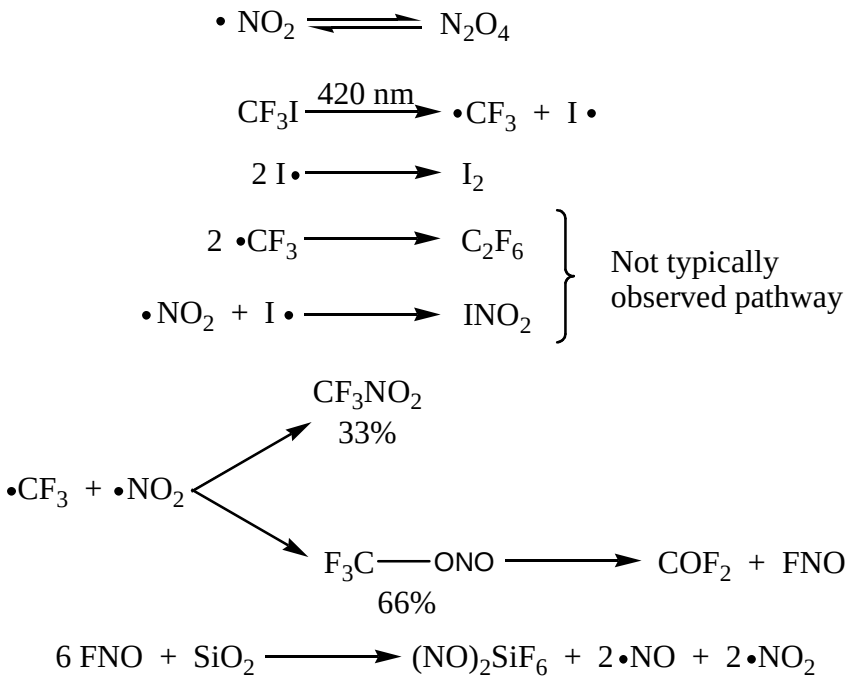

Scheme 1.5. Photochemical Generation of CF_3NO_2

A similar photochemical reaction was found by Jander *et al.* Shaking and irradiating trifluoroiodomethane, CF_3I, with an excess of ·NO and a small amount of mercury with UV light generates CF_3NO. If the reaction was not shaken and the pressure was kept under an atmosphere, CF_3NO_2 was generated.[1.29]

A series of kinetic studies were done in the 1980s and 1990s investigating the combination of the $\cdot CF_3$ with $\cdot NO_2$ radical using ultraviolet light or a pulsed laser as an energy source of the C-X bond.[1.30-1.39] The photolysis was achieved with 248 nm wavelength light,[1.39] while the wavelength of the lasers was varied for each experiment. Surprisingly, very few of these studies observed evidence for the generation of CF_3NO_2. All agreed that the O-bonded product is the major pathway, which decays into COF_2 and FNO, even though FNO is not typically detected due to its high reactivity. The FNO molecule is isoelectronic with ozone, O_3; and similar to ozone, FNO is a strong oxidizer. In order to handle FNO, special materials such

as Monel or PTFE are necessary. The studies seem to agree that once formed, the O-bonded molecule decays before it has a chance to dissociate back into $\cdot NO_2$ and $\cdot CF_3$ radicals. The best explanation for the lack of CF_3NO_2 in these experiments is the photo sensitivity of CF_3NO_2. Rossi *et al.* found that CF_3NO_2 absorbs light at 277 nm, and shorter wavelengths, undergoing a $n \rightarrow \pi^*$ transition followed by the cleavage of the C-N bond.[1.40] With the N-bonded product being the minor product, it is quickly destroyed leading to the eventual formation of only FNO and COF_2.

1.2.7 Method 7. Thermal Generation of CF_3NO_2

Perfluoroalkyl iodides are known to break up and to form perfluoroalkyl and iodine radicals at elevated temperatures. At 200 °C, N_2O_4 is entirely dissociated into $\cdot NO_2$ radicals. Therefore, it was reasonable to give this direct route a try. Thermal cracking of trifluoroiodomethane, CF_3I, in the presence of an excess of $\cdot NO_2$ forms CF_3NO_2 with isolated yields between 37-54%. This method leads to the same byproducts as the photochemical method namely COF_2, FNO, and I_2. The thermal method has been used in batches of up to 1.10 moles of CF_3I. Since the reaction is not exothermic, the amount generated is limited only by the size of the reactor. With this new synthetic method for generating larger quantities of CF_3NO_2, a more effective method of purification was needed. The procedure that accomplished this task will be discussed in Chapter 4.

1.3 CF_3NO_2 as a Replacement for Refrigerants or Dielectric Gases

With the high temperature/high pressure synthetic method, large quantities (e.g. 300 g) of CF_3NO_2 can now be prepared. This will allow the testing of some of the proposed uses of CF_3NO_2 in the aforementioned patents.[ii] In order to determine if CF_3NO_2 will be a viable replacement for the current or dielectric gases, several properties need to be measured. These include cost, environmental benefits/detriments of CF_3NO_2 compared to the currently used compounds, and the range of its stability over the temperature, pressure and electrical conditions that will be applied.

A major sticking point for new compounds to be released into the environment is their global warming potential, GWP, their ozone depletion potential, ODP and the radiative forcing, RF, must be assessed. Calculating the GWP is dependent on the RF, and these values are closely related. A high value of any one of these properties can result in detrimental effects on the environment. This means the compound would probably not be suitable for commercialization. Another important variable is the reactivity of the molecule with ·OH in the atmosphere. If the ·OH radical can break down a high GWP molecule into molecules with lower GWP. This would offset the damage caused by the initial molecule allowing for the possibility of that molecule to be used more liberally. All these factors must be investigated before mass producing a new compound that has the possibility of entering the environment.

There are two types of radiative forcing: adjusted, ARF, and instantaneous, IRF. ARF is calculated with the assumption that there is a fixed initial tropospheric temperature and a radiative equilibrium in the stratosphere. With these two variables made constant, ARF is now the change in the net total of IR, visible and UV radiation flux, F, due to the changes in gas

[ii] Several specialty catalogs list CF_3NO_2 for sale, but upon inquires, no orders for any quantity were accepted.

concentration. The IRF is calculated when the initial stratospheric temperature is fixed as well.[1.41]

Global warming potential, GWP, has been integrated into the RF concept to create the absolute global warming commitment, AGWC, calculation. This is the formula, Equation 1, used to calculate the values in Table 2:

$$GWC_x(t) = \int_0^t \Delta Fx(\tau)\, d\tau \qquad \text{(Eq. 1)}$$

$\Delta Fx(t)$ is the gaseous substance, and the time periods calculated are typically 20, 100, and 500 years. This number is usually compared to CO_2 with the relative value of 1.0.[1.41]

Ozone depletion potential, ODP, is defined as the potential of a substance to destroy ozone compared to CCl_3F. It is a relative value, and the ODPs of many common refrigerants are shown in Table 1.2.

Using CF_3NO_2 as a replacement for refrigerants is less promising than its use as a dielectric gas. Ever since chlorofluorocarbons, CFCs, were found to be detrimental to the ozone layer, replacement refrigerants, minus the ozone depletion potential have been investigated. Hydrochlorofluorocarbons, HCFCs, and hydrofluorocarbons, HFCs, were the first replacement compounds, since they had less of an environmental impact but not significant enough to be a long term replacement. These compounds are now being phased out as well.[1.42] A summary of many common refrigerants and some dielectric gases, with their estimated environmental lifetimes and GWP, are summarized in Table 1.2.[1.43]

As a possible refrigerant replacement, CF_3NO_2 must have a significantly lower GWP than the current refrigerants, and no harmful byproducts should be produced when it breaks down in the atmosphere. The GWP of CF_3NO_2 to date is still unknown and must be determined,

but CF_3NO_2 is known to photodissociate under irradiation at or below 277 nm creating $\cdot CF_3$ and $\cdot NO_2$. The quantum yield has not been determined, so the degree of photodissociation in the atmosphere and hence its lifetime is still unknown.[1.40] Nitrogen dioxide is a major pollutant especially in the lower atmosphere, and its levels are monitored closely, especially in major pollution areas. If the photodissociation of CF_3NO_2 is too fast in the lower atmosphere, it will be very problematic as a replacement refrigerant. Even though CF_3NO_2 has many advantageous properties needed in a viable refrigerant replacement, such as boiling point, bp, in the range between -20 to -40 °C, high chemical resistance and good thermal stability, the decay products of any leaked CF_3NO_2 may be just as problematic as a compound with a higher GWP.

Table 1.2. Global Warming Potential of Various Compounds[1.43]

Common Name	**Chemical Formula**	**Lifetime (years)**	**Radiative Efficiency (W m^{-2} ppb^{-1})**		**Global Warming Potential for Given Time Horizon**		**ODP [relative to CCl_3F][1.42]**
				20 Years	**100 Years**	**500 Years**	
Carbon Dioxide	CO_2		1.4×10^{-5}	1	1	1	0
Methane	CH_4	12	3.7×10^{-4}	72	25	7.6	
Nitrous Oxide	N_2O	114	3.03×10^{-3}	289	298	153	
CFC-11	CCl_3F	45	0.25	6730	4750	1620	1
CFC-12	***CCl_2F_2***	***100***	***0.32***	***11000***	***10900***	***5200***	**0.82**
CFC-13	$CClF_3$	640	0.25	10800	1440	16400	
CFC-113	CCl_2FCClF_2	85	0.3	6540	6130	2700	
CFC-114	$CClF_2CClF_2$	300	0.31	5040	10000	8730	
CFC-115	$CClF_2CF_3$	1700	0.18	5310	7370	9990	
Halon-1301	$CBrF_3$	65	0.32	8480	7140	2760	
Halon-1211	$CBrClF_2$	16	0.3	4750	1890	575	5.1
Halon-2402	$CBrF_2CBrF_2$	20	0.33	3680	1640	503	
Carbon	CCl_4	26	0.13	2700	1400	435	

Tetra-chloride							
Methyl Bromide	CH_3Br	0.7	0.01	17	5	1	
Methyl Chloroform	CH_3CCl_3	5	0.06	506	146	45	
HCFC-22	$CHClF_2$	12	0.2	5160	1810	549	0.05
HCFC-123	$CHCl_2CF_3$	1.3	0.14	273	77	24	0.022
HCFC-124	$CHClFCF_3$	5.8	0.22	2070	609	185	0.022
HCFC-141b	CH_3CCl_2F	9.3	0.14	2250	725	220	0.12
HCFC-142b	CH_3CClF_2	17.9	0.2	5490	2310	705	0.065
HCFC-225ca	$CHCl_2CF_2CF_3$	1.9	0.2	429	122	37	
HCFC-225cb	$CHClFCF_2CClF_2$	5.8	0.32	2030	595	181	
HFC-23	CHF_3	270	0.19	12000	14800	1200	0.0004
HFC-32	CH_2F_2	4.9	0.11	2330	675	205	0
HFC-125	CHF_2CF_3	29	0.23	6350	3500	1100	0.00003
HFC-134a	CH_2FCF_3	14	0.16	3830	1430	435	0.000015
HFC-143a	CH_3CF_3	52	0.13	5890	4470	1590	0
HFC-152a	CH_3CHF_2	1.4	0.09	437	124	38	0
HFC-227ea	CCF_3CHFCF_3	34.2	0.26	5310	3220	1040	
HFC-236fa	$CCF_3CH_2CF_3$	240	0.28	8100	9810	7660	0
HFC-45fa	$CHF_2CH_2CF_3$	7.6	0.28	3380	1030	314	0
HFC-365mfm	$CH_3CF_2CH_2CF_3$	8.6	0.21	2520	794	241	
HFC-43-10mee	$CF_3CHFCHFCF_2CF_3$	15.9	0.4	4140	1640	500	
Sulfur Hexa-fluoride	*SF_6*	*3200*	*0.52*	*16300*	*22800*	*32600*	
Nitrogen Trifluoride	NF_3	7400	0.21	12300	17200	20700	
PFC-14	CF_4	50000	0.10	5210	7390	11200	
PFC-116	C_2F_6	10000	0.26	8630	12200	18200	
PFC-218	C_3F_8	2600	0.26	6310	8830	12500	
PFC-318	$c\text{-}C_4F_8$	3200	0.32	7310	10300	14700	
PFC-3-1-10	C_4F_{10}	2600	0.33	6330	8860	12500	
PFC-4-1-12	C_5F_{12}	4100	0.41	6510	9160	13300	
PFC-5-1-14	C_6F_{14}	3200	0.49	6600	9300	13300	
PFC-9-1-18	$C_{10}F_{18}$	>1000	0.56	>5500	>7500	>9500	
Trifluoro-	SF_5CF_3	800	0.57	13200	17700	21200	

methyl Sulfur-penta-fluoride							
Methylene Chloride	CH_2Cl_2	0.38	0.03	31	8.7	2.7	0
Methyl Chloride	CH_3Cl	1.0	0.01	45	13	4	0.02

Fazekas *et al.* found the photochemical decomposition of CF_3NO_2 in the upper atmosphere can undergo two main photodissociation pathways. The first pathway is due to the splitting of the C-N bond followed by radical recombination to both the N and O bonded material and the subsequent decay of the O-bonded material into COF_2 and FNO. This cycle will continue until no CF_3NO_2 remains. FNO will decay producing F·, and ·NO, while the oxygen atom will react readily with various compounds in the upper atmosphere including ozone. In the second proposed decay pathway, Equation 2, an oxygen atom is lost:

$$CF_3NO_2 + h\nu \rightarrow CF_3NO + O \qquad \text{(Eq. 2)}$$

The majority of CF_3NO_2 was destroyed after 1 hour of photodecomposition.[1.44] These two decay pathways may be problematic or they may balance each other out. At the moment the exact effect of CF_3NO_2 in the upper atmosphere is unknown. The generation of $\cdot NO_2$ in the upper atmosphere is not desired due to the destruction of an oxygen atom typically used for the generation of ozone, Equations 3-4.

$$\cdot NO_2 + O \rightarrow \cdot NO + O_2 \qquad \text{(Eq. 3)}$$

$$\cdot NO + O_3 \rightarrow \cdot NO_2 + O_2 \qquad \text{(Eq. 4)}$$

These two equations are the natural source of ozone depletion in the upper atmosphere. The other CF_3NO_2 destruction pathway creates an oxygen atom which can actually be used to help generate ozone. Depending on which destruction pathway is the dominate path the destruction of CF_3NO_2 may not have a large detrimental effect on the ozone layer.

Trifluoronitromethane, CF_3NO_2, as a replacement for sulfur hexafluoride, SF_6, as a dielectric gas in certain applications is promising. Sulfur hexafluoride is the most used dielectric gas/insulator and is used as an interrupting medium in circuit breakers, gas-insulated capacitors, gas-insulated substations and high-fidelity loudspeakers. Sulfur hexafluoride is used because it is nontoxic and easy to handle. It is useful over a large temperature range, has excellent dielectric properties and has excellent arc interrupting properties.[1.45] Sulfur hexafluoride has the downside of a high GWP and is difficult to destroy once it is formed. Due to its useful properties, SF_6 is used more every year, and loss through generation and use is a concern due to its high GWP, see Table 2. For this reason, alternative dielectric gases are being investigated, and CF_3NO_2 has been suggested as a possible replacement. As an undiluted dielectric gas, CF_3NO_2 has not garnered much interest due to its high cost of production. A mixture of trifluoronitromethane (10% mass) with a good, inexpensive dielectric gas, such as CCl_2F_2, would greatly reduce CCl_2F_2 carbonization. Carbonization is the decay of a molecule into elemental carbon and other small molecules.[1.9] Carbonization is one of the major problems with carbon containing dielectric gases. A reduction of the amount of carbonization is highly advantageous because other mixtures can now be tested with CF_3NO_2 and other dielectric compounds that are more environmentally benign than SF_6. A low concentration of CF_3NO_2 in such a mixture would not have as severe an environmental effect as pure CF_3NO_2 would.

1.4 Preparative Methods for Other Perfluoronitroalkanes

Very few methods are known to introduce the nitro group into longer perfluoroalkyl chains. The various perfluoronitroalkanes include the linear or primary R_f-CF_2-NO_2, secondary, R_f-$CF(R_f)$-NO_2 and tertiary R_f-$CF(R_f)(R_f')$-NO_2 molecules. Only a few linear perfluoronitroalkanes are known to exist, and examples with perfluoroalkyl chains longer than eight carbons are unknown. Furthermore, no examples of perfluoronitroalkanes with the nitro group attached to either secondary or tertiary carbon atoms have been reported.[iii] Some success in adding the nitro group to perfluoroalkanoic acids was achieved by Scribner.[1.21,1.22] For example, using the same techniques described in Method 2 in Section 1.2, nitrogen dioxide was successfully added to linear perfluoroalkanoic acids with up to seven carbon atoms at reaction temperatures under 200 °C.

Brice *et al.* carried out some high temperature (450-650 °C), vapor phase chemistry on R_fCF_2X (X = H, Cl, Br, I and SO_2F) derivatives (see Scheme 1.6). They were not successful in adding $\cdot NO_2$ to the perfluoroalkyl group. Instead, in all cases, an acid fluoride end group was formed, except when X = H or when a carbon was eliminated from the chain. This elimination also forms a COF_2 molecule for every carbon removed in this manor. If Br_2 or I_2 was present along with $\cdot NO_2$, the $-CF_2H$ group was capable of reacting and forming the acid fluoride after hydrogen extraction occurred.[1.46]

[iii] Abundance was determined by a search on SciFinder

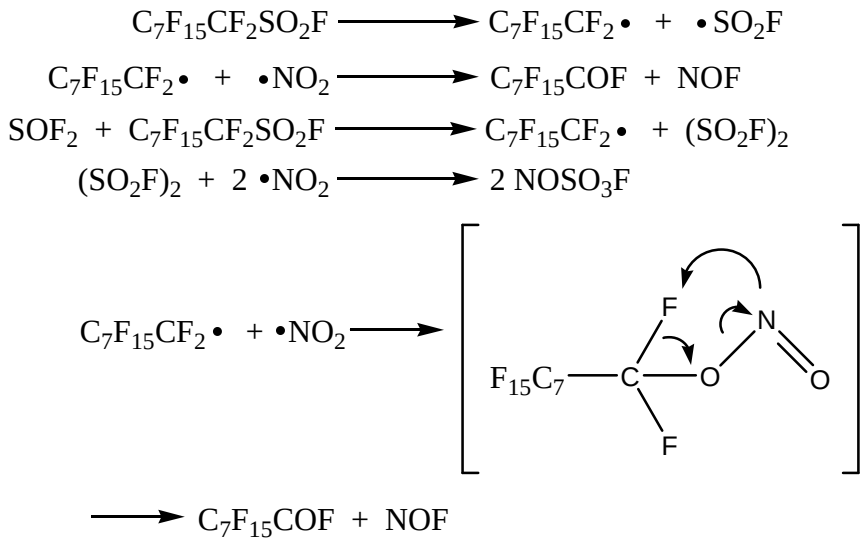

Scheme 1.6. ·NO_2 Addition Mechanism for High Temperature Reactions

At these elevated temperatures, the loss of one or more carbon atoms is typically due to the loss of COF_2 (see Scheme 1.7).[1.46]

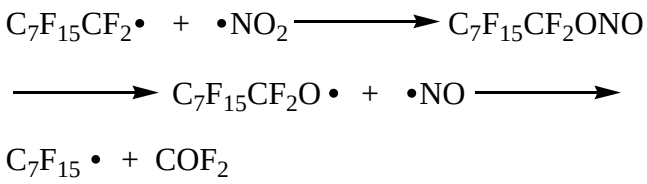

Scheme 1.7. Mechanism of Carbon Loss from Perfluoroalkanes in the Presence of ·NO_2

Brice *et. al.* found that the reaction did not reach the reaction threshold until 450 °C, and the product distribution remained constant until 650 °C. The ideal conditions for this reaction were 550 °C with a contact time of 15-20 seconds.[1.46]

Adding nitro groups to perfluoroalkyl compounds is an area that has definite potential for expansion. The research described in this dissertation will focus on the generation of CF_3NO_2 by photochemical and thermal activation. However, some scouting experiments were also carried

out on the thermal addition of $\cdot NO_2$ to linear perfluoroalkyl iodides, C_6-C_{12}, as well as the secondary and tertiary perfluoroalkyl iodides.

1.5 References

1.1 Jander, J.; Haszeldine, R. N. *Naturwissenschaften* **1953**, *40*, 579.

1.2 Gmelin Handbuch, F perfluorohalgenoorgano-Verbindungen; Springer-Verlag: Berlin-Heidelberg, 1980, pp 2-18.

1.3 Yabe, M.; Inagaki, Y. Jpn. Patent 63,193,348, 1988.

1.4 Hara, H.; Teraoka, T.; Kamimura, S.; Noguchi, M. Jpn. Patent 04,110,387, 1992.

1.5 Quay, S. C. WO Patent 93/05819, 1993.

1.6 Unger, E. C. U.S. Patent 5,585,112, 1996.

1.7 Unger, E. C. WO Patent 9,851,282, 1998.

1.8 Unger, E. C. WO Patent 9,851,284, 1998.

1.9 Wootton, R. E. U.S. Patent 4,275,260, 1981.

1.10 Luly, M. H.; Richard, R. G. U.S. Pat. Appl. 20080135817, June 12, 2008.

1.11 Lu, N.; Thrasher, J. S. *J. Fluorine Chem*. **2002**, *117*, 181.

1.12 Haszeldine, R. N. *J. Chem. Soc*. **1953**, 2075.

1.13 Haszeldine, R. N. GB Patent 770619, 1957.

1.14 Huckel, W. *Nachr. Akad. Wiss. Gottingen, Math.-physik. Klasse* **1946**, 36.

1.15 Vorobe'ev, M. D.; Filatov, A. S.; Englin, M. A. *Zh. Org. Khim.*, **1973**, *9*, 324.

1.16 Jander, J.; Haszeldine, R. N. *J. Chem. Soc*. **1954**, 919.

1.17 Yakubovich, A. Y.; Makarov, S. P.; Ginsburg, V. A.; Privenzentseva, N. F.; Martynova, L. L. *Dokl. Akad. Nauk SSSR* **1961**, *141*, 125-128.

1.18 Ginsburg, V. A.; Martynova, L.L.; Vasil'eva, M. N. *Zh. Obshch. Khim*. **1967**, *37*, 1083.

1.19 Yakubovich, A. Y.; Ginsburg, V. Al; Makarov, S. P.; Shpanskii, V. A.; Privezentseva, N. F.; Martynova, L. L.; Kir'yan, B. V.; Lemke, A. L. *Dokl. Akad. Nauk SSSR* **1961**, *140*, 1352.

1.20 Boschan, R. *Inorg. Chem*. **1960**, *53*, 1450.

1.21 Scribner, R. M. *Inorg. Chem*. **1963**, *29*, 284.

1.22 Scribner, R. M. U.S. Patent 3,057,931, 1962.

1.23 Tittle, B.; Cady, G. H. *Inorg. Chem*. **1965**, *4*, 259.

1.24 Ginsburg, V. A.; Yakubovich, A. Y.; Filatov, A. S.; Shpaskii, V. A.; Vlasova, E. S.; Zelenin, G. E.; Sergienko, L. F.; Martynova, L. L.; Markarov, S. P. Dokl. *Akad. Nauk SSSR* **1962**, *142*, 88.

1.25 Muralidharan, K.; Chakraborty, R.; Shreeve, J. M. *J. Fluorine Chem*. **2004**, *125*, 1967.

1.26 Haszeldine, R. N.; Jander, J. *J. Chem. Soc.* **1953**, 4172.

1.27 Ginsburg, V. A.; Medvedev, A. N.; Lebedeva, M. F.; Vasil'eva, M. N.; Martynova, L. L. *Zh. Obshc. Khim*. **1967**, *37*, 611.

1.28 Pye, K.; Smith. S. *Eur. Polym. J*. **1991**, *27*, 155.

1.29 Jander, J.; Haszeldine, R. N. *J. Chem. Soc*. **1954**, 912.

1.30 Felder, P. *Chem. Phys*. **1990**, *143*, 141.

1.31 van Veen, G. N. A.; Baller, T.; de Vries, A. E. *Chem. Phys*. **1985**, *93*, 277.

1.32 Young, M. A.; Pimentel, G. C. *J. Phys. Chem*. **1990**, *94*, 4884.

1.33 McFarlan, J.; Polanyi, J. C.; Shapter, J. G. *J. Photochem. Photobio., A*. **1991**, *58*, 139.

1.34 Demore, W. B.; Sander, S. P.; Golden, D. M.; Hampson, R. F.; Kurylo, M. J.; Howard, C. J.; Ravishankara, A. R.; Kolb, C. E.; Molina, M. J. *Chemical Kinetics and Photochemical Data for Use in Stratospheric Modeling, Evaluation No. 12,* JRL Publication, No. 97-4, NASA, Pasadena, CA, 1997.

1.35 Giles, M. K.; Turnipseed, A. A.; Talukdar, R.K.; Rudich, Y.; Villalta, P. W.; Huey, L. G.; Burkholder, J. B.; Ravishankara, A. R. *J. Phys. Chem.* **1996**, *100*, 14005.

1.36 Ryan, K. R.; Plumb, I. C. *J. Phys Chem*. **1992**, *86*, 4678.

1.37 Bozzelli, J. W.; Kaufmann, M. *J. Phys. Chem*. **1973**, *77*, 1748.

1.38 Vakhtin, A. B. *Int. J. Chem. Kinet*. **1996**, *28*, 443.

1.39 Breheny, C.; Hancock, G.; Morrell, C. *Phys. Chem. Chem. Phys*. **2000**, *2*, 5105.

1.40 Rossi, M. J.; Barker, J. R.; Golden, D. M. *J. Chem. Phys*. **1989**, *71*, 3722.

1.41 Frolkis, V. A.; Karol, I. L.; Kiselev, A. A. *Ecological Indicators*. **2002**, *2*, 109 and reference therein.

1.42 Restrepo, G.; Weckert, M.; Bruggemann, R.; Gerstmann, S.; Frank, H. *Environ. Sci. Technol*. **2008**, *42*, 2925.

1.43 Foster, P.; Ramaswamy, V.; Artaxo, P.; Berntsen, T.; Betts, R.; Fahey, G.W.; Haywood, J.; Lean, J.; Lowe, C.C.; Myhre, G.; Nganga, J.; Prinn, R.; Raga, G.; Schulz, M.; Van Dorland, R. 2007: Changes in Atmospheric Constituents and In Radiative Forcing. *In: Climate Change 2007: They Physical Science Basis. Contribution of Working Group I to the Fourth Assessment Report of the Intergovernmental Panel on Climate Change* [Solomon, S.; Quin, D.; Manning, M.; Chen, Z.; Marquis, M.; Averyt, K.B.; Tignor, M.; Miler, H.L. (eds.)] Cambridge University Press, Cambridge, United Kingdom and New York, NY, USA.

1.44 Fazekas, G. B.; Takacs, G. A. *J. Photochem*. **1983**, *21*, 9.

1.45 Boggs, S. A. *IEEE Electrical Insulation Magazine* **1989**, *5*, 18.

1.46 Severson, W. A.; Brice, T. J. *Inorg. Chem*. **1957**, *80*, 2313.

CHAPTER TWO

PHOTOCHEMICAL GENERATION OF TRIFLUORONITROMETHANE, CF_3NO_2

2.1 Introduction

Trifluoronitromethane, CF_3NO_2, has been known for over fifty years. It was discovered soon after trifluoronitrosomethane, CF_3NO, which garnered much interest for the making of "nitroso rubbers" for the space program.[2.1] A large number of oxidizing agents are found to convert CF_3NO to CF_3NO_2 in various yields.[2.2, 2.3]

$$CF_3NO \xrightarrow[NaOH_{(aq)},\ NaOCl,\ NaHPO_3,\ CH_3PHO_2Na,\ NO \text{ or Heat}]{Mn_2O_7,\ KMnO_4,\ MnO_2(Hg),\ PbO_2,\ CrO_3,\ H_2O_2,\ O_2,\ S_2F_{10}} \begin{matrix} CF_3NO_2 \\ \text{Trace to} \\ \text{90\% Yields} \end{matrix}$$

There is no inexpensive and straightforward synthesis for CF_3NO_2, and multiple reactions and/or purification steps are necessary to produce CF_3NO_2. To date, there have bee no uses for CF_3NO_2 found. However, the lack of an efficient way to make CF_3NO_2 has not led to a lack of proposed uses. Trifluoronitromethane has been proposed as a solvent for optical recording material,[2.4] as a heat transfer fluid,[2.5] as a gaseous ultrasound contrast media,[2.6] as a gas for gaseous precursor-filled microspheres used for topical and subcutaneous delivery vehicles,[2.7] as a media for generating a solid porous matrix for pharmaceutical uses,[2.8] as an acoustically active drug

delivery system[2.9] and as a dielectric gas, pure or as a mixture gas, for the replacement of sulfur hexafluoride, SF_6.[2.10] A simple one-step method for generating large quantities of CF_3NO_2 is very desirable, particularly if any of the proposed uses for this compound turns out to be viable.

In 2002, Lu and Thrasher published the first one-step synthesis of CF_3NO_2.[2.11] This process involved the irradiation of iodotrifluoromethane, CF_3I, with an excess of nitrogen dioxide, $\cdot NO_2$, with a diazo blue light source (λ_{max} = 420 nm).[11] The reaction is initiated by the photochemical splitting of CF_3I into $\cdot CF_3$ and $\cdot I$ radicals. The trifluoromethyl radical, $\cdot CF_3$, reacts with the excess $\cdot NO_2$ present in the system, forming the desired CF_3NO_2 molecule in 33% yield. The CF_3NO_2 isomer involving the nitrogen to carbon bond is known as the N-bonded molecule. The spin density of the free electron in $\cdot NO_2$ can be found on the nitrogen and the two oxygen atoms of the molecule. Thus, the N-bonded molecule is not the major product of this photochemical reaction. Instead the major product of this reaction is the O-bonded CF_3ONO molecule. This molecule is formed when the $\cdot CF_3$ reacts with one of the two oxygen atoms. The O-bonded molecule is not stable and quickly decays into COF_2 and FNO. The compound FNO will react further with the glass of the reaction vessel as indicated in Equation 1.[2.12]

$$6\ NOF\ +\ SiO_2\ \rightarrow\ (NO)_2SiF_6\ +\ 2\ \cdot NO\ +\ 2\ \cdot NO_2 \qquad \text{(Eq. 1)}$$

All byproducts can be removed by several physical and chemical procedures that are summarized in Chapter 4. The overall photochemical reaction is shown in Scheme 2.1.[2.11]

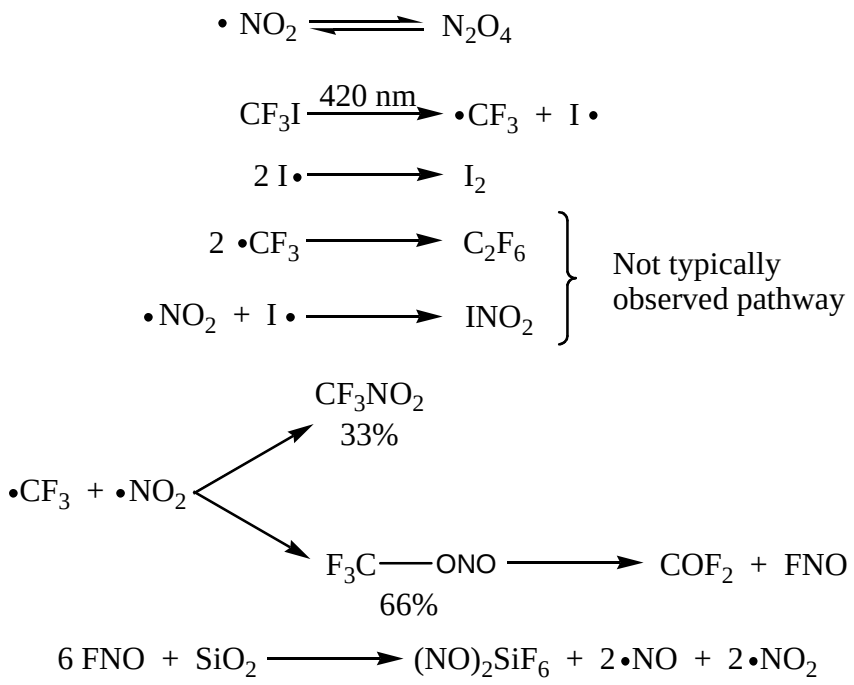

Scheme 2.1. Mechanism for the Generation of CF_3NO_2

Since 2002, only one other reaction has been found that generates CF_3NO_2 in one step. This reaction was reported in 2004 by the Shreeve *et al*. and involves the electrophilic trifluoromethylation of $NaNO_2$ in DMSO using 5-(trifluoromethyl) dibenzothiophenium tetrafluoroborate as the trifluoromethylation agent (Scheme 2.2).[2.13]

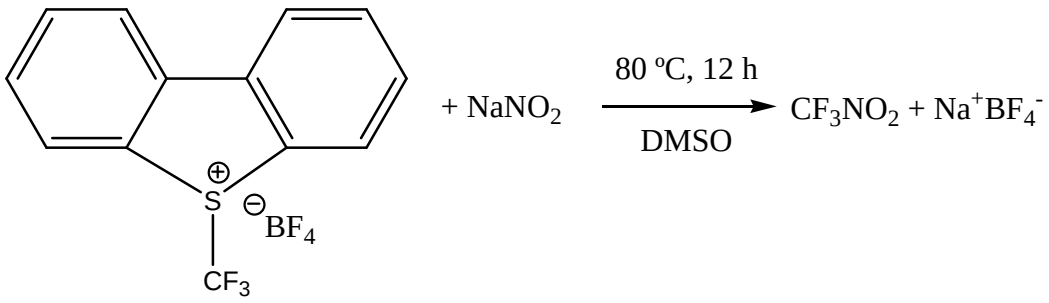

Scheme 2.2. Alternate One-step Method for Generating CF_3NO_2

Trifluoronitromethane is produced in ~90% yield in this reaction and is easy to isolate, but the reaction is vastly more expensive due to the cost of the trifluoromethylation reagent (ca. $50 per gram – SynQuest Laboratories, Inc. 2007/08 catalogue).

One of the goals of this project was to determine if the photochemical method was scalable. Many variables such as pressure, temperature, stoichiometry, reaction time and others need to be considered to find the best conditions for the generation of large quantities of CF_3NO_2.

2.2 Results and Discussion

The initial work in the Thrasher group focused on the generation of SF_5NO_2 using the diazo blue light with small amounts of starting materials at 25-40 °C. After the successful synthesis of SF_5NO_2,[2.14-2.16] the method involving the use of diazo blue light instead of the typical UV-light was expanded to make the already known CF_3NO_2. A typical reaction was run under the following conditions: CF_3I (2.07 g, 10.6 mmol) and $\cdot NO_2$ (0.874 g; 19.0 mmol), which is a 1 : 1.8 stoichiometric ratio of CF_3I : $\cdot NO_2$, were added to a 4-L Pyrex® reaction vessel resulting in a pressure of 0.18 atm. The yield of CF_3NO_2 in the reaction was typically about 0.40 g (3.5 mmol) or ca. 33% yield.[2.11] No attempts were made to scale up this photochemical method to produce 5-10 g (or more) of CF_3NO_2 a batch.

2.2.1 Properties of CF_3NO_2

Trifluoronitromethane, CF_3NO_2, is a colorless gas with a boiling point of -32 °C.[2.1] The ^{19}F-NMR spectrum of CF_3NO_2 shows a 1 : 1 : 1 triplet at δ = -73.6 ppm, with a ^{19}F to ^{14}N coupling constant $^2J_{FN}$ = 14.6 Hz. The ^{14}N-NMR spectrum is a quartet at δ = 279.1 ppm with a ^{19}F to ^{14}N coupling constant of $^2J_{FN}$ = 20.5 Hz. This splitting is possible due to the highly symmetric environment of the ^{14}N-nucleus.[2.11] The ^{13}C-NMR spectrum is a quartet at δ = 113 ppm with a coupling constant $^1J_{FC}$ = 298 Hz.[17] The IR spectrum of CF_3NO_2 has the following stretching frequencies: $\nu_{as}NO_2$ = 1627 cm^{-1}, ν_sNO_2 = 1312 cm^{-1}, $\nu_{as}CF$ = 1289 cm^{-1} and 1273 cm^{-1}, ν_sCF = 1159 cm^{-1}, ν_sCN = 862 cm^{-1} and νNO_2 = 751 cm^{-1}.[2.11]

2.2.2 Properties of $\cdot NO_2$

Nitrogen dioxide, $\cdot NO_2$, is an red-brown paramagnetic gas with a boiling point of 21.15 °C and a melting point of -11.2 °C.[2.18] The $\cdot NO_2$ molecule exists in equilibrium with its dimer N_2O_4. While the lone electron of $\cdot NO_2$ is delocalized over all the atoms of the molecule, the combination of radicals forms a nitrogen-nitrogen bond, Equation 2.

$$2\ \cdot NO_2 \rightleftharpoons O_2N\text{-}NO_2 \qquad \text{(Eq. 2)}$$

This bond is very long, 0.175-0.178 nm,[2.19] with a bond dissociation energy of 12.88 kcal/mol.[2.20] The N_2O_4 molecule is colorless and much less reactive than $\cdot NO_2$. Temperature and pressure equilibrium data for the system $\cdot NO_2/N_2O_4$ mixtures are shown in Table 2.1.

Table 2.1. Equilibrium Ratio of $\cdot NO_2/N_2O_4$ for Various Temperatures and Pressures[2.19]

Temp. (℃)	$K_{(eq)}$, atm	1 atm	0.7 atm	0.5 atm	0.3 atm	0.1 atm
-33	1.418×10^{-3}	0.038	0.046	0.055	0.071	0.127
-13	1.194×10^{-2}	0.166	0.139	0.170	0.221	0.41
7	7.418×10^{-2}	0.312	0.383	0.467	0.645	1.31
27	3.612×10^{-1}	0.806	1.021	1.285	1.855	3.817
47	1.443	2.123	2.793	3.65	5.65	15.361

Table 2.1 shows the concentration of $\cdot NO_2$ divided by the concentration of N_2O_4 at various pressures and temperatures and the equilibrium constants, $K_{(eq)}$, at those temperatures. What is important to note is that with declining pressures and increasing temperatures, the concentration of $\cdot NO_2$ increases. The higher partial pressure of $\cdot NO_2$ is key to all of the following experiments because it is the $\cdot NO_2$ that is the reactive species and is the crux of the chemistry for the photochemical reaction.

2.2.3 Analysis of the Photochemical Reaction Mixtures

The products were routinely analyzed by ^{19}F-NMR spectroscopy. IR spectroscopy was used occasionally as a supplemental technique to confirm the absence of NO_x. At the end of the reaction, left over CF_3I (^{19}F-NMR spectrum, singlet δ = -5.1 ppm) and occasionally small amounts of CF_3NO (^{19}F-NMR spectrum, singlet δ = -89.8 ppm) are found.

Infrared spectroscopy is used to detect any NO_x compounds in CF_3NO_2 which contains no other fluorine-containing impurities after a typical purification, see Chapter 4. A visual inspection of the condensed gases is a good indicator of the absence of both CF_3NO and N_2O_3

due to their royal blue color at -196 °C. The CF_3NO molecule retains this color in the gas phase, while N_2O_3 dissociates into ·NO (colorless) and ·NO_2 (brown-orange color).

2.2.4 Sample Analysis

The sample purification performed before the ^{19}F-NMR spectral analysis is minimized, in order to keep as many of the byproducts formed during the reaction present in the sample. After the reaction, the volatile contents of the cylinder were vacuum transferred into a clean metal cylinder. The less volatile I_2 was left behind in the reaction vessel. The stainless steel cylinder was then cooled to -78 °C, and all of the volatile materials were removed and placed in a fresh cylinder. While most of the nitrogen dioxide remains behind in the -78 °C vessel as N_2O_4, any CF_3I, CF_3NO_2, CF_3NO and some N_2O_3 are transferred. A sample from this cylinder was analyzed by ^{19}F-NMR spectroscopy.

^{19}F-NMR spectroscopy was used to estimate the mol% of CF_3NO_2 in the fluorine-containing products, in all reactions, including unreacted CF_3I. This was achieved by integrating the two peaks resulting from these materials, followed by using Equation 3:

$$CF_3NO_2\ \text{mol\%} = \frac{\text{Integrated intensity of } CF_3NO_2}{(\text{Integrated intensity of } CF_3NO_2 + \text{Integrated Intensity of } CF_3I)} \quad \text{(Eq. 3)}$$

This method is not suitable to give reliable numbers, if the sample is not completely in the vapor phase due to the different vapor pressures of CF_3NO_2 and CF_3I. This was not a problem for the blue light photochemical reactions where the entire sample could be expanded into the vacuum

line. From this value the %-yield can be back calculated. Many of the runs have lower than the expected 33% yield, since not all of the CF_3I has been consumed. If no CF_3I was found, then the isolated yield is shown. It must be noted that the values for mol% of CF_3NO_2 given in this work are calculated from the material present in the sample. Approximately 66% of the sample decays into other byproducts, such as FNO and COF_2, neither of which makes it to the analysis step. Therefore, the mol% of CF_3NO_2 is only relative to the sample remaining.

2.2.5 Effects of Stoichiometric Ratio on the Generation of CF_3NO_2

The stoichiometric ratio of the starting materials CF_3I : $\cdot NO_2$ was the first variable studied. It is one of the easiest to investigate, and it was assumed to have the smallest effect on the overall reaction. With only two starting materials, CF_3I and $\cdot NO_2$, an excess of one or the other is easily tested. Due to the close boiling points of CF_3NO_2 and CF_3I, -33 °C and -22 °C, respectively, an excess of CF_3I is undesirable and would complicate the purification process. The primary reason to consider $\cdot NO_2$ as the limiting reagent would be for large-scale purification purposes. If $\cdot NO_2$ were the limiting reagent, it would eliminate the need for many of the purification steps that are necessary for removing left over $\cdot NO_2$ from the product CF_3NO_2. However, the difficulty in separating excess CF_3I from CF_3NO_2 is the primary reason for using an excess of $\cdot NO_2$. The co-reactant $\cdot NO_2$ was used in excess in most batch reactions that were irradiated with super-blue light.

The stoichiometric ratios of CF_3I to $\cdot NO_2$ ranged from 1 : 1.1 to 1 : 5. The total pressure at ambient temperature was kept near 0.3 atm in all reaction, and the reaction time was limited to 18 hours. The temperature inside the blue light reaction system rose during the irradiation to

45-50 °C. Prior to each reaction, the reaction vessel was washed with acetone, rinsed with deionized water and then heated overnight at 175 °C prior to being evacuated. The results from these experiments are summarized in Table 2.2. Reactions with a ~3 : 1 molar excess of CF_3I : $\cdot NO_2$ were carried out in order to determine if other byproducts were formed when $\cdot NO_2$ was the limiting reagent. The mol ratio of CF_3I : $\cdot NO_2$ is the starting stoichiometric ratio of the reaction. The mol ratio of CF_3I : CF_3NO_2 is the composition of the reaction mixture upon completion. The mol% CF_3NO_2 was calculated as described in Section 2.2.3.

Table 2.2. Stoichiometric Ratios of CF_3I : $\cdot NO_2$

Experiment	**Mol ratio of CF_3I to $\cdot NO_2$**	**Mol ratio of CF_3I to CF_3NO_2**	**Mol% CF_3NO_2**
#1	1 to 1.06	1 to 3.50	77.8%
#2	1 to 1.13	1 to 2.89	74.3%
#3	1 to 3.02	1.11 to 1	47.4%
#4	1 to 3.08	1 to 1.02	50.5%
#5	1 to 4.72	1 to 1.04	51.0%
#6	1 to 5.05	1 to 1.19	54.3%
#7	2.79 to 1	1 to 0.44	30.6%
#8	2.37 to 1	1 to 0.35	25.9%

The results show that 18 hours were not sufficient to bring the reaction to completion. Runs #1 and #2 had the smallest molar excess of $\cdot NO_2$ and gave the best conversions. At the lowest stoichiometric excess, the partial pressure of the $\cdot NO_2$ is also at its lowest. This will push the $\cdot NO_2 \rightleftharpoons N_2O_4$ equilibrium towards the $\cdot NO_2$ radical. When the difference in stoichiometric ratios is larger, the opposite happens. The partial pressure of N_2O_4 is increased at the expense of $\cdot NO_2$.

For the experiments with a 3 : 1 and 5 : 1 stoichiometric ratio of $\cdot NO_2$: CF_3I, the mol% of CF_3NO_2 is ~50% for each experiment. With the total pressure of these reactions at 0.3 atm, the

results suggest that the partial pressure of $\cdot NO_2$ for these two stoichiometric ratios is similar enough that the yield is not influenced. Because the total pressure is kept to 0.30 atm, every time the stoichiometric ratio of $\cdot NO_2 : CF_3I$ is increased, the $2\ \cdot NO_2 \rightleftharpoons N_2O_4$ equilibrium is shifted to the right side.

The 3 : 1 $CF_3I : \cdot NO_2$ reaction produced a large number of impurities. The largest and only impurity whose identity was confirmed was hexafluoroethane, C_2F_6 (^{19}F-NMR spectrum, δ = -89.0 ppm), which consisted of 4.6 mol% of the major product mixture. Hexafluoroethane is a logical byproduct in the radical reaction, but hexafluoroethane was not observed when $\cdot NO_2$ was used in excess. Without any $\cdot NO_2$ to react with, $\cdot CF_3$ radicals can react directly with one another to form C_2F_6. Runs #7 and #8 were the only reactions where C_2F_6 was identified in the reaction mixture.

Since a stoichiometric excess of $\cdot NO_2$ works well over a wide range, especially if the reaction vessel is kept well above room temperature, increasing the amount of CF_3I in the reaction is necessary for a scale up. A reduction in the amount of $\cdot NO_2$ will allow a greater amount of CF_3I to be put into the Pyrex® vessel while keeping the necessary excess of $\cdot NO_2/N_2O_4$.

2.2.6 Effects of Pressure on the Generation of CF_3NO_2

Initially, the experiments for the photochemical generation of CF_3NO_2 were done at a total pressure between 0.5-1.0 atm. This turned out to be an unworkable condition at temperatures of 45-65 °C. A closer look at the chemistry of $\cdot NO_2$ explains this lack of reaction, see Table 2.1. This table gives the ratio of $\cdot NO_2 : N_2O_4$ at various temperatures and pressures.

At 47 °C, a molar ratio of $\cdot NO_2$: N_2O_4 of greater than 5 : 1 only exists for pressures less than or equal to 0.3 atm. The partial pressure of $\cdot NO_2$ increases as the temperature increases and the pressure decreases.

To better understand the effect of pressure on the system, a set of experiments were performed with the total pressure at ambient temperature ranging from 0.1 to 0.5 atm while holding the stoichiometric ratio at 3 : 1 and the reaction time at 18 hours. A clean and dry 4-L Pyrex® reaction vessel was used in all runs. The reaction temperature reached 45 to 50 °C after approximately 120 minutes. These results are summarized in Table 2.3.

These results are problematic for the scalability of the photochemical process. To achieve a better than 75% yield, the total pressure should not exceed 0.20 atm. The amount of CF_3NO_2 can be maximized by adjusting the stoichiometric ratios of the two reactants, CF_3I and $\cdot NO_2$, as close as possible, say 1 : 1.1, as demonstrated in Section 2.2.4.

Table 2.3. Results from Reactions at Various Pressures with a 3 : 1 Molar Ratio of $N_2O_4/\cdot NO_2$: CF_3I and 18 Hour Reaction Time

Experiment	Pressure (atm)	Mol ratio of CF_3I to CF_3NO_2	Mol% CF_3NO_2
#9	0.1	1 to 230	99.6%
#10	0.1	1 to 37	97.4%
#11	0.2	1 to 4.68	82.4%
#12	0.2	1 to 2.85	75.0%
#13	0.3	1.11 to 1	47.4%
#14	0.3	1 to 1.02	50.5%
#15	0.4	1 to0.62	38.2%
#16	0.4	1 to 0.56	36.0%
#17	0.5	1 to 0.47	31.8%
#18	0.5	1 to 0.36	26.4%

Unless a flow system is created for a continuous process or some alternative method for generating CF_3NO_2 is found, the volume of our largest reaction vessel, 16-L, sets an upper limit of 1-3 g of pure CF_3NO_2 per reaction in this set-up.

2.2.7 Effects of Temperature on the Yield of CF_3NO_2

Similar to pressure, temperature has a significant effect on the equilibrium $2 \cdot NO_2 \rightleftharpoons N_2O_4$. The higher the temperature, the more the equilibrium shifts towards the $\cdot NO_2$ radical. For example, at a temperature of 100 °C and a pressure of 1 atm, about 90% of all gas molecules will be $\cdot NO_2$. At 35 °C and 1 atm, the mixture consists of 70% N_2O_4.[2.18] The equilibrium was studied between 10 to 70 °C and at less than 0.5 atm. Experiments #23-#26 were carried out at low temperatures by placing the reactor in a temperature-controlled room held at 5 °C and activating the fan at the bottom of the irradiation chamber to push warm air out. The temperature measured at the half-height of the reaction vessel was typically between 10-13 °C. Elevated temperatures are reached by leaving the fan off. Depending on the temperature in the laboratory, the temperature inside the super-blue light reactor was found to be between 47-55 °C.

Unless otherwise noted, all reactions shown in Table 2.4 were run for a period of 18-20 hours. The product mixture was analyzed by ^{19}F-NMR spectroscopy following the method described in 2.2.3. Instead of listing the CF_3NO_2 isolated, which varies drastically between runs (a typical photochemical reaction will give a yield of 22-33%), the conversion of CF_3I into CF_3NO_2 is a better measure for monitoring the success of the reaction. The differences

between the yields are often due to changes in the purification procedure and will be discussed in detail in Chapter 4.

Regardless of the stoichiometric ratio of CF_3I to $\cdot NO_2$, as long as the pressure of the system was 0.3 atm or less and the temperature above 50 °C, the amount of CF_3I left after 18-20 hours of irradiation was below the detection limit by ^{19}F-NMR spectroscopy.

Table 2.4. Temperature of Reaction at Various Pressures and Stoichiometric Ratios

Reaction #	CF_3I to $\cdot NO_2$	Pressure (atm)	Temp. (°C)	Mol% CF_3NO_2
#19	1 to 5.05	0.44	52	83.3%
#20	1 to 3.22	0.30	50	100%
#21	1 to3.27	0.16	55	100%
#22	1 to 1.56	0.14	49.3	99.4%
#23	1 to 4.87	0.30	12.2	30.6%
#24	1 to 5.21	0.30	11.7	27.0%
#25	1 to 1.07	0.30	12.0	31.0%
#26	1 to 1.01	0.30	10.5	34.2%

When the total pressure of the reactants exceeds 0.3 atm, the CF_3I remaining at the end of the reaction increases. This is due to the decrease in partial pressure of $\cdot NO_2$ and the increase of partial pressure of N_2O_4. At elevated temperatures, the partial pressure of $\cdot NO_2$ increases enough to drive the reaction to completion. When the temperature of the system is lowered to below 15 °C, little conversion occurs even with a relatively low pressure of 0.3 atm. This is due to N_2O_4 now being the dominant species. At low temperature, Runs #23-#36, the stoichiometric ratios have no effect on the yield of the reaction.

The blue light reactor has no temperature control other than a fan. The only way to raise the temperature was to utilize the heat from the light-tubes. Typical heating methods such as heat tapes, heat guns or hot plates were not effective due to space constraints or unwanted

shading of light reaching the reaction vessel. Another factor that must be taken into account is the effect of temperature on the pressure of the system. The higher the temperature the system is operated at, the greater will be the pressure inside the reaction vessel. For safety reasons, the pressure was kept below 1 atm but not monitored during the reaction.

2.2.8 Effects of Reaction Time on the Yield of CF_3NO_2

All reactions to this point have been run for 18-20 hours. If the reaction time can be reduced, even slightly, more reactions can be done in a shorter period of overall time, thus producing a greater amount of CF_3NO_2 in the same period of time. A shorter reaction time may overcome the pressure problem that is limiting the quantity of reactants that can be used in a single reaction. A series of experiments were performed where the reaction was stopped after 1, 4, and 16 hours in order to determine if the 18-20 hours of reaction time was necessary. The results of these experiments are summarized in Table 2.5.

Table 2.5. Effects of Reaction Time on the Generation of CF_3NO_2

Starting Mole Ratio of CF_3I : $\cdot NO_2$	Temp. (°C)	Pressure (atm)	Mol% CF_3NO_2	Time (h)
1 to 1.9	41	0.15	20.7%	1
1 to 1.8	41	0.15	15.2%	1
1 to 1.8	41	0.15	18.2%	1
1 to 1.7	46	0.15	58.2%	4
1 to 1.6	46	0.14	52.6%	4
1 to 2.1	45	0.16	67.1%	4
1 to 1.6	49	0.14	99.5%	16
1 to 1.5	49	0.13	99.9%	16

This series of experiments shows that the initial reaction time chosen for this reaction turned out to be sufficient to complete the reaction in a temperature range of 40-50 °C. At 16 hours, the reaction has almost reached completion. If the reaction had been run for the standard 18 hours, the amount of CF_3I would most likely have been below the detection limit (*vida supra*).

If more heat could be added to the reaction, 5-10 °C, a reaction time of 16 hours should be enough to complete the conversion of CF_3I to CF_3NO_2. Due to the previously discussed problems with heating the system, a minimal benefit would be achieved. A very fast decay of CF_3I into I_2 and C_2F_6 will occur at 300 °C,[2.21] but the photochemical reactor has no way of reaching this temperature. A reaction temperature of 70 °C was the highest temperature observed. Iodotrifluoromethane is thermally stable in the 10-70 °C range of this study. The high-temperature chemistry of CF_3I will be utilized in the large-scale preparation of CF_3NO_2 discussed in Chapter 3.

2.2.9 Other Variables Affecting the Yield of CF_3NO_2

Other variables were found to influence the reaction, but it was more difficult to quantify their effects. One such variable is the ever-changing interior surface of the glass reaction vessel due to cleaning and drying procedures and the reaction of the glass surface with varying amounts of FNO. The side product FNO reacts with glass, forming $(NO)_2SiF_6$, see Equation 2. On average, 0.5 grams of Pyrex® were lost during each run. This reaction causes the glass surface to corrode, which undoubtedly decreases the transparency of the Pyrex® vessel, decreasing the ability of the super-blue light to pass through the Pyrex®. Another effect not accounted for stems

from the production of iodine, I_2. Iodine is continuously formed during the reaction, and it collects as large crystals at the coolest parts of the reaction vessel (often near the bottom) as well as in a thin film covering the entire inside of the reaction vessel. This film is removed with acetone. The reaction vessel was cleaned once a week, unless otherwise stated. Leaving iodine in the reaction vessel does not appear to affect the photochemical reactions. If I_2 was left in the reaction vessel and another experiment was performed in the "dirty" vessel, full conversion of CF_3I into CF_3NO_2 was still observed as long as the right pressure, temperature and time conditions were used. The vapor pressure of iodine at 20 °C in only 0.28 mbarr (0.22 torr) and is continually removed from the gas phase by crystallization. To check the effect of iodine, mercury was added to the reaction vessel prior to the photochemical reaction. The mercury was intended to scrub iodine more effectively via the formation of mercury (II) iodide, HgI_2, a red solid with a vapor pressure of 0.001 mbar at 60 °C. The removal of iodine by mercury is slow and gave no improvement in the yield of the reaction.

2.2.10 Generation of CF_3NO

A small amount of trifluoronitrosomethane, CF_3NO, was occasionally observed as a byproduct during the photochemical reaction. Trifluoronitrosomethane is a richly colored blue gas with a boiling point of -84 °C. This allows for easy separation by trap-to-trap purification from CF_3NO_2. This byproduct was most likely formed by a blue shift of the light coming from the diazo blue lamps. The spectral properties of the lamps will typically change after several hundred hours of operation. When research was begun, no CF_3NO was observed. By the end of the experiments, typically 1-2% of CF_3NO was observed. This is important because $\cdot NO_2$

photodissociates in high quantum yields at wavelengths below 400 nm (see Figure 2.1) into molecules such as O_2, ·NO, and N_2.[2.21] This is one of the main reason why CF_3NO_2 and SF_5NO_2 were not photochemically prepared until Thrasher and Lu switched to a super-blue light source from the mercury-UV photolysis lamps typically used for photochemical reactions.[2.11]

Once formed, the ·NO radical can react with the $\cdot CF_3$ radical forming CF_3NO.[2.1,2.11] If the stoichiometric ratio of the starting materials $\cdot NO_2$ and CF_3I is low, 1.1 : 1, little possibility exists for oxidizing the CF_3NO (with either O_2, ·NO, or $\cdot NO_2$) further to CF_3NO_2 and thereby eliminating the CF_3NO impurity. Fortunately, as has already been mentioned, CF_3NO and CF_3NO_2 are well separable, and the CF_3NO can be readily oxidized to CF_3NO_2 by a number of methods.[2.2, 2.3]

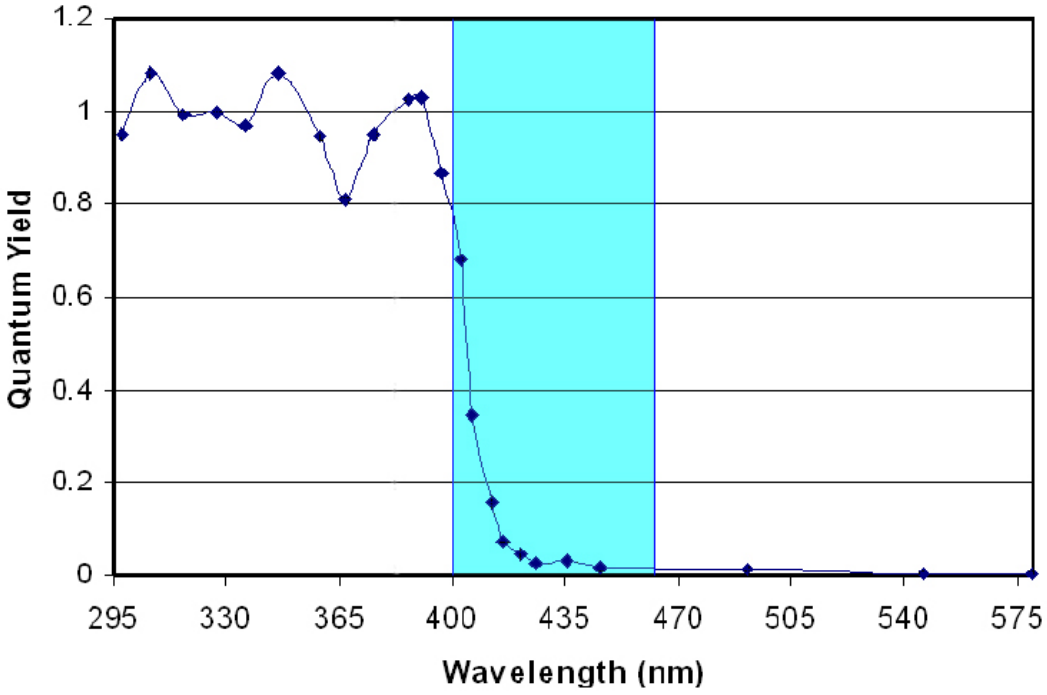

Figure 2.1. Wavelength dependence on the quantum yield for $\cdot NO_2$ photodissociation.[2.22]

2.3 Conclusions

The goal of this photochemical study using the diazo blue light reactor was to find the best reaction conditions for producing CF_3NO_2 from the photolysis of CF_3I and $\cdot NO_2$. The scalability of the photochemical reaction between CF_3I and $\cdot NO_2$ is controlled by the equilibrium between $2\ \cdot NO_2 \rightleftharpoons N_2O_4$. Even under the best conditions, only a maximum of 33% yield of the target molecule can be obtained as shown in Scheme 2.1. The problem created by the $\cdot NO_2/N_2O_4$ equilibrium does not make the scale-up of the photochemical method feasible. However, the photochemical method is excellent for synthesizing small amounts of CF_3NO_2, up to 3 grams per batch in a 16-L reaction vessel. The best conditions found for generating CF_3NO_2 with the diazo blue light photochemical method are a reaction time of 18-20 hours, an initial temperature and pressure of 20 °C and 0.3 atm, respectively, a reaction temperature between 55-65 °C and a stoichiometric ration of $\cdot NO_2$: CF_3I of 1.1 : 1. In this way, 1-3 grams of pure CF_3NO_2 are produced per batch.

2.4 Experimental Section

2.4.1 Instrumentation

Infrared spectra were recorded on one of three instruments: 1) Bio-Rad FTS-40, 2) JASCO FT/IR-410 or 3) JASCO FT/IR-4100 infrared spectrometer. The infrared spectra were taken on gas samples at pressures between 5-25 torr in a 10- or 20-cm glass cell fitted with silicon windows.

The ^{19}F-NMR spectra were recorded on either a Bruker 360 MHz or Bruker 500 MHz NMR spectrometer. All NMR samples were condensed into a NMR tube (5 mm O.D., equipped with a Teflon valve) on a vacuum line. Trichlorofluoromethane, $CFCl_3$, was used as an internal standard, and deuterochloroform, $CDCl_3$ (dried over P_4O_{10}), was used as the solvent.

2.4.2 Starting Materials

2.4.2.1 Trifluoroiodomethane, CF_3I

Trifluoronitromethane, CF_3I, was used as received from SynQuest Laboratories, Inc., Cat #1100-J-01, CAS #2314-97-8. The purity, which was guaranteed to be 99.0%, was checked by IR and ^{19}F-NMR spectroscopy. No impurities were detected.

2.4.2.2 Nitrogen dioxide, $\cdot NO_2$

Nitrogen dioxide, $\cdot NO_2$, was not always used as received from Matheson Trigas, CAS #10102-44-0. The $\cdot NO_2$ was condensed and held at -78 °C (nominally N_2O_4) and if a blue color was present (due to N_2O_3), the sample was kept at -78 °C under dynamic vacuum at 10^{-4} torr in order to remove the $\cdot NO$. The $\cdot NO$ molecule can form over time in a carbon steel storage cylinder. At low temperature, the $\cdot NO$ impurity is in an equilibrium with $\cdot NO_2$, $\cdot NO + \cdot NO_2 \rightleftharpoons N_2O_3$. The equilibrium allows for the slow extraction of $\cdot NO$ at -78 °C, while the N_2O_4 will remain behind. No more blue color indicates the successful removal of the $\cdot NO$. The sample is then warmed and transferred into a clean cylinder for use later.

2.4.2.3 Cesium fluoride, CsF

Cesium fluoride was stored and handled in a glove box. Before being used, a weighed quantity was placed in a platinum crucible, removed from the glove box, fused above its melting point, poured into a mortar and transferred back into the glove box. The solid CsF cake was ground into a powder. The crudely ground CsF was placed in a jar mill containing ceramic milling pieces. The jar mill was then sealed, removed from the glove box and placed on a mechanical tumbler for overnight grinding of the CsF. After cycling the jar mill back into the glove box, the finely ground CsF was weighed into the reaction cylinder for further use.

2.4.2.4 Aluminum trifluoride, AlF_3

Aluminum trifluoride was synthesized from sublimed anhydrous aluminum trichloride, $AlCl_3$ and HF free fluorine, F_2, as a 20% mixture with N_2. The sublimed $AlCl_3$ (110 g, 0.825 mol) was handled in the glove box and ground, as previously described for CsF. All the $AlCl_3$ was spread out in a copper boat, which was sealed in a double-end-capped, stainless steel cylinder equipped with two valves. The cylinder was then evacuated of all gases, and the tare weight of the cylinder was recorded. The cylinder was attached to a stainless steel vacuum line, and F_2/N_2 gas was allowed to flow into the vessel until a pressure of 200 torr was reached. The vessel was then heated to 200 °C with a heating sleeve overnight while monitoring the pressure of the system through the vacuum line. The following day, upon cooling the reaction vessel back to room temperature, any remaining gases were removed by vacuum through a soda lime tower. The reaction vessel was disconnected from the vacuum line, and the vessel and its contents were

reweighed. This process was repeated until the mass of the vessel and its contents remained constant. This reaction typically takes 2 weeks. Upon completion 63 g (0.75 mol) of AlF_3 was recovered with a 91% yield. The reaction is quantitative, and any losses are due to handling.

2.4.3 Preparation of CF_3NO_2

2.4.3.1 Method 1. Generation of CF_3NO_2 in the Presence of Mercury

Into a 4-L Pyrex® glass reaction vessel, 18.17 g of Hg was added by pipette followed by a Teflon stir bar. The reaction vessel was sealed, connected to a vacuum line and cooled to -196 °C. All non-condensable gases were removed by the freeze-pump-thaw method, 3 cycles. The vacuum line was filled with $\cdot NO_2/N_2O_4$ to a pressure of 258 torr, 2.55 g (55.4 mmol), which was then condensed into the -196 °C reaction vessel. Upon warming to room temperature, the weight of the vessel with the $\cdot NO_2$ was confirmed. Then 9.53 g of CF_3I (48.6 mmol) were added to the reaction vessel. The reaction was closed and allowed to warm back to room temperature. Once the reaction vessel was at room temperature, it was placed in the diazo blue light reaction chamber and irradiated with the blue light for ~18 hours. A thermocouple was taped to the surface of the reaction tube. This batch was purified following Method #2 described in Chapter 4.

Note: All masses for Method 1 were calculated from PV = nRT with the exception of the mercury, which was weighed.

2.4.3.2 Method 2. Generation of CF_3NO_2, General Method

An evacuated ~16.3-L Pyrex® glass reaction vessel was attached to the vacuum line and cooled to -196 °C. A total of 6.63 g (144 mmol) of $\cdot NO_2$ was vacuum transferred into the vessel, usually in three aliquots. After the reaction vessel was warmed back to room temperature, it was weighed. The vessel was reattached to the vacuum line, re-cooled to -196 °C and 8.77 g (44.8 mmol) CF_3I were added by vacuum transfer. The valve to the reaction vessel was then closed, and the reaction, mixture was allowed to warm to room temperature. Upon warming, the vessel was weighed again. The stoichiometric ratio of CF_3I : $\cdot NO_2$ was 1 : 3.2, and the pressure in the reaction vessel at RT was 0.30 atm. The reaction vessel was then placed into the blue light reactor and irradiated for 18 hours. This reaction was purified following Purification Method #2 as described in Chapter 4. This reaction yielded 1.40 g (12.2 mmol), representing a 27 %-yield of CF_3NO_2.

2.4.3.3 Method 3. Generation of CF_3NO_2, Timed Reactions

Following the procedure in Method 2, 2.85 g (61.9 mmol) of $\cdot NO_2$ and 6.49 g (33.1 mmol) of CF_3I were added to a ~16.3-L reaction vessel. The stoichiometric ratio of CF_3I : $\cdot NO_2$ was 1 : 1.87, while the pressure in the vessel was 0.15 atm. Upon warming to room temperature, the cylinder was placed in the blue light reactor and irradiated for 1, 4, or 16 hours depending on the specific time for the experiment. Each timed experiment was repeated 3 times, except the 16-hour reaction, which was performed twice, with slightly varying masses for the two reactants, CF_3I and $\cdot NO_2$.

2.5 References

2.1 Jander, J.; Haszeldine, R. N. *Naturwissenschaften* **1953**, *40*, 579.

2.2 Gmelin Handbuch, F perfluorohalgenoorgano-Verbindungen; Springer-Verlag: Berlin-Heidelberg, 1980, pp 2-18.

2.3 Haszeldine, R. N. GB Patent 770,619, 1957.

2.4 Yabe, M.; Inagaki, Y. Jpn. Patent 63,193,348, 1988.

2.5 Hara, H.; Teraoka, T.; Kamimura, S.; Noguchi, M. Jpn. Patent 4,110,387, 1992.

2.6 Quay, S. C. WO Patent 9,305,819, 1993.

2.7 Unger, E. C. U.S. Patent 5,585,112, 1996.

2.8 Unger, E. C. WO Patent 9,851,282, 1998.

2.9 Unger, E. C. WO Patent 9,851,284, 1998.

2.10 Wooton, R. E. U.S. Patent 4,275,260, 1981.

2.11 Lu, N.; Thrasher, J. S. *J. Fluorine Chem*. **2002**, *117*, 181-184.

2.12 Andreades, S. *J. Org. Chem*. **1962**, *27*, 4157-4162.

2.13 Muralidharan, K.; Chakraborty, R.; Shreeve, J. M. *J. Fluorine Chem*. **2004**, *125*, 1967.

2.14 Lu, N. Preparation, Characterization, and Properties of SF_5NO_2 and Related Compounds, Ph.D. Dissertation, University of Alabama, Tuscaloosa, AL, 2001.

2.15 Lu, N.; Thrasher, J. S.; Ahsen, S. V.; Willner, H.; Hnyk, D.; Oberhammer, H. *Inorg. Chem*. **2006,** *45*, 1783-1788.

2.16 Lu, N.; Kumar, H. P. S.; Fye, J. L.; Sun Blanks, J.; Thrasher, J. S.; Willner, H.; Oberhammer, H. *Angew. Chem. Int. Ed.* **2006,** *45*, 938-940.

2.17 DeMarco, R. A.; Fox, W. B.; Moniz, W. B.; Sojka, S. A. *J. Magn. Reson*. **1975**, *18*, 522-526.

2.18 Braker, W.; Mossman, A. L. Matheson Gas Data Book, 5th and 6th ed.; East Rutherford, NJ, Secaucs, NJ, 1979, 1980.

2.19 Bauer, S. H. *Chem. Rev*. **2002**, *102*, 3893.

2.20 Sisk, W.N.; Miller, C. E.; Johnston, H.S. *J. Phys. Chem*. **1993**, *97*, 9916-9923.

2.21 Yamamoto, T.; Yasuhara, A.; Shiraishi, F.; Kaya, K.; Abe, T. *Chemosphere* **1997**, *35*, 643.

2.22 Jones, I. T. N.; Bayes, K. D. *J. Chem. Phys.* **1973**, *59*, 4836.

CHAPTER THREE

THERMAL GENERATION OF TRIFLUORONITROMETHANE, CF_3NO_2

3.1 Introduction

The main goal of Chapter 2 was to prove or disprove the scalability of the photochemical generation of trifluoronitromethane, CF_3NO_2, using a diazo blue light source with a λ_{max} focused around 420 nm. The equilibrium between 2 $\cdot NO_2 \rightleftharpoons N_2O_4$ was found to hinder the photochemical reaction too much to allow for a successful scale up. The photochemical method proved to be an excellent method for small-scale synthesis, 1-3 g, but this method failed in the generation of the desired large-scale amounts that was set as the goal of this project, namely 10-100 grams a charge. A new inexpensive method for generating CF_3NO_2 that can be scaled up to make large quantities of product is highly desired and was the goal of this next set of experiments.

At 53.3 kcal/mol, the C-I bond is the weakest bond in trifluoroiodomethane.[3.1-3.5] There are several ways the bonds can be broken but photochemical dissociation and thermal decay are the two main methods. In both cases, the dissociation is homolytic in nature, Equation 1:

$$CF_3I \rightleftharpoons \cdot CF_3 + \cdot I \qquad \text{(Eq. 1)}$$

This information, as well as the results in Chapter 2, offered a promising starting point for suggesting the thermal method as a new reaction pathway for generating CF_3NO_2. Trifluoroiodomethane will decompose quickly in the temperature range of 300 to 400 °C, and by a temperature of 600 °C, the compound is completely dissociated.[3.6] Some studies have been performed on the thermal decay of CF_3I at very high temperatures, 760-1600 °C, and rate constants for C-I bond homolysis were reported for that temperature range.[3.1-3.5] On the other hand, little work on the kinetics has been reported at lower temperatures, namely ≤500 °C. One experiment by Whittle *et al.* investigated the thermal bromination of CF_3I to determine the bond dissociation energy of the C-I bond and found that temperatures of at least 170 °C were required for the reaction to occur.[3.3]

A few reports have appeared on the generation of CF_3NO_2 under thermal conditions from the reactions of nitrogen dioxide with either trifluoroacetic anhydride[3.7] and trifluoroacetic acid.[3.8-3.10] The experiment involving trifluoroacetic anhydride (Scheme 3.1) was performed at 100 °C producing some CF_3NO_2 once trifluoroacetic acid is generated. The formation of N_2O_3 impedes the reaction causing the yield for this method to be very poor, namely only 7% isolated yield.[3.7]

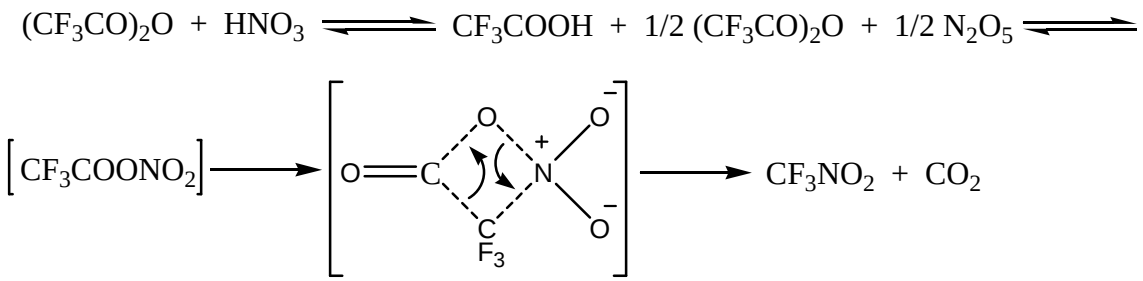

Scheme 3.1. Thermal Generation of CF_3NO_2 Using Trifluoroacetic Anhydride

Another report claimed a generation of CF_3NO_2 by reacting trifluoroacetic acid with $\cdot NO_2$ at a temperature of 200 °C was possible. For this reaction, %-yields of 30% were reported; but in the paper and patent, no isolated product was recovered. The yield was calculated by GC/MS, gas chromatography-mass spectrometry.[3.8-3.9] This synthetic application was taken a step further. The reaction of various chain length perfluorinated alkanes containing a carboxylic acid end group were reacted with $\cdot NO_2$, and the carboxylic acid end group was replaced with an $-NO_2$ group.[3.8-3.10] Brice and Severson also investigated perfluoroalkanesulfonyl fluorides and perfluoroalkanes with a CF_2X end group (X = H, Cl, Br, I) at temperatures between 450-600 °C. In most cases, the halogen radical and the corresponding perfluoroalkanes radical are formed. The radical then reacts with $\cdot NO_2$ forming the perfluoroalkane carbonyl fluoride, R_f-COF. Some chain shortening can occur before the perfluoroalkanes carbonyl fluoride is formed. The loss of a carbon generates a COF_2 molecule for every carbon lost producing various chain length perfluoroalkanes carbonyl fluorides for the final decay product.[3.11-3.12]

This Chapter will discuss the successful generation of CF_3NO_2 by the thermal reaction of CF_3I with $\cdot NO_2$ at a temperature of 200 °C. This method allows for the synthesis of CF_3NO_2 to be scaled up to batch sizes ranging from 10-60 g of pure material, and this method should be easily scalable to generate unlimited amounts of CF_3NO_2.

3.2 Results and Discussion

The successful thermal generation of CF_3NO_2 was discovered as much by chance as by a normal systematic approach. Very little literature exists on thermal additions of $\cdot NO_2$ to perfluoroalkyliodides.[3.8-3.10,3.12] The temperatures of most of these experiments were performed

at 400-600 °C, and CF_3I is known to undergo rapid thermal decomposition in this range.[3.6] The generation of the $\cdot CF_3$ radical[3.3,3.5] or longer perfluoroalkyl radicals[3.8-3.10] is well known, but what was not known is how thermally stable the CF_3NO_2 molecule or other $-NO_2$ analogs would be in the temperature range between 400-600 °C. Another question that arises is whether the perfluoroalkyl radicals would more readily combine with each other to yield perfluoroalkanes than with nitrogen dioxide to give nitroperfluoroalkanes.

As will be described in detail in Chapter 5, CF_3NO_2 was found to be stable with respect to thermal decomposition up to approximately 290 ºC. Therefore, this temperature was set as the upper limit for this experimentation. This helps explain why no CF_3NO_2 was observed in any of the previously reported attempts at temperatures above 300 °C. In this research, the initial attempts at generating CF_3NO_2 directly from CF_3I and $\cdot NO_2$ were carried out at much lower temperatures.

The initial thermal reactions were not successful in generating trifluoronitromethane, CF_3NO_2. The first thermal experiments were performed in a stainless steel autoclave containing a 3.30 : 1 ratio of $\cdot NO_2$: CF_3I, 8.21 g (178 mmol) $\cdot NO_2$ and 10.64 g (54.3 mmol) CF_3I in the presence of mercury (~10 g, 50 mmol). The purpose of the mercury was to eliminate any possibility of CF_3I reforming after its thermal dissociation via the formation of HgI_2. The reaction was initially run at 100 °C overnight followed up by a reaction at 125 °C the following night. After each reaction period, the system was allowed to cool, and a gas-phase IR spectrum was taken on the volatile contents of the autoclave. In each case, no CF_3NO_2 was observed. For a third period time, the intent was to raise the temperature of the reaction to 150 °C and continue upward, stepwise, until 250 °C was reached. Unfortunately, the autoclave sprang a leak around 150 °C and could not be resealed. After cooling, the autoclave was opened, and several large

yellow crystals were found on the inside surface of the head of the autoclave. No unreacted mercury was apparent in the bottom of the autoclave, but instead, a canary yellow powder, with a melting point above 300 °C, was present. The crystals and the powder appeared to be the same material. Both the crystal and powder begin to slowly decompose at a temperature of 260 °C, emanating a brownish-orange gas, which is most likely $\cdot NO_2$. Also, around this temperature, the substance begins to sublime and collect at the top of a sealed melting point tube. No melting was observed up to 300 °C. The crystal was determined by X-ray diffraction to be mercury(II) iodide nitrate, $HgINO_3$. The compound $HgINO_3$ was initially prepared by Persson and Holmberg by adding KI to an aqueous solution containing excess $Hg(NO_3)_2$ and HNO_3. The orange HgI_2 forms upon dissolving in the aqueous solution and displacing the nitrate from the mercury. The system was then heated to ~60 °C until all the HgI_2 dissolved, and at this point, colorless needle-like crystals were isolated by filtration.[3.13] Their method is both an easier and less expensive route to $HgINO_3$. However, before the current sample was characterized, the possibility of a new crystalline material kept the research focused on this thermal reaction.

In order to study the reactivity of CF_3I and $\cdot NO_2$ in the presence of mercury at higher temperatures, the reactants were placed in a Hoke® cylinder. Two reactions were carried out at this point. One reaction was at 150 °C and the other reaction was at 200 °C. Both cylinders were heated for 24 hours with mercury present. The final products were purified through an aqueous caustic solution, and the results are displayed in Table 3.1.

These results proved that CF_3NO_2 could be synthesized from the thermal reaction of CF_3I and $\cdot NO_2$ in the presence of mercury. However, several new questions now needed to be addressed. (1) Is mercury necessary for the reaction to proceed? Mercury(II) complexes are typically very poisonous, and mercury is considered a major pollutant. Therefore, removal of

mercury from the reaction would be preferred. (2) What conditions of pressure, temperature and stoichiometric ratio will allow the reaction to go to completion? (3) Will the thermal reaction fall victim to the same pitfalls of the photochemical reactions? Can added temperature overcome the 2 $\cdot NO_2 \rightleftharpoons N_2O_4$ equilibrium? (4) Will the isolated yield be greater than 33% even though both methods follow the same radical pathway? (5) If a large excess of $\cdot NO_2$ is required to drive the reaction to completion, can the $\cdot NO_2$ be recycled, or will it contain impurities that will contaminate future reactions upon reuse? (6) What is the kinetics of the thermal reaction? (7) Can this method be applied to other fluorine-containing primary iodides, secondary iodides and tertiary iodides for replacing the iodo with a nitro group?

Table 3.1. Initial Thermal Reactions with Mercury Present

CF_3I	$\cdot NO_2$	Hg	Stoichiometric Ratio of $CF_3I : \cdot NO_2$	Temp. (°C)	Pressure (atm)	Mol% CF_3NO_2
6.29 g (32 mmol)	5.09 g (111 mmol)	12.07 g (60 mmol)	1 : 3.44	150	30.51	3.2%
6.33 g (32 mmol)	5.01 g (109 mmol)	12.14 g (61 mmol)	1 : 3.37	200	33.75	20.0%

3.2.1 Effects of Temperature, Pressure and Stoichiometric Ratio on the Thermal Generation of CF_3NO_2

With the success of synthesizing trifluoronitromethane, CF_3NO_2, thermally in the presence of mercury, a new set of experiments were performed to determine if CF_3NO_2 could be formed without mercury. Thereafter, the ranges of stoichiometric ratios, pressures and temperatures required to optimize the yield of the reaction were investigated. Due to the

difficulty of separating CF_3I from CF_3NO_2, an excess of $\cdot NO_2$ was used in all the reactions. The first reaction carried out, without mercury, was an attempt to push the reaction to completion. A twenty fold excess of $\cdot NO_2$ was added to the cylinder, and the reaction mixture was reacted for ~96 hours at 200 °C. Upon cooling the reaction vessel to -78 °C and removing the volatile material through an aqueous caustic scrubber, the remaining isolated material contained only CF_3NO_2 and N_2O_3. However, no CF_3I was present. The thermal reaction was successful without mercury, and therefore, a wide range of variables could now be investigated. The results from these reactions are summarized in Table 3.2. All the reactions were heated to 200 °C for 72-96 hours, and in all cases, no unreacted CF_3I was detectable by ^{19}F-NMR spectroscopy at the end of the reaction. Unless otherwise noted, the variation in the yields is primarily due to differences in the purification techniques. When a standard purification method was developed, the %-yield covered a range from 37-54%.

This new thermal method to synthesize CF_3NO_2 displays a wide range of successful conditions. Stoichiometric ratios of CF_3I : $\cdot NO_2$ as high as 1 : 20 and as low as 1 : 1.1 of CF_3NO_2 : $\cdot NO_2$ were successful. Pressures ranging from 20 to 52 atm were successful, and this range should be expandable in both directions. The heat added to the system is significant enough to overcome the issues with the $2\ \cdot NO_2 \rightleftharpoons N_2O_4$ equilibrium, but sufficient time is still required to complete the reaction. In general, the thermal reaction required at least 24 hours for completion at 200 °C. This new thermal method is still a batch reaction. Like the photochemical method, it is possible that the nitrogen dioxide/dinitrogen tetroxide equilibrium can still have an effect. A flow process could avoid this pressure problem by allowing the addition of heat to the system by adjusting the pressure to a lower level by increasing the flow of the reactants. The feasibility of a flow reaction is an area that will need investigation at a later point.

Table 3.2. Thermal Reactions at Various Stoichiometric Ratios and Pressures

Reaction #	CF_3I:CF_3NO_2	Pressure (atm)	Isolated%-Yield
1	1 to 19.90	52.01	43.4%
2	1 to 8.74	24.01	18.1%*
3	1 to 7.05	39.82	47.1%
4	1 to 3.33	33.80	4.2%*
5	1 to 3.13	22.86	54.1%
6	1 to 2.75	20.55	81.2%**
7	1 to 2.27	43.91	46.0%
8	1 to 2.09	37.92	35.3%***
9	1 to 2.04	39.27	33.6%***
10	1 to 2.04	37.15	29.3%***
11	1 to 1.99	26.54	14.9%*
12	1 to 1.80	35.05	37.1%
13	1 to 1.62	39.81	36.5%
14	1 to 1.50	41.54	42.4%
15	1 to 1.41	42.09	33.6%
16	1 to 1.12	45.30	66.4%**

*** - Leak in cylinder or during purification caused change in yield**
**** - Product mixture was only purified with deionized water; N_2O_3 still present**
***** - Product mixture was purified through activated carbon**

The new thermal method has many advantages over the initial photochemical method. One such advantage is more starting material can be placed in the stainless steel reaction cylinder. A 75-mL stainless steel reaction vessel can generate 2-3 times as much product as the ~16-L blue light reactor. Most of the reactions were carried out in a nominal 2.25-L (measured to be 2.44-L by gravimetric methods) stainless steel reaction vessel, and batches of 10-60 grams of CF_3NO_2 were typically generated in each run. The upper pressure limits of the reaction were not investigated for safety reasons, but by simply maximizing the reaction conditions that were tested, a 1 : 1.1 molar ratio reaction of CF_3I : $\cdot NO_2$ at 50 atm could produce between 75-100 g of CF_3NO_2 per batch in the 2.25-L reaction vessel. The thermal method also gives a slightly better isolated yield than the photochemical method with a typical yields being 37-54%.

Several proposed methods exist for the decay of CF_3NO_2. The irreversible decay of the CF_3ONO molecule into FNO and COF_2 has already been discussed.[3.14] Trifluoronitromethane will photoabsorb light at a wavelength at 277 nm. This absorption is attributed to a $n \rightarrow \pi^*$ excitation, which is followed by the cleavage of the C-N bond in CF_3NO_2.[3.16] At this point, the radicals have a chance to reform the O-bonded molecule. The second pathway is the isomerization of CF_3NO_2 into CF_3ONO and its subsequent decay into FNO and COF_2. This pathway can be either photochemical or thermal in nature. These pathways are unlikely to occur in the photochemical reaction due to the reduced energy, 420 nm wavelength of light, of the super blue light system. The occurrence of these pathways would lead to a decrease in the overall recovery of CF_3NO_2 when compared to the photochemical method, and this is not the case.

The modest increase in yield, 37-54% for the thermal reaction, needs to be explained. All the thermal reactions were performed at 200 °C, which is well below the thermal decay temperature, ~270 °C, of CF_3NO_2, which was determined in Chapter 5**.** Because the thermal decay temperature has not been reached, the isomerization pathway is the one route that would lead to a decrease in the isolated yield. A loss in the yield is not observed. Instead, the thermal reaction gives a modest increase in the %-yield of 37-54%, increased from a maximum of 33% for the photochemical method. The dissociation of the C-O bond in CF_3ONO back into the $\cdot CF_3$ and $\cdot NO_2$ radicals does not occur at room temperature in the photochemical reaction, instead it decays into COF_2 and FNO.[3.14] At elevated temperatures, 200 °C, this may not be the case, and the O-bonded CF_3ONO molecule may dissociate back into $\cdot CF_3$ and $\cdot NO_2$ radicals. These two radicals can now reform back into the desired CF_3NO_2 molecule. The CF_3ONO molecule will still be the dominant species, and it will still continue to decay into COF_2 and FNO. However,

the dissociative pathway will now compete with the CF_3ONO decomposition route, allowing for a moderate increase in the yield as shown in Scheme 3.2.

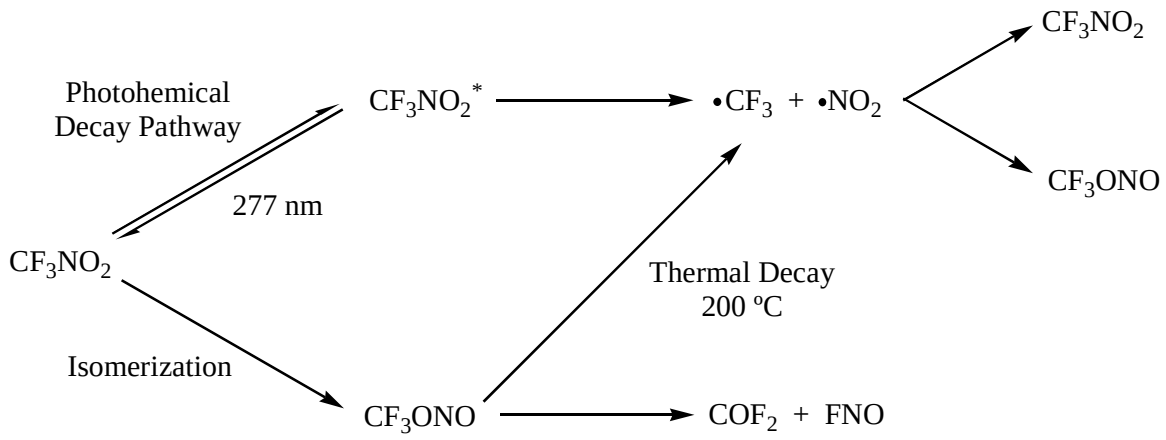

Scheme 3.2. Mechanism for the Formation of CF_3NO_2

This new thermal method for generating CF_3NO_2 works well over a wide range of stoichiometric ratios of $\cdot NO_2$: CF_3I (from 1.1 : 1 up to 20 : 1) and a moderate pressure range of 20-55 atm and can produce much larger quantities of CF_3NO_2 (10-60 g in a single batch) than the initial photochemical method. The thermal method does not require a new purification method or more expensive starting materials but achieves what the photochemical method could not, the ability to be scaled up. With the basic reaction conditions worked out and a more detailed understanding of the underlining chemistry at hand, one can now take a closer look at specific parts of the reaction. Some important variables include product recycling, various observations during the runs, and the kinetics of the reaction.

3.2.2 Thermal Reaction Odds and Ends

If the $\cdot NO_2$ can be recycled and used again with no adverse affects on the reaction, it will be advantageous to do so from the viewpoint of this making the reaction as "green" and cost effective as possible.

A thermal reaction, Reaction 3 (Table 3.2), was performed with recycled $\cdot NO_2$ from Reaction 1. Before the reaction, the $\cdot NO_2$ was purified by cooling it to -78 °C and removing any material that was volatile at this temperature. IR spectroscopy indicated that some impurities existed in the recycled $\cdot NO_2$. A ^{19}F-NMR spectrum confirmed that these impurities did not contain fluorine, but the impurities were not identified because separation from $\cdot NO_2$ was not possible. The impurities are most likely one or more of the NO_x compounds that are formed during the thermal reaction. The isolated percent yield of CF_3NO_2 in Reaction 3 was 47%.

Recycling the $\cdot NO_2$ is advantageous, especially on the laboratory scale because it cuts down on the cost of the reaction. However, it is unlikely that the current method for purifying the unreacted nitrogen dioxide would be used on an industrial scale.

In many of the earlier runs, a large amount of flaky, inorganic, non-crystalline material was recovered with the iodine. This material was not soluble in many different solvents including water, acetone, hexane, dichloromethane, chloroform, ether and THF. The color of the material ranged from a light whitish color to a dark brownish red. Three samples of this flaky material from Reactions 1 and 16 and a reaction with a 1 : 8.74 stoichiometric ratio ($\cdot NO_2$ excess) and 24 atm of pressure that leaked during the purification process (Reaction 17) were submitted for EDAX analysis. Each sample was run in duplicate, and the averages of the results are summarized in Table 3.3.

Table 3.3. EDAX Results of Flakes Isolated from Thermal Reaction

Sample	N	O	F	Si	P	Mo	S	I	Cr	Mn	Fe	Ni
Rxn 1	2.35	36.64	29.14	0.50	0.32	0.07	3.09	1.91	5.52	0.56	18.41	1.87
Rxn 16	3.04	10.62	60.27	0.57	0.27	0.75	0.0	0.20	5.04	0.32	17.09	1.95
Rxn 17	2.69	11.91	58.81	0.42	0.44	0.62	0.0	0.33	5.48	0.56	17.20	1.76

When these results are compared to the contents of stainless steel 316 (see Table 3.4[3.15]), the make up of the flakes begins to makes sense. The stainless steel vessel used in Reaction 1 was passivated with SF_4 prior to the thermal reaction, and the stainless steel reaction vessels for Reactions 16 and 17 were not. The passivation of the cylinder with SF_4 in Reaction 1 accounts for the presence of sulfur. No sulfur was found in the flakes from either of the other two reactions which were not passivated with SF_4. All the metals present in the flakes presumably comes from metal oxides or fluorides formed during the reaction.

Table 3.4. Contents of Stainless Steel 316[3.15]

	C	Mn	Si	P	S	Cr	Mo	Ni	N
Min	--	--	--	0	--	16.0	2.00	10.0	--
Max	0.08	2.0	0.75	0.045	0.03	18.0	3.00	14.0	0.10

3.2.3 Thermal Generation of CF_3NO_2 Using Trifluoroacetic Acid

The Scribner method for generating CF_3NO_2 is the most analogous to the thermal synthetic method discussed in this Chapter. Scribner reacted trifluoroacetic acid (TFA) with $\cdot NO_2$ at 200 °C and achieved a 30% yield of CF_3NO_2 in 6 hours with minimal purification

steps.[3.8] The shorter reaction time, 6 hours as opposed to 24 hours, and a better atom economy, no I_2 being generated as a byproduct, are both advantages over the new thermal method. Scribner's yield was not an isolated yield but a crude yield calculated from a GC/MS analysis. Scribner never attempted to optimize his reaction, and from what one can find in various literatures, others have not pursued this reaction further. The reaction was reinvestigated herein to determine whether or not the reaction could be reproduced and optimized.

The experimental conditions for this experiment were kept as close to Scribner's conditions as possible with one major exception, the volume of the reaction cylinder. Scribner's reaction was performed in an 80-mL stainless steel pressure reactor, while the new experiment was performed in a 150-mL stainless steel Hoke® cylinder with a burst disk. This change was made for safety reasons. If all of the reactants in the cylinder were to enter the gaseous state from overheating, the pressure in the cylinder would be over 1500 psi which is the upper limit for the cylinder; and for this reason the vessel volume was doubled. To the cylinder, 3.35 g (29.4 mmol) of TFA and 6.59 g (143 mmol) of $\cdot NO_2$ were added under a vacuum, which is a 1 : ~5 ratio of TFA : $\cdot NO_2$. The cylinder was heated to 200 °C for 6 hours, and upon cooling to room temperature, the contents were purified by pumping off any volatiles present after cooling the cylinder to -78 °C. The purification yielded 0.22 g, which represents a 6.5% yield of relatively pure CF_3NO_2. The ^{19}F-NMR spectrum showed the product mixture contained no other fluorinated impurities, but the mixture contained the typical blue color associated with the N_2O_3 contamination observed in the thermal reaction of CF_3I and $\cdot NO_2$. This mixture was not placed over NaOH pellets to finish the purification. Instead it was set aside, and unreacted starting materials were heated further at 200 °C in an attempt to push the reaction further towards completion and the 30%-yield that was claimed by Scribner.

The materials in the cylinder were allowed to react for an additional 2 weeks. Upon cooling, the basic purification technique of removing the volatiles at -78 °C was performed. A quantity of 0.97 g of material was collected, which increased the total product mass from the two reaction periods to 1.19 g. The two products were combined and further purified by being placed over NaOH pellets for several days. Trifluoronitromethane is not degraded by NaOH, but any NO_x compounds are removed. This is the typical final purification step developed for CF_3NO_2 and discussed in detail in Chapter 4. Upon removing the purified CF_3NO_2, only 0.14 g was recovered. This is a %-yield of 2.1%. The majority of the mass of this reaction turned out to be the various NO_x compounds formed upon heating $\cdot NO_2$. The added mass of the NO_x compounds could account for the higher %-yield observed by Scribner. In general, GC/MS is a poor analytical technique for analyzing low molecular weight gasses, and it is possible that the NO_x impurities were never observed during the Scribner experiments accounting for the elevated %-yield calculation. A detailed analytical procedure was not laid out in his paper. Therefore, duplication of Scribner's GC/MS method was not possible. Regardless, his result of a 30% yield could not be duplicated, which throws some doubt on any advantages the Scribner method might have over this new thermal method reported herein.

3.2.4 Thermal Addition of $\cdot NO_2$ to Larger Primary Iodoperfluoroalkanes

With the successful addition of $\cdot NO_2$ to the smallest iodoperfluoroalkane, CF_3I, it was desirable to see if this thermal method could be applied to larger, more complex molecules. The logical next step is to try longer primary iodoperfluoroalkanes. These compounds should have similar dissociation energies for their C-I bonds, and they have the advantage of having much

greater boiling points, so larger samples can be reacted without the same pressure concerns that occur when using CF_3I. A reaction was attempted with 39.36 g of a mixture of C_6-C_{12} chain-length iodoperfluoroalkanes with an approximate 5-fold excess of $\cdot NO_2$, which was estimated by assuming the mixture to only be the C_6 molecule. The reaction mixture was heated for 4 days at 200 °C. Upon purification, the resulting yellow-colored product mixture was analyzed by GC/FID, gas chromatography-flame ionization detector, and GC/MS to confirm that the reaction worked. One question that arose, was whether or not carbon chain shortening occurred during the run? Chain shortening would occur by elimination of COF_2 and would result in a re-distribution of the remaining chain lengths. Table 3.5 shows the initial starting mixture of the C_6-C_{12} 1-iodoperfluoroalkanes determined by GC/FID and the resulting mixture of the 1-nitroperfluoroalkanes. The numbers expressed are in average mol% which was calculated from two injections on the GC/FID.

Table 3.5. Thermal Reaction of $\cdot NO_2$ with 1-Iodoperfluoroalkanes C_6-C_{12}

Chain Length	Starting Mixture (mol%)	Final Product (mol%)
C2		1.19
C4		10.77
C6	34.79	30.01
C8	27.85	40.26
C10	16.75	10.82
C12	9.20	5.69
C14	5.90	0.48
C16	5.51	

This Table displays some interesting results. The mixture is actually broader than what is stated in the catalog. The mixture is actually C_6-C_{16} 1-iodoperfluoroalkanes. Upon reaction

completion, a 31.7% isolated yield of the desired 1-nitroperfluoroalkanes mixture is recovered, and the substitution was confirmed by GC/MS. The carbon chain is cleaving during the reaction. No C_{16} and very little C_{14} product remained upon completion, and new C_2 and C_4 compounds were formed. The major product is the C_8 molecule, which is the one chain length that increased in mol%. The C_8 molecule went up ~13%, and this is approximately the same mol% of C_{14} and C_{16} that was destroyed. This suggests that the C_8 molecules represents the most thermally stable of the various chain lengths. A search on SciFinder could not find any known molecules greater than the C_8 1-nitroperfluoroalkanes. Therefore, this method can successfully add the nitro group to longer chain perfluoroalkyl compounds than was previously known. Unfortunately, isolation of these new compounds was not successful, and a larger batch reaction is needed for a proper distillation. With the successful addition of $\cdot NO_2$ to many different chain lengths of primary iodoperfluoroalkanes, the focus shifted to the secondary and tertiary iodides.

3.2.5 Thermal Addition of $\cdot NO_2$ to Secondary and Tertiary Iodoperfluoroalkanes at 165 °C in a Stainless Steel Vessel

The two model compounds used for the secondary and tertiary iodoperfluoroalkane reactions were 2-iodoheptafluoropropane, a secondary iodide, and 2-iododecafluoro-2-(trifluoromethyl)pentane, a tertiary iodide. The two reactions were set up with an ~3 : 1 excess of $\cdot NO_2$: R_f-I. The reactants were placed in separate stainless steel cylinders that were heated to 165 °C for 72 hours, Schemes 3.3 and 3.4. Based on steric effects, both the secondary and tertiary iodides should require a lower temperature to cleave the C-I bond. This is why a 200 °C reaction temperature was not used like it was for the primary iodides. Upon purification of the

completed reaction, the contents of the two collection traps, one held at -78 °C and the other at -196 °C, were analyzed by ^{19}F and ^{1}H-NMR spectroscopy, IR spectroscopy, and GC/MS. Neither of the reactions was successful in giving the desired product at this temperature.

In the reaction with 2-iodoheptafluoropropane (see Scheme 3.3) only the -196 °C trap collected any material (1.19 g). The reaction cylinder contained iodine. A visual inspection of the inside of the reaction cylinder showed no white material. A possible decay product of the reaction is tetrafluorethylene (TFE), which could polymerize into poly-TFE, a white polymeric solid. No solid product other than I_2 was observed. The reaction produced several volatile products. Two of these compounds were characterized. The major volatile material was CF_3NO_2, which made up the majority of the mixture. The only other identifiable material was CF_3I, which was a minor product in the mixture. The other compounds present in the collection trap could not be identified.

Very little information could be gained from the IR or the GC/MS. The GC/MS results were especially disappointing. The only peak that was generated during the GC/MS run was a broad peak at 3 minutes, which represented the CF_3 and I ions. Conditions could not be found that did not cause the destruction of all the species present in the mixture. No other peaks were present in the injections. Not even CF_3NO_2 was detected. More experimentation with the GC/MS system is required to find conditions that do not destroy the compounds or separates them well enough for characterization to occur.

The thermal reaction with 2-iododecafluoro-2-(trifluoromethyl)pentane was not successful at 165 °C, Scheme 3.4. During the attempted purification of the products from this reaction, 1.29 g of material stopped in a -196 °C trap, while 0.56 g of material collected in a -78 °C trap. The -78 °C trap contained some CF_3I and CF_3NO_2 and many unidentified

compounds. These unidentified compounds appear to be chain-shortened perfluoroalkanes, but again, it is difficult to tell because no successful GC/MS data was obtained. The IR spectrum did eliminate the possibility of the formation of any alkenes. The only double bond stretching frequencies observed were those from the CF_3NO_2 molecule and other NO_x compounds. The starting material was 98.5% pure, and the impurities contained some hydrogen atoms. This muddles the interpretation of the NMR spectra even further, as both product collection traps contained some molecules with hydrogen. The -196 °C trap contained primarily CF_3NO_2 and CF_3I. Again, CF_3NO_2 was the dominant species, with a 4.4 fold excess when integrated against CF_3I.

The thermal reactions with both the secondary and tertiary iodide undergo a radical reaction, and due to this mechanism, a greater amount of possible products can be formed upon reaction completion. The most commonly lost group is the $\cdot CF_3$ radical, which can react with the I· radical or the $\cdot NO_2$ present in system to form the dominant species of the reaction, which are CF_3I and CF_3NO_2. The activation barrier to the CF_3NO_2 formation is lowered using the larger molecule. With CF_3I, no reaction generating CF_3NO_2 occurs, even after 3 days at 170 °C in a stainless steel vessel. Because the ·I radical can now be removed at a lower temperature and $\cdot CF_3$ can be generated, it can react and form CF_3NO_2 even at lower temperatures. If the proper species was chosen as a starting material, one that generated the $\cdot CF_3$ radical at a relatively low temperatures >100 °C in the gaseous phase, it would be possible to avoid the disadvantages of high temperature reactions like pressure and cost of construction materials.

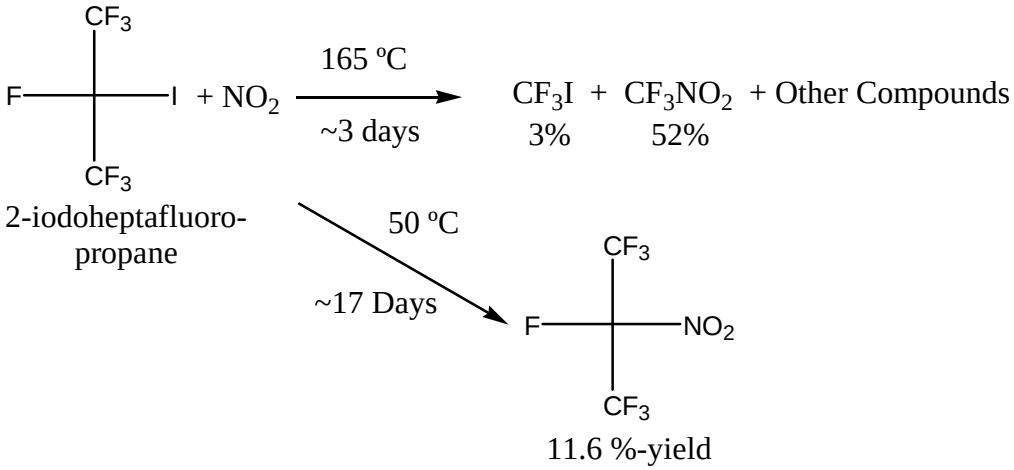

Scheme 3.3. Summary of Thermal Reaction for 2-Iodoheptafluoropropane

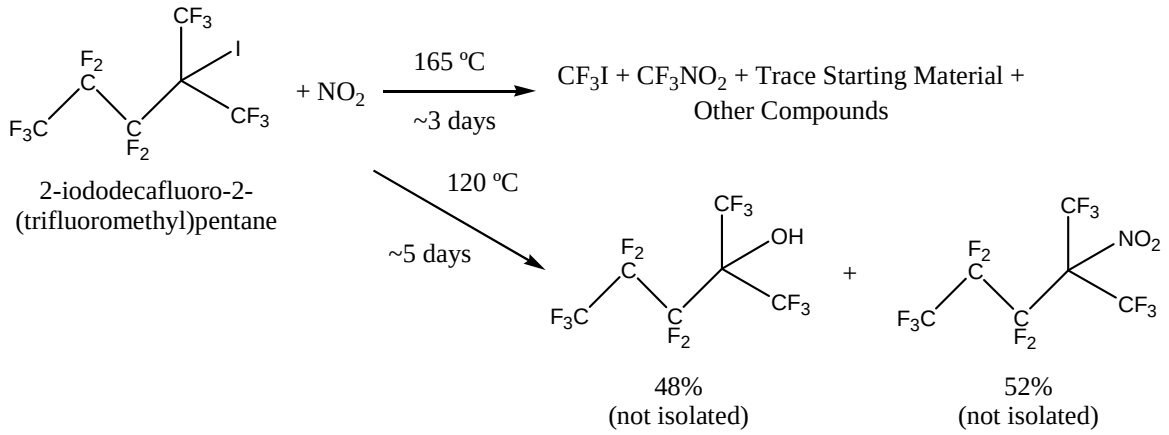

Scheme 3.4. Summary of Thermal Reaction for 2-Iododecafluoro-2-(trifluoromethyl) pentane

3.2.6 Thermal Addition of $\cdot NO_2$ to Secondary and Tertiary Iodoperfluoroalkanes at Temperatures Slightly above the Boiling Point of the Respective Iodoalkane in a Monel Vessel

The literature suggests that 2-iododecafluoro-2-(trifluoromethyl)pentane is not thermally stable in stainless steel at elevated temperatures,[3.31] so another set of experiments was attempted in a Monel cylinder at a reduced temperature of 120 °C. This temperature is just above the boiling point of 2-iododecafluoro-2-(trifluoromethyl)pentane, which is 116 °C. Similar conditions will be attempted with 2-iodoheptafluoropropane. Again, a Monel cylinder was used for this reaction, but the reaction temperature was held at 50 °C. The boiling point of 2-iodoheptafluoropropane is 39 °C. Due to the reduction in the reaction temperature, the reaction time was lengthened considerably. However, the progress of the reaction was not monitored, so the reaction may be completed well before the time the reaction was stopped.

To the Monel cylinder, an amount of 2.99 g (6.70 mmol) of 2-iododecafluoro-2-(trifluoromethyl)pentane was added and followed by the addition of 0.75 g (16.3 mmol) of $\cdot NO_2$. This mixture was placed in a 120 °C oven and allowed to react for ~5 days. The product mixture was cooled to -196 °C and allowed to warm slowly. The material was separated by a trap-to-trap distillation through a -78 °C trap and two -196 °C traps. The collections from the -196 °C traps were combined, and 0.44 g of material was collected. This collection was a mixture of many different compounds, with the exception of trace amounts of CF_3NO_2 and CF_3I none were identified.

The -78 °C trap was much more interesting. The trap consisted of colorless crystals on the walls of the trap above a large amount of yellow-brown liquid. This collection was

transferred into a fresh cylinder, and a ^{19}F-NMR spectrum was taken. The spectrum was relatively clean and contained two major products with a trace of the starting material, see Figure 3.1. The two compounds that were observed in the reaction mixture were 2-nitrodecafluoro-2-(trifluoromethyl)pentane and 2-trifluoromethyl-decafluoro-2-pentanol. Integration of the peaks show a ~50 : 50 mix of the two compounds, 48 % was the alcohol and 52% was the desired nitro compound. The characterization of the alcohol was initially a surprise. The NMR spectrum was taken before the caustic workup, and the appearance of an alcohol suggested an impurity was present in the starting material or on the cylinder wall that the nitrite molecule could react with. There is a small impurity present in the starting material, 1% or less, which contains protons. The concentration is not great enough to protonate the nitrite to the degree observed in the final mixture. The set up of the cylinder precludes the contamination of water which would be the other major compound that could form the alcohol in situ. The cylinder was dried several days in an oven at 200 °C. The nitrite, the -C-O-N-O molecule, reacts very quickly with acids or bases to form an alcohol.[3.10-3.11] The acidity of the solvent used for collecting the NMR spectrum, duterated-chloroform, is strong enough to protonate the nitrite and form the alcohol. Once the mixture was worked up over a caustic solution, only the alcohol and the nitro species remained. If the gaseous IR of the species had been taken before the caustic work up, it would be expected that the nitrite would have been observed and little to no alcohol would be present. EI GC/MS showed a single peak that eluted at 3.37 minutes and consisted of two compounds. No signal was observed in the positive mode, but the negative mode confirmed the creation of the alcohol with the peak being 334.9 ($C_6F_{13}O^-$). The nitro compound will not be easily protonated and cannot be deprotonated. Therefore, this EI GC/MS, electron impact ionization, method was not very effective for characterizing the molecule. The typical GC/MS

experiment still did not work for the reasons given in the previous section. IR confirmed the existence of the nitro compound by the characteristic N-O stretching peaks at ~1600 cm^{-1}.

Attempts were made to separate the alcohol from the nitro molecule. Trap-to-trap and similar vacuum techniques were not successful in separating the compounds. Instead of doing the typical purification procedure, placing the material over NaOH pellets, the product mixture was transferred into a 250-mL round bottomed flask containing 100 mL of 1 M NaOH aqueous solution. The mixture was allowed to sit overnight. The expectation was that the alcohol would become protonated thus staying behind in the aqueous layer while the nitro molecule would separate out easily. Unfortunately, both molecules were soluble in the aqueous solution. The solution was acidified, and both compounds were recovered with a 91% recovery. The yellow color was removed during this process, and a clear colorless liquid was collected. More experiments will be required to determine if these two compounds can be successfully separated. If more material was present, flash column chromatography may be successful. Also, if the boiling points are different enough, a spinning band column distillation would be another good option for separation.

With the success of the tertiary iodide, the reaction involving the secondary iodide was retried. To a 60-mL Monel cylinder, an amount of 4.73 g (16.0 mmol) of 2-iodoheptafluoropropane was added followed by 1.24 g (77.5 mmol) of $\cdot NO_2$. This reaction mixture was heated at 50 °C for ~17 day, see Scheme 3.3. Thereafter, the cylinder was cooled to -78 °C and all volatiles were removed by vacuum and collected in a -196 °C trap, 0.39 g. The typical N_2O_3 blue discoloration was present in this collection. The collection was transferred into a fresh cylinder containing NaOH pellets and allowed to sit overnight. Removal of the purified product yielded 0.28 g of material. Analysis by ^{19}F-NMR spectroscopy showed a pure

sample of the desired 2-nitrofluoropropane, see Figure 3.2. IR was used to confirm the presence of the nitro functional group and GC/MS was again not useful for characterization. This is an 8.1% yield. The material left in the reaction cylinder was not investigated.

No attempts were made to optimize the reaction, but with some work, it should be expected that the yield could be increased. These experiments also lay down the ground work for expanding this chemistry. The reaction vessel is very important and the high heat, coupled with a stainless steel vessel enhances the decay of the radical species into undesired smaller molecules. An interesting set of experiments would be to see what would occur at higher temperature in the Monel cylinder or at lower temperatures, in the stainless steel cylinder. This would help determine whether the decay is caused by the heat, the material of construction or a combination of the two. Regardless, the $\cdot NO_2$ can successfully be added to primary, secondary and tertiary iodides allowing for the expansion to a set of molecules where very few molecules are known or characterized.

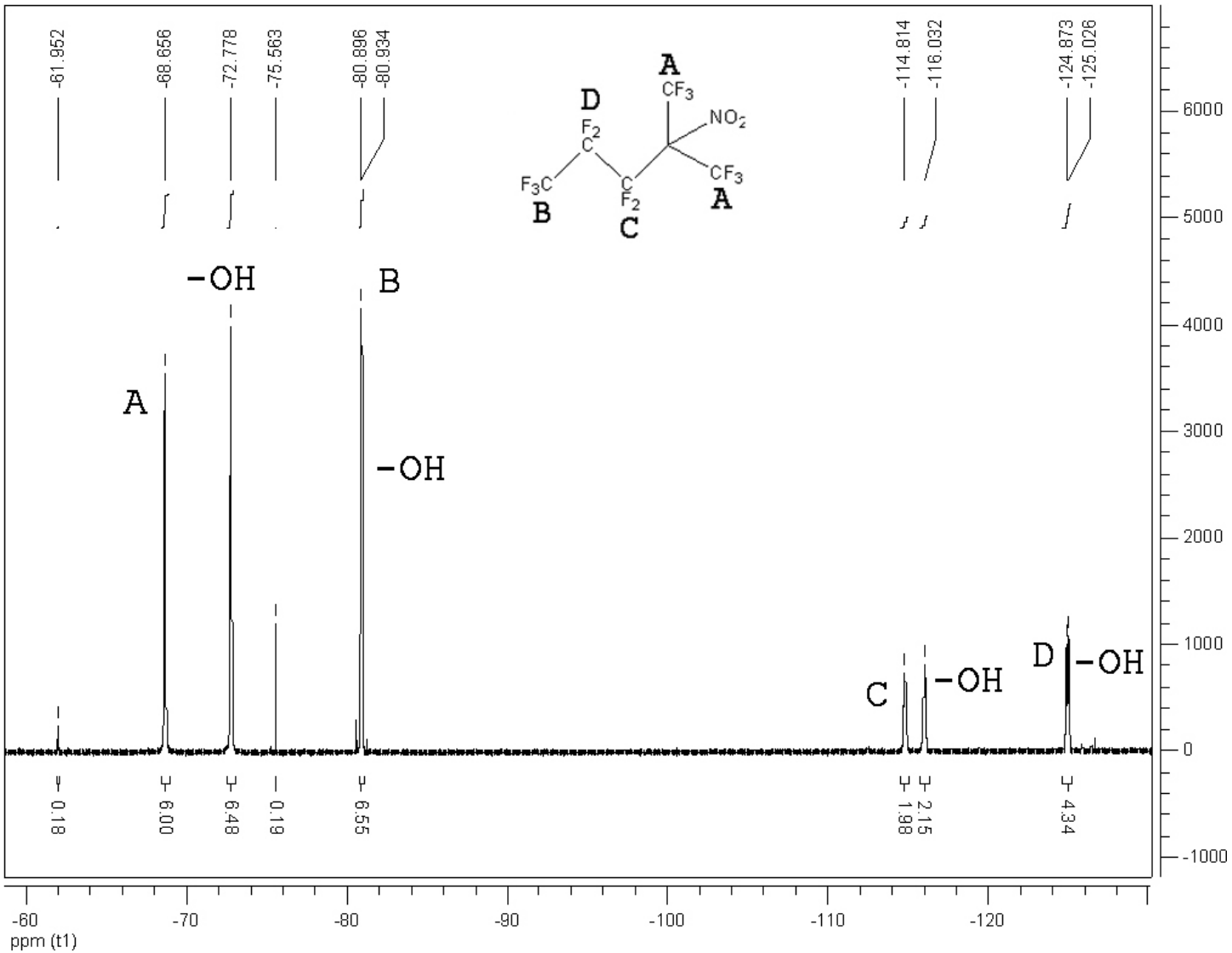

Figure 3.1 **^{19}F-NMR spectrum of 2-iododecafluoro-2-(trifluoromethyl)pentane reaction mixture collected at -78 °C from Monel cylinder at 120 °C.**

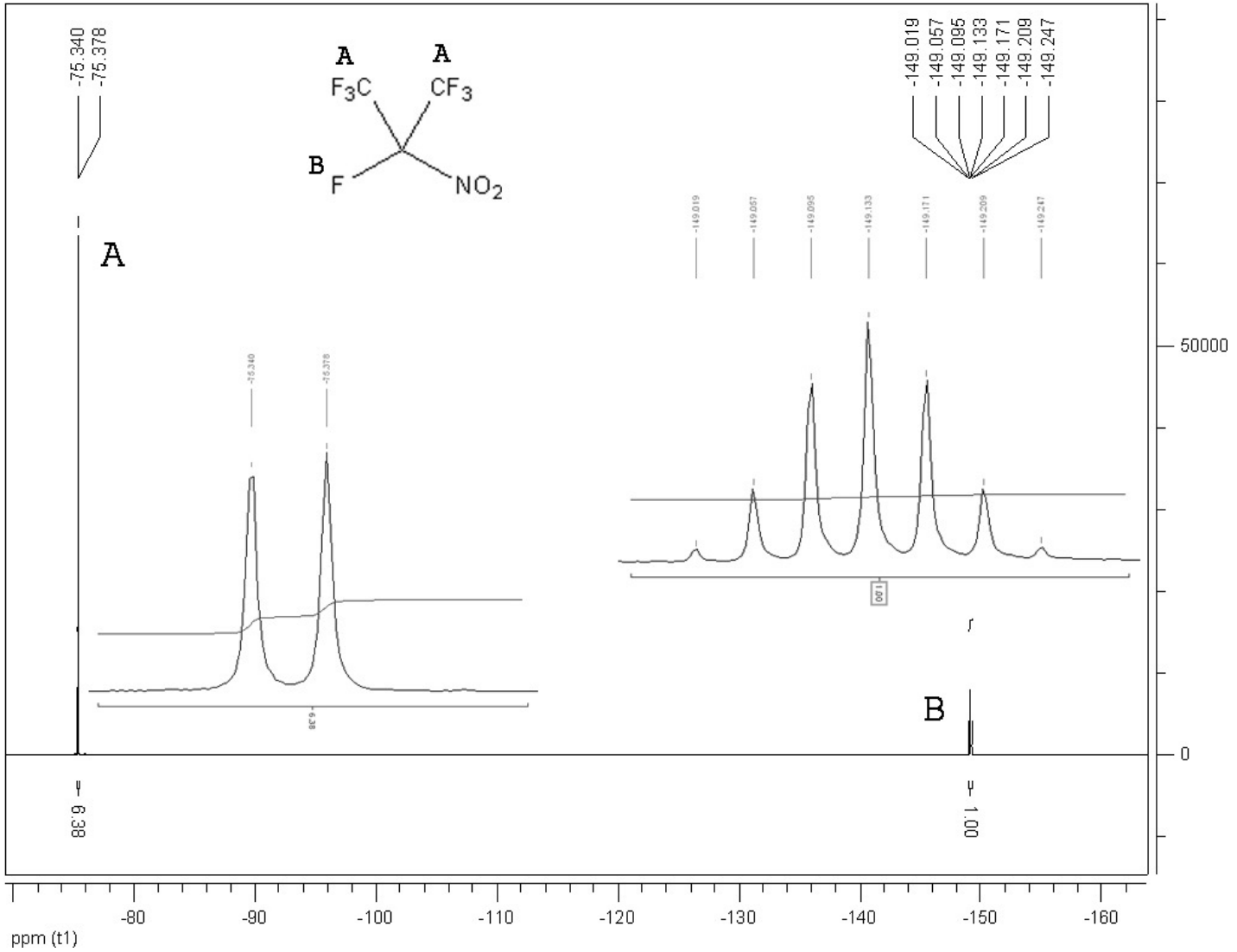

Figure 3.2 **^{19}F-NMR spectrum of 2-nitroheptafluoropropane from reaction in Monel cylinder at 50 °C with 2-iodoheptafluoropropane and ·NO$_2$.**

3.2.7 Preparation of the Kinetic Experiments CF_3NO_2 in Various Materials

With many of the synthetic details worked out for the thermal generation of CF_3NO_2 such as the stoichiometric ratio range, low and high temperatures and a reasonable pressure window, one major area still remains which is the kinetics of the reaction. Some research has been done on the kinetics of $\cdot NO_2$ reacted with the $\cdot CF_3$ radical, see Table 3.6.[3.16-3.24] Unfortunately, none of the experiments are similar experimentally for comparison to the new thermal reaction was were attempted at temperatures between 170-250 °C and pressures ranging from 10-60 atm. The previous kinetic experiments are summarized in Table 3.6 and were preformed at low pressures, ≤1 atm, and low temperatures, ≤27 °C, and the majority is under photochemical conditions, except when noted.

Table 3.6. Summary of Various Kinetic Experiments of $\cdot CF_3 + \cdot NO_2$

Reference	Pressure range (torr)	Rate Constant (10^{-11} cm^3 mol^{-1} s^{-1})	Comments
Rossi *et al.*[3.16]	0.005	0.27 ± 0.05	
Bevilacqua *et al.*[3.22]	0.8-2 (He)	1.0 ± 0.7	
Sehested *et al.*[3.23]	2-10 (Ar/N_2)	1.6 ± 0.3	IR Fluorescence
Pagsberg *et al.*[3.24]	3-17 (Ar)	1.5 ± 0.2	
Hancock *et al.*[3.19]	1.5-110 (Ar/N_2)	1.75 ± 0.26	
Sehested *et al.*[3.23]	760 (SF_6)	2.10 (+0.7)(-0.3)	Pulse Radiolysis
Francisco and Li[3.21]	4-5 (He/Ar)	2.5 ± 0.3	
Oum and Hancock[3.18]	5 (Ar)	2.4 ± 0.5	
Sugawara *et al.*[3.17]	4-20 (Ar)	2.5 ± 0.3	
Vahktin[3.20]	300-600 (He)	3.2 ± 0.7	

Surprisingly, very few of these experiments observed the generation of CF_3NO_2,. Typically, only FNO and COF_2 were observed. Occasionally, the O-bonded CF_3ONO molecule was observed briefly. This lack of formation of CF_3NO_2 is most likely due to the low pressure

that these experiments were performed at or the high energy of the irradiation light. Evidence was found that as the pressure increased, the amount of CF_3NO_2 produced also increased, but this finding was not pursued.[3.17]

Kinetic experiments can be complex especially when the system does not follow true first order kinetics. The kinetic experiment in this research is very basic and a much more detailed set of experiments needs to be performed to get to the exact nature of the kinetics. This research lays down the groundwork for the next set of kinetic research. Many different assumptions have been made in order to set up the experiments described. First, the reaction is assumed to be first order in nature. This is not entirely true since both the O-bonded and N-bonded molecules are both formed. It is unknown if the molecules are formed at different rates or if the molecules split back into their radicals. The increase in yield during the thermal run has led to the hypothesis that an equilibrium is formed between the O-bonded species and its radicals. The N-bonded molecule appears to be stable, not forming an equilibrium. For this reason, the appearance of CF_3NO_2 cannot be used as the variable to monitor for the kinetic experiments. The back reaction of the O-bonded species makes this very difficult. If the kinetics were being investigated in the blue light system, this would not be the case because the equilibrium does not appear to be established under photochemical conditions. Instead, the O-bonded molecule irreversibly decays into COF_2 and FNO. This decay occurs before the equilibrium can be established and the generation of CF_3NO_2 by the one pathway can be measured. Even though this direct measurement is lost, useful information can still be gathered. The major variable that was monitored during this experiment was the disappearance of CF_3I, and an assumption must again be made. In this case, the assumption is that once the C-I bond is broken, it will not be reformed this makes the bond-breaking step the rate limiting step of the reaction. To further eliminate the

chance for an equilibrium to establish itself, the experiments were set up as pseudo-first order with an excess of $\cdot NO_2$. These assumptions will give us insight into the decay rate of CF_3I and a rough estimate of the C-I bond dissociation energy, BDE, which can be compared to the literature values.

Two different kinetic experiments were attempted. The first experiment was not successful but gave insight on how best to set up the second kinetic experiment, as well as pointing out mistakes in the initial set of assumptions. The second experiment investigated the kinetics of $CF_3I + \cdot NO_2$ in a sealed Pyrex® glass NMR tube at temperatures of 170, 185, 200, 215, 230 and 250 °C, while the first experiment explored the kinetics in a stainless steel cylinder at 170, 185 and 200 °C. From the data of the second experiment, the rate constants at the various temperatures and the BDE of CF_3I can be calculated.

The first attempt at a kinetic experiment was set up in a ~2.44-L stainless steel vessel. The vessel was charged with a 3 : 1 ratio of $\cdot NO_2$: CF_3I and placed in an oven at a preset temperature and heated for a predetermined period of time. The cylinder was removed after the set time period, and while still hot, a sample was transferred into a ¼-inch stainless steel tube and sealed by valves at both ends of the sample tube. The isolated sample is added to a glass vessel containing NaOH pellets, which remove the majority of unreacted NO_x compounds. This purified sample was analyzed by GC/FID to determine the ratio of CF_3I to CF_3NO_2. This initial experiment turned out to be more problematic than expected. First, the cylinder requires a long time period to warm up to the set temperature, typically an hour or more. Also, after sampling the cylinder contents, it takes another 20-30 minutes to get back to the set temperature. Second, the system is changed every time a sample is removed. The experiment was set up to minimize this effect, however, every sample removed about 1% of the total mass. This will be a source of

error in the experiment. Unfortunately, the results from this experiment were inconclusive and fit in poorly with previous literature, and a new experiment had to be devised. One useful piece of information was obtained from this experiment. At 150 °C, no reaction took place in stainless steel. The initial thermal experiments at 150 °C contained elemental mercury, and a 3.2 mol% of CF_3NO_2 was converted, suggesting mercury has a slight catalytic effect on the reaction.

To help eliminate the problems observed during the initial kinetic experiments, it was decided to scale the reaction down to the scale of an NMR tube. The experiment was setup in a thick walled NMR tube with known amounts of $\cdot NO_2$ and CF_3I. Sealing the NMR tube eliminates the changes in the stoichiometric ratio and mass. Changes in the generation of CF_3NO_2 will be dependent only on the heat of the system. The major concern with this experiment is the lack of a reference solvent present in the NMR tube for better shimming and more accurate integration. This can be circumvented, to a degree, by shimming on a known solvent, typically D_2O and running a greater number of scans on the kinetic sample. A greater signal-to-noise ratio at the baseline is expected in this experiment due to the lack of a solvent, but a greater number of scans, 128, should help overcome this problem and allow for a decent integration for the desired kinetic calculations. This experiment was also not as pseudo-first order as typical kinetic experiments. The majority of experiments were ~3 : 1. Typically, a 20 : 1 ratio of reactants is needed for true pseudo-first order kinetics. A sacrifice to the ratio had to be made in order to have enough material to detect a peak above the noise of the baseline.

A series of kinetic experiments, at the following temperatures, were run in the NMR tube at 170, 185, 200, 215, 230 and 250 °C. The data forming the straightest line, at least three points, was plotted, and these points are used for determining the rate constant from the slope of these lines. Typically, these points were chosen from the start of the experiment. The rate

constant calculated from the slope was then used in the Arrhenius plot to calculate the BDE of the CF_3I molecule.

3.2.7.1 Initial Kinetic Experiment, Stainless Steel Cylinder

This experiment was set up in a 2.25-L cylinder that contained 69.47 g (1.510 mol) of $\cdot NO_2$ and 151.08 g (774.76 mmol) of CF_3I. The temperature was monitored by a thermocouple taped to the outside of the cylinder. Each sample takes at least 5 minutes of handling outside the oven to collect the sample, and typically, 20-40 minutes were required to get the cylinder surface back up to the set temperature, ±0.5 °C.

3.2.7.1.1 Kinetics at 150 °C in a Stainless Steel Cylinder

No reaction occurred at this temperature, even after ~3 days of reaction. This is contrary to one of the earlier thermal reactions at 150 °C, which had mercury present in the cylinder. This mercury containing reaction saw a 3.2% conversion after ~24 hours.

3.2.7.1.2 Kinetics at 170 °C in a Stainless Steel Cylinder

This experiment was the first temperature where the reaction began to progress forward in the generation of CF_3NO_2. Three samples were taken, and the results are summarized in Table 3.7.

Table 3.7. Kinetics at 170 °C in a Stainless Steel Cylinder

Reaction	Time (sec)	Mol% CF_3I	Mol/L CF_3I	Mol% CF_3NO_2	Mol/L CF_3NO_2
1	26160	96.5	0.306	3.5	0.011
2	63540	88.0	0.280	12.0	0.038
3	87900	92.0	0.292	8.0	0.025

The rate found for this experiment was 5 x 10^{-6} mol * L/sec. There is very poor R^2 in this experiment, and the value holds little significance. At this point, some of the problems of this experiment began to become apparent. A new method needs to be devised.

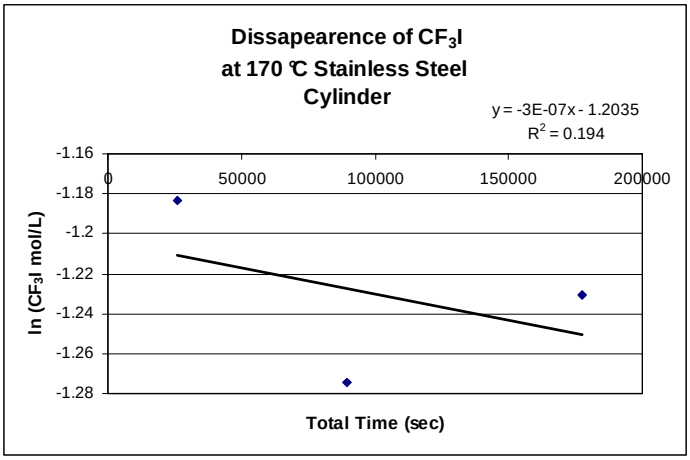

Figure 3.3. Disappearance of CF_3I in 170 °C kinetic experiment, stainless steel cylinder.

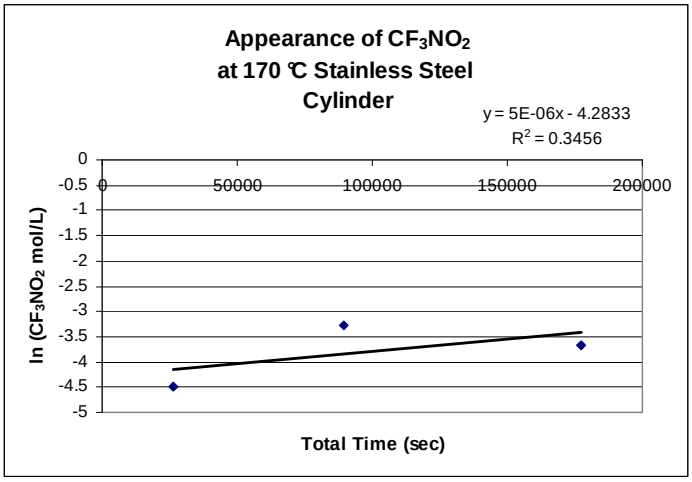

Figure 3.4. Appearance of CF_3NO_2 in 170 °C kinetic experiment, stainless steel cylinder.

Some of the workup procedures were changed after this initial kinetic experiment. This helped achieve better results for the next two kinetic experiments at 185 and 200 °C. The first and most important change was to open the cylinder to the samplings tube with the cylinder standing in an upright position, instead of on its side. This kept any liquid that may be present in the cylinder from entering the sampling tube thus allowing for the samples to come from the more unified gaseous sample, instead of a mixture of liquids. The cylinder was also insulated when removed from the oven with glass wool and cloth.

3.2.7.1.3 Kinetics at 185 °C in a Stainless Steel Cylinder

With the changes made to the procedure, the results for this kinetic experiment were much more successful, but the R^2 factor was still not as high as desired, only ~0.7. Ideally it should be higher than 0.95. The results are summarized in Table 3.8.

Table 3.8. Kinetics at 185 °C in a Stainless Steel Cylinder

Reaction	Time (sec)	Mol% CF_3I	Mol/L CF_3I	Mol% CF_3NO_2	Mol/L CF_3NO_2
1	10260	84.5	0.268	15.5	0.049
2	21300	77.9	0.247	22.1	0.070
3	32040	70.9	0.225	29.1	0.093
4	43260	72.1	0.229	27.9	0.089

The rate constant for this reaction was found to be 6 x 10^{-6} mol * L/sec.

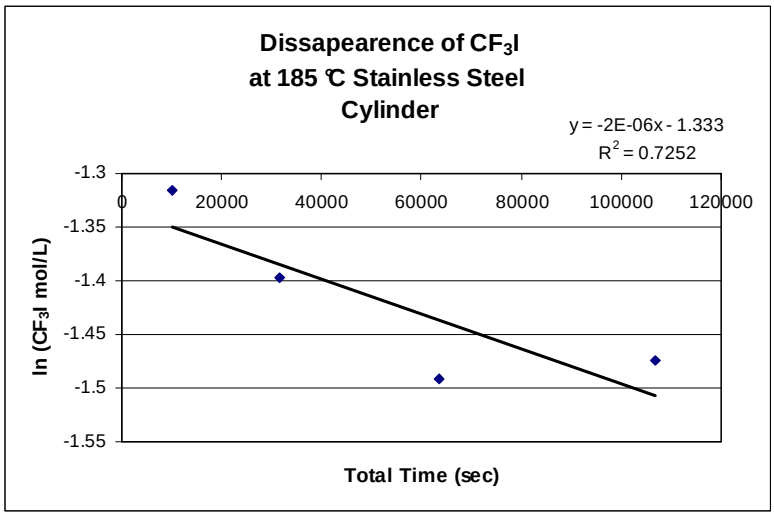

Figure 3.5. Disappearance of CF_3I in 185 °C kinetic experiment, stainless steel cylinder.

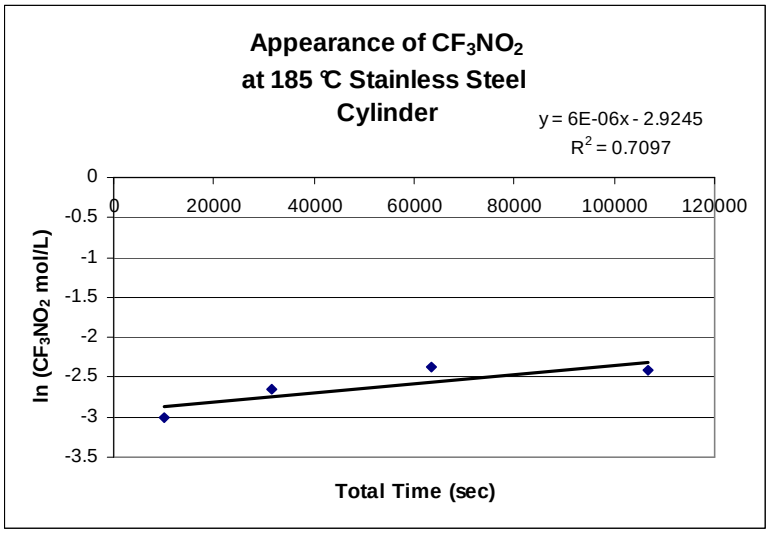

Figure 3.6. Appearance of CF_3NO_2 in 185 °C kinetic experiment, stainless steel cylinder.

3.2.7.1.4 Kinetics at 200 °C in Stainless Steel Cylinder

For this experiment, the best R^2 values were achieved using the stainless steel cylinder. The results from this experiment are slower than those found in the glass kinetic experiments. The results are summarized in Table 3.9.

Table 3.9. Kinetics at 200 °C in a Stainless Steel Cylinder

Reaction	Time (sec)	Mol% CF_3I	Mol/L CF_3I	Mol% CF_3NO_2	Mol/L CF_3NO_2
1	6360	76.5	0.243	23.5	0.075
2	19320	62.5	0.198	37.5	0.119
3	30600	53.5	0.170	46.5	0.148

The rate for this reaction was found to be 1 x 10^{-5} mol * L/sec.

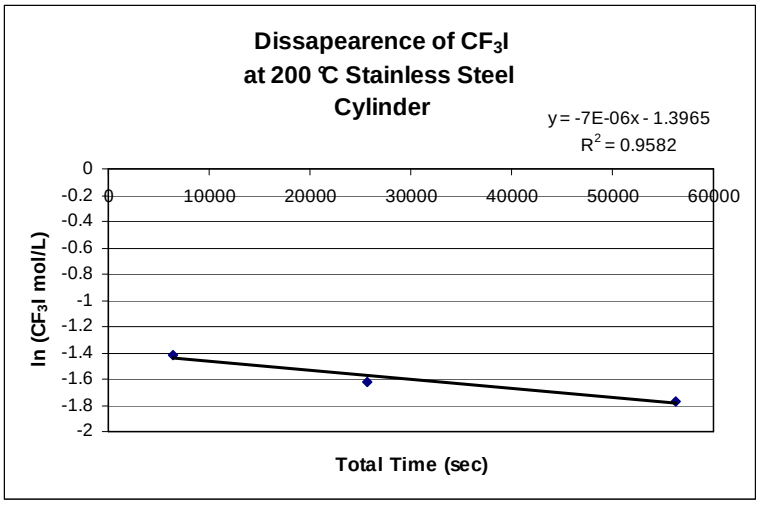

Figure 3.7. Disappearance of CF_3I in 200 °C kinetic experiment, stainless steel cylinder.

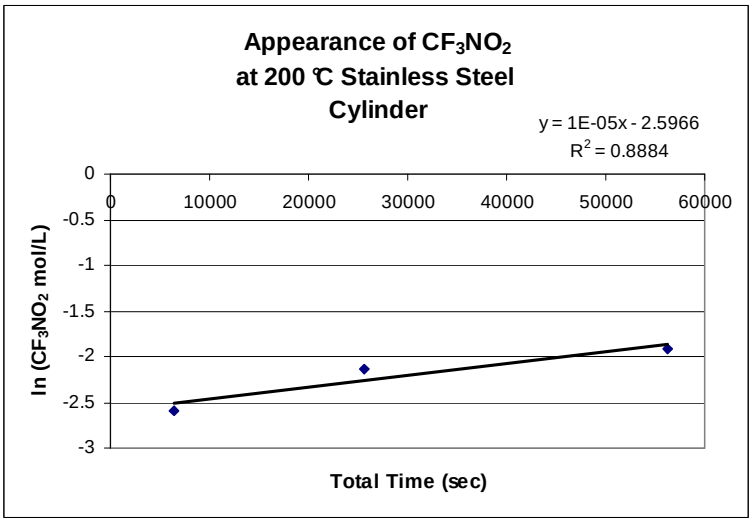

Figure 3.8. Appearance of CF_3NO_2 in 200 °C kinetic experiment, stainless steel cylinder.

These kinetic data points, Table 3.10, when plotted on a Arrhenius Plot, Figure 3.9, gave deceptively good results with a high $R^2 = 0.92$. It must be remembered that the first point, at 170 °C, is very suspect. The fact that it lines up well with the other two is more of a coincidence than anything else. Also, when looking at the results, the dissociation energy of CF_3I,

Table 3.12, or the E_a from the Arrhenius plot is extremely low, 9.61 kcal/mol, the accepted value is around 53 kcal/mol.[3.3] This large difference confirms the shortcomings of this kinetic experiment and points out the necessity for a different experimental setup.

The lowering of activation energy may be due to a catalytic effect from the stainless steel, but this is difficult to tell from the poor results. The surface area in this cylinder is also an important factor to take into account. The inside surface of the cylinder will continually change as the surface is oxidized by the $\cdot NO_2$ and any $\cdot F$ radicals are formed by the generation of FNO. As the surface reacts with the various oxidizers, the active areas will be deactivated but may be reactivate as the surface flakes. Many inorganic flakes are recovered in these thermal reactions in stainless steel. If catalysis is occurring in this kinetic experiment, this is an undesirable result. A bond dissociation energy that can be compared to the previous kinetic experiment is desired for comparison reasons.

Table 3.10. Summary of Kinetic Experiments in Stainless Steel Cylinder

Experiment	Disappearance of CF_3I (mol/L * sec)	Appearance of CF_3NO^2 (mol/L * sec) k_1	Factor (CF_3NO_2/CF_3I)	Half Life ($t_{1/2}$) (sec)
170 °C	**-3×10^{-7}**	**5×10^{-6}**	**16.66**	**138629**
185 °C	**-2×10^{-6}**	**6×10^{-6}**	**3**	**115524**
200 °C	**-7×10^{-6}**	**1×10^{-5}**	**1.43**	**69314**

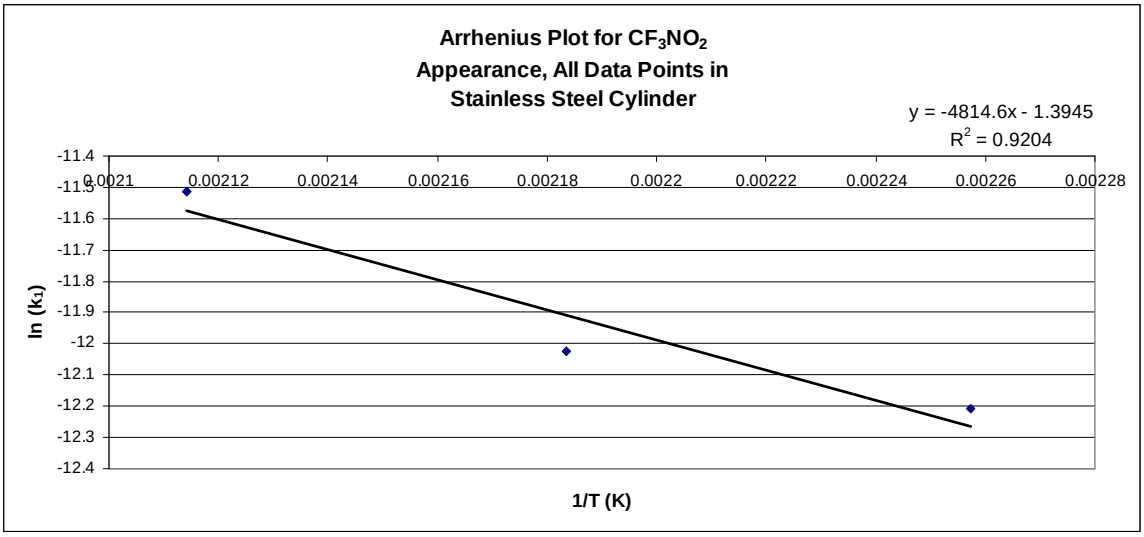

Figure 3.9. Arrhenius plot for all kinetic experiments in stainless steel cylinder, CF_3NO_2 appearance.

Table 3.11. Summary of Data for Plotting Arrhenius Plot of Kinetic Experiments Carried Out in Stainless Steel

Experiment	k	ln k	T (K)	1/T (K)
170 °C	5×10^{-6}	-12.206	443	0.00226
185 °C	6×10^{-6}	-12.024	458	0.00218
200 °C	1×10^{-5}	-11.513	473	0.00211

Table 3.12. Summary of Parameters from the Arrhenius Plot of the Data from All of the Kinetic Experiments Carried Out in Stainless Steel

Plot	Equation	X = 0 Intercept (ln A)	A	Slope (Ea/R)	E_a (kJ/mol)	E_a (kcal/mol)
All Points CF_3NO_2	**y =-4814.6 x – 1.3948**	**-1.3945**	**2.47×10^{-1}**	**-4814.6**	**40.02**	**9.61**

Ideally, for all of these kinetic experiments, more sampling would have been advantageous. However, each sample takes ~1% of the total mass of the system. This will have a small but definite effect on the equilibrium of the system. The more samples taken, the greater the opportunity for changes in the kinetics. Also, each gas in the system, CF_3I, CF_3NO_2, $\cdot NO_2$ and other NO_x compounds, has a different vapor pressure curve. At the given temperatures, the amount of each gas in the vapor phase will vary, unless the temperature is greater than the critical temperature for all the gasses. CF_3I has a critical temperature of 123.44 °C.[3.25] For CF_3NO_2, the critical point is unknown, and if it is significantly higher, problems can occur with the measurements. If CF_3I and CF_3NO_2 are not completely in the gaseous phase, a drastic effect can be had on the ratio of the gasses in the sample tube. This is not an issue for the NO_x compounds, since they are not being monitored by ^{19}F-NMR spectroscopy. The difference in the critical temperatures of CF_3NO_2 and CF_3I may be significant because the temperature of the system can only be monitored on the skin surface. How quickly the internal temperature falls while sampling is unknown. It is possible that by the time a sample is taken, CF_3I, CF_3NO_2 or both gasses have fallen below their critical temperature upsetting the results.

Too many factors and questions are present with the kinetic experiment using the stainless steel reaction vessel. A new approach is needed that would avoid the shortcomings of the stainless steel cylinder kinetic experiment, which includes possible changes in concentrations for each sample, loss of mass upon each sample and lengthy heating and reheating times during sampling warm up and cool down. This led to the new kinetic experiments being performed in the thick-walled NMR tubes. The NMR tubes eliminate all of the previous shortcomings while only one major issue is created, the monitoring of the gaseous samples by ^{19}F-NMR spectroscopy,

3.2.7.2 Kinetics in Glass NMR Tubes

Upon determining that the stainless steel kinetic experiment was not suitable for gathering useful kinetic results, a new system was devised using thick walled NMR tubes. Many of the major experimental problems found during the stainless steel experiments were eliminated with the change to the sealed NMR system including changes to the sample makeup, changes to the system materials and slow heating and cooling of the sample between NMR measurements. Several disadvantages of this experimental approach include the relatively low concentration of sample in the NMR tube, the lack of a deuterium-containing solvent for locking and shimming the NMR spectrometer, and the loss of true pseudo-first order conditions. The signal-to-noise ratio of the baseline is relatively large, which makes an exact integration more difficult than with a typical NMR spectrum, but this can be overcome by line broadening the spectrum and taking more scans. This is one of the major sources of error for this experiment.

3.2.7.2.1 Kinetics at 170 °C in Glass NMR Tube

This was the first kinetic experiment attempted; a 3.25 : 1 ratio of $\cdot NO_2$: CF_3I (0.0147 g $\cdot NO_2$, 0.0192 g CF_3I) was added to the NMR tube and sealed under vacuum at -196 °C. The NMR tube was placed in a preheated protective metal cylinder in the oven at 170 °C and heated. The sample was removed from the oven and its protective container and allowed to cool. Transfer takes ~15 seconds, while cooling takes ~30 seconds. Once cooled, the reaction progress is investigated by ^{19}F-NMR spectroscopy. The results are shown in Table 3.13.

Table 3.13. Kinetics in Glass at 170 °C

Reaction	Time (sec)	Mol% CF_3I	CF_3I (Mol/L)	Mol% CF_3NO_2	CF_3NO_2 (Mol/L)
1	23280	100	0.134	0	0
2	83280	100	0.134	0	0
3	413700	90.1	0.121	9.9	0.013
4	836100	69.5	0.093	30.7	0.041
5	1164900	38.6	0.052	61.4	0.082
6	1640700	16.1	0.022	83.9	0.113

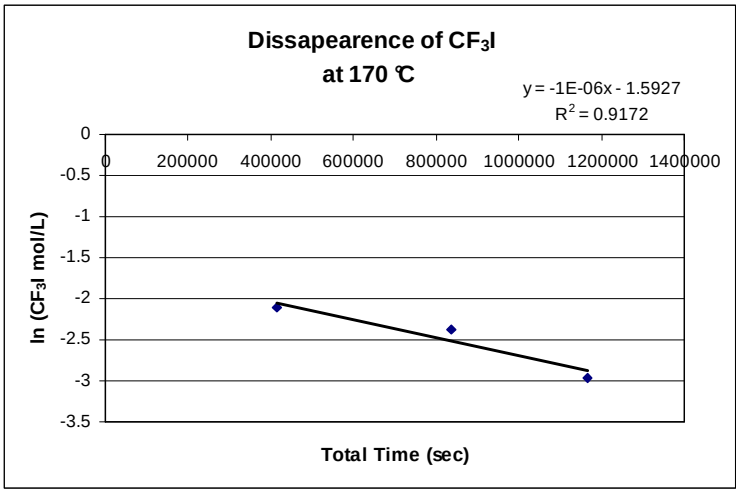

Figure 3.10. Disappearance of CF_3I in 170 °C kinetic experiment.

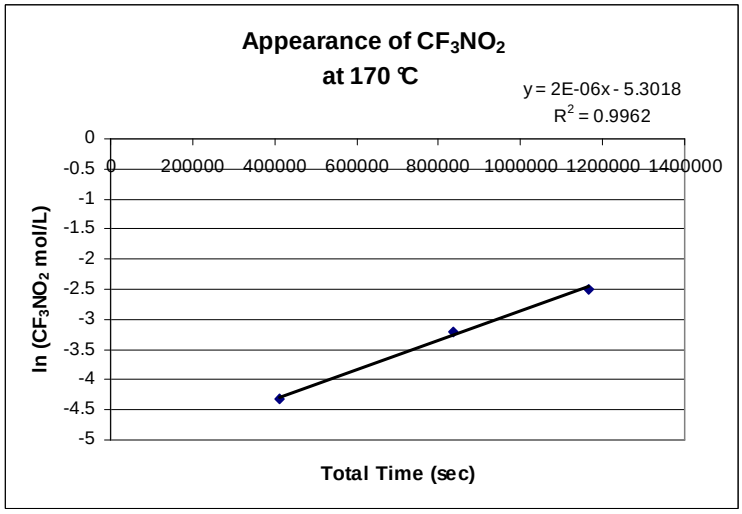

Figure 3.11. Appearance of CF_3NO_2 in 170 °C kinetic experiment.

The rate of the disappearance is determined by the slope and is 1 x 10^{-6} mol/L * sec. The addition of $\cdot NO_2$ and CF_3I in these very small amounts to the NMR tube is very difficult. Multiple transfers into a pre-weighed cylinder had to be performed in order to approach the desired addition amounts of reactants for adding into the NMR tube. A new method was developed for all the following kinetic experiments

3.2.7.2.2 Kinetics at 185 °C in Glass NMR Tube

This experiment was prepped differently from the 170 °C run, and this procedure was used for all the remaining kinetic experiments and is described in the Experimental section. The results for this experiment are summarized in Table 3.14.

Table 3.14. Kinetics in Glass at 185 °C

Reaction	Time (sec)	Mol% CF_3I	Mol/L CF_3I	Mol% CF_3NO_2	Mol/L CF_3NO_2
1	166860	17.0	0.063	83.0	0.306
2	249540	4.1	0.015	95.9	0.353
3	313140	1.0	0.004	99.0	0.365

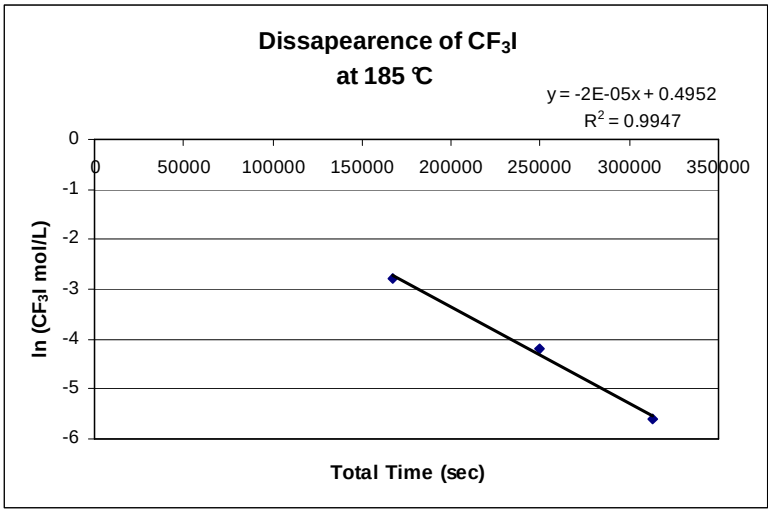

Figure 3.12. Disappearance of CF_3I in 185 °C kinetic experiment.

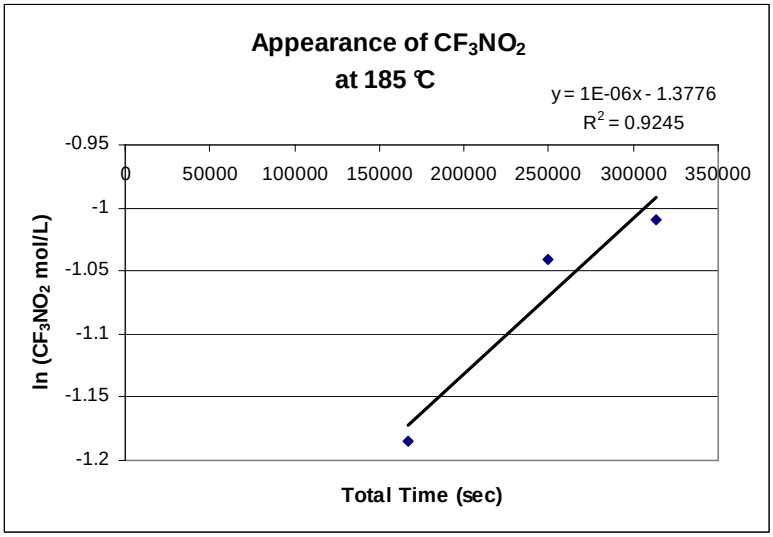

Figure 3.13. Appearance of CF_3NO_2 in 185 °C kinetic experiment.

The rate of disappearance for this experiment was 2 x 10^{-5} mol/L * sec.

3.2.7.2.3 Kinetics at 200 °C in Glass NMR Tube

This experiment was attempted twice because the data from the first experiment did not fit the Arrhenius plot well, and the rate of CF_3NO_2 appearance was faster for the 200 °C experiment than the 215 °C experiment. Possible reasons for this difference will be discussed below. In both experiments, the rate constants found were very similar, but unfortunately, they were both faster than the 215 °C experiments. Also, the appearance of CF_3NO_2 was faster than the disappearance of CF_3I by a x2.5 and x11. For this reason, these results where discarded when setting up the final Arrhenius plot. The results are summarized in Tables 3.15 and 3.16.

Table 3.15. Kinetics in Glass at 200 °C, Experiment 1

Reaction	Time (sec)	Mol% CF_3I	Mol/L CF_3I	Mol% CF_3NO_2	Mol/L CF_3NO_2
1	7380	95.5	0.312	4.5	0.015
2	12720	84.6	0.276	15.4	0.050
3	18120	69.7	0.227	30.3	0.099
4	23640	53.2	0.174	46.8	0.153

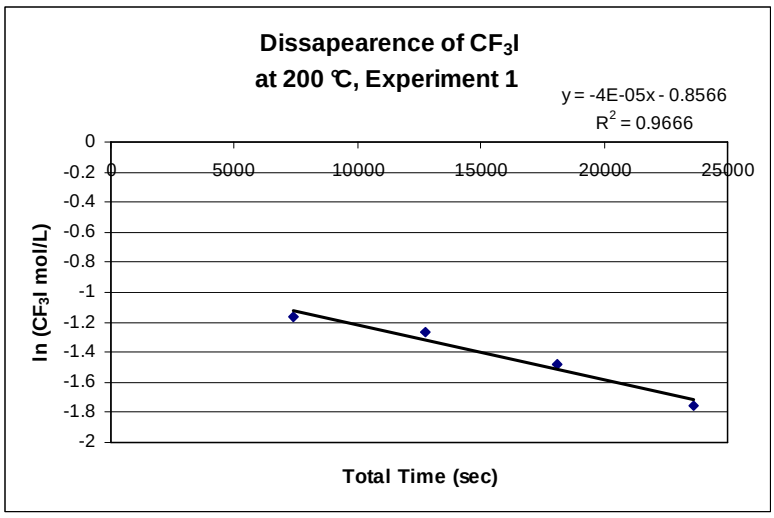

Figure 3.14. Disappearance of CF_3I in 200 °C kinetic experiment 1.

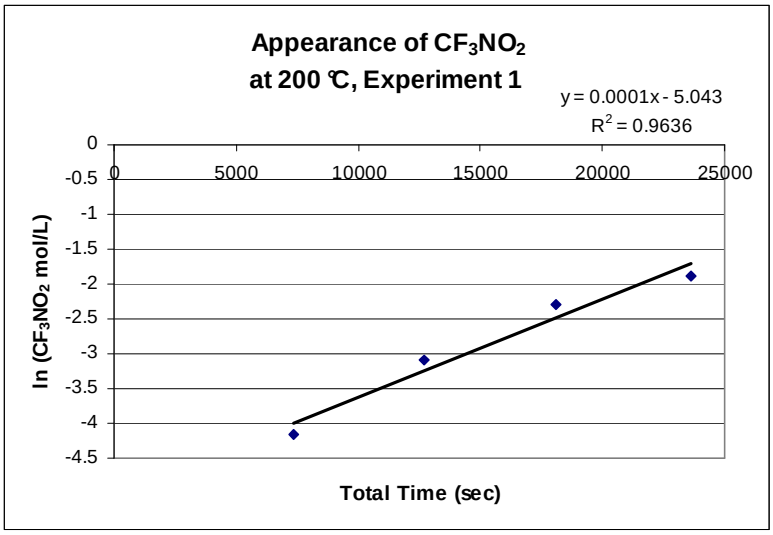

Figure 3.15. Appearance of CF_3NO_2 in 200 °C kinetic experiment 1.

The rate of disappearance of CF_3I for this Experiment is 4 x 10^{-5} mol/L * sec.

Table 3.16. Kinetics in Glass at 200 °C, Experiment 2

Reaction	Time (sec)	CF_3I (Mol%)	CF_3I (Mol/L)	CF_3NO_2 (Mol%)	CF_3NO_2 (Mol/L)
1	1560	100	0.099	0	0
2	3540	99.5	0.099	0.5	0.0005
3	6660	97.5	0.097	2.5	0.002
4	9780	93.9	0.093	6.1	0.006
5	12300	89.8	0.089	10.2	0.010

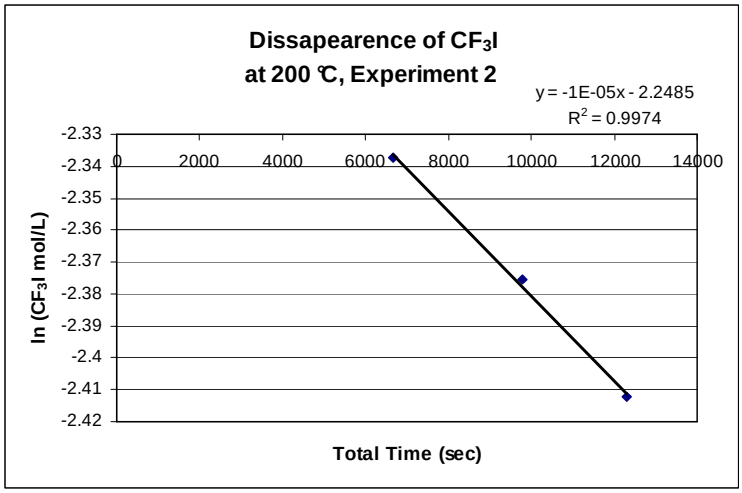

Figure 3.16. Disappearance of CF_3I in 200 °C kinetic experiment 2.

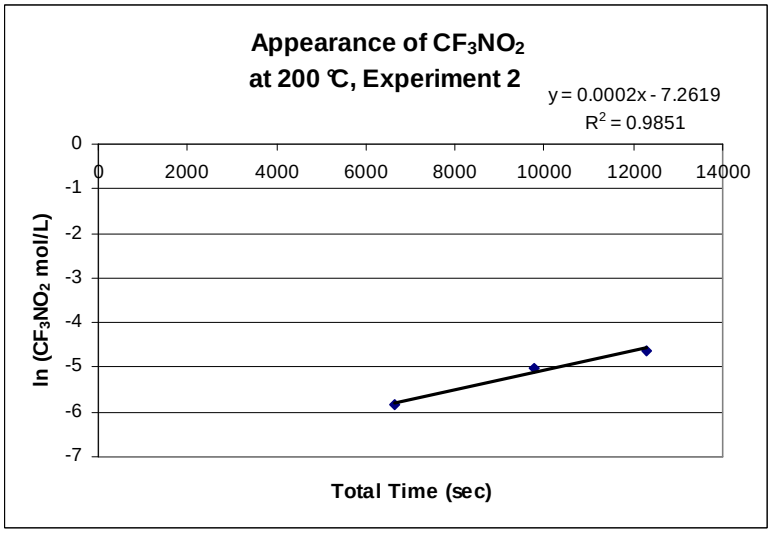

Figure 3.17. Appearance of CF_3NO_2 in 200 °C kinetic experiment 2.

The rate of disappearance of CF_3I for this experiment is 1×10^{-5} mol/L * sec

3.2.7.2.4 Kinetics at 215 °C in Glass in Glass NMR Tube

The results for this reaction are summarized in Table 3.17.

Table 3.17. Kinetics in Glass at 215 °C

Reaction	Time (sec)	CF_3I (Mol%)	CF_3I (Mol/L)	CF_3NO_2 (Mol%)	CF_3NO_2 (Mol/L)
1	10800	37.9	0.111	62.1	0.182
2	16200	13.5	0.040	86.5	0.254
3	18060	10.0	0.029	90.0	0.264
4	19920	6.6	0.020	93.3	0.274

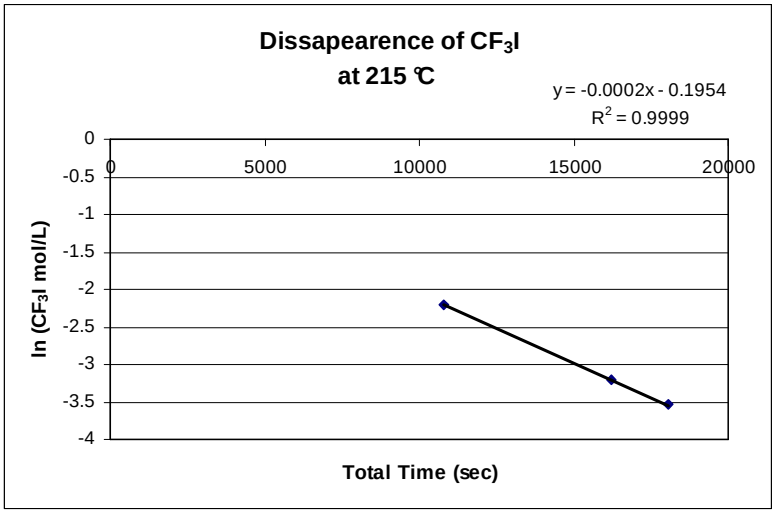

Figure 3.18. Disappearance of CF_3I in 215 °C kinetic experiment.

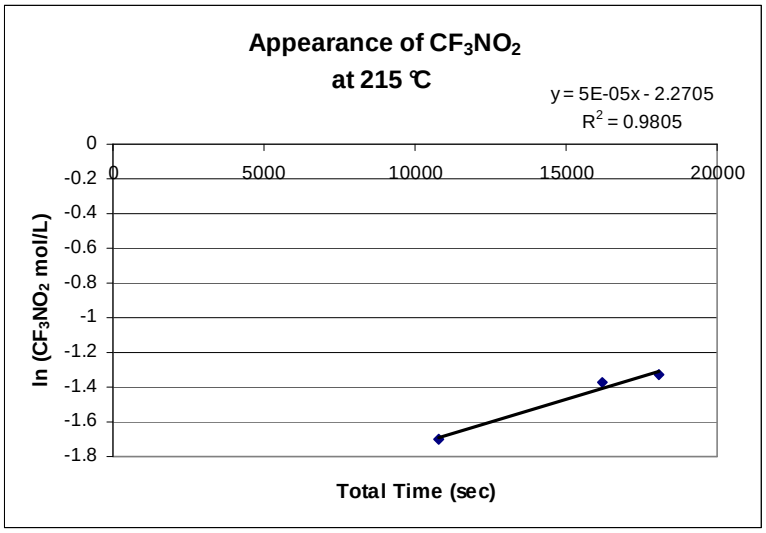

Figure 3.19. Appearance of CF_3NO_2 in 215 °C kinetic experiment.

The rate of disappearance for this experiment was 2 x 10^{-4} mol/L * sec.

3.2.7.2.5 Kinetics at 230 °C in Glass NMR Tube

This experiment was done twice in an attempt to get a better fit for the Arrhenius plot. The result from Experiment 2 was discarded for the final Arrhenius plot because the rate of CF_3I disappearance was much less, x11, than the appearance of CF_3NO_2. The results for these reactions are summarized in Tables 3.18 and 3.19.

Table 3.18. Kinetics in Glass at 230 °C Experiment 1

Reaction	Time (sec)	Mol% CF_3I	Mol/L CF_3I	Mol% CF_3NO_2	Mol/L CF_3NO_2
1	1560	88.2	0.098	11.8	0.013
2	3360	47.3	0.052	52.7	0.058
3	5160	14.6	0.016	85.4	0.094
4	6960	3.4	0.004	96.6	0.107

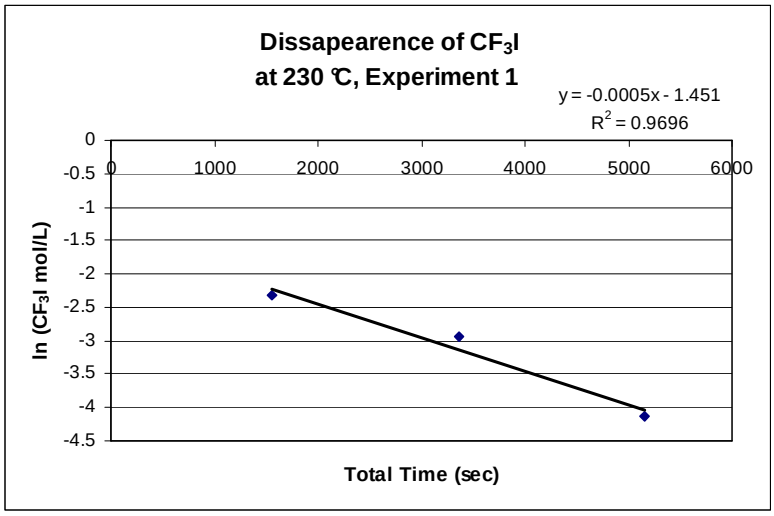

Figure 3.20. Disappearance of CF_3I in 230 °C kinetic experiment 1.

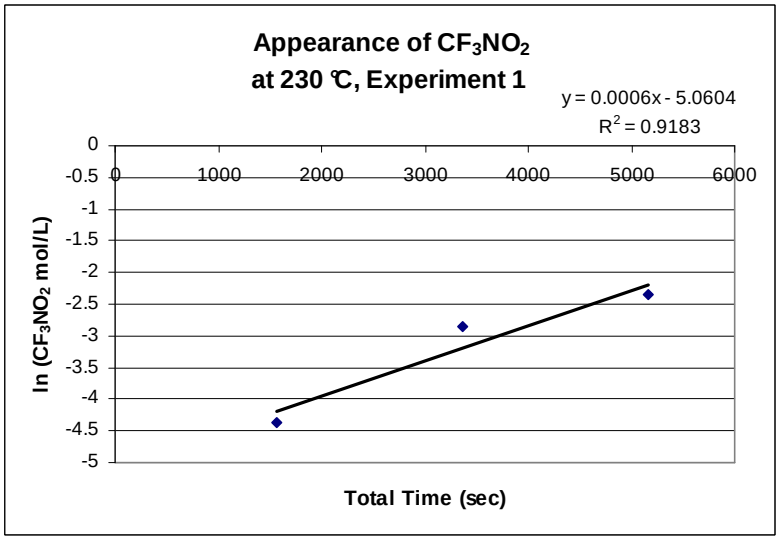

Figure 3.21. Appearance of CF_3NO_2 in 230 °C kinetic experiment 1.

The rate of disappearance for the experiment is 5×10^{-4} mol/L * sec.

Table 3.19. Kinetics in Glass at 230 °C Experiment 2

Reaction	Time (sec)	CF_3I (Mol%)	CF_3I (Mol/L)	CF_3NO_2 (Mol%)	CF_3NO_2 (Mol/L)
1	300	100	0.091	0	0
2	600	99.7	0.090	0.3	0.0003
3	900	99.3	0.090	0.7	0.0007
4	1320	97.2	0.088	2.8	0.003
5	1740	94.9	0.086	5.1	0.005
6	2160	90.9	0.082	9.1	0.008
7	2580	86.0	0.078	14.0	0.013
8	3060	78.6	0.071	21.4	0.019
9	3480	72.2	0.065	27.8	0.025

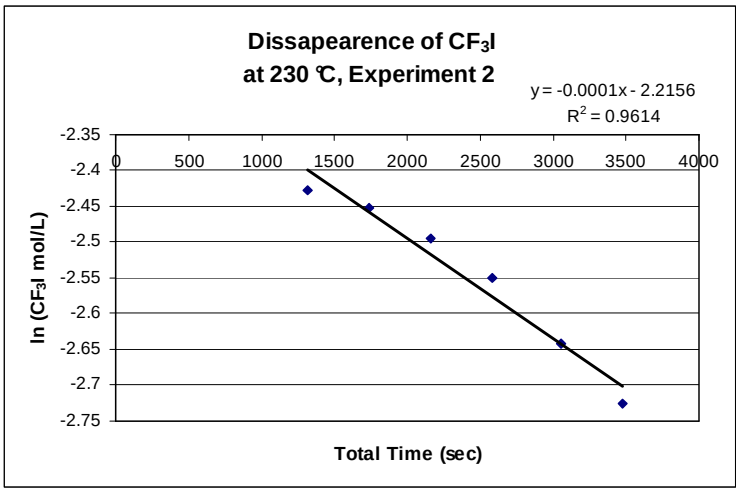

Figure 3.22. Disappearance of CF_3I in 230 °C kinetic experiment 2.

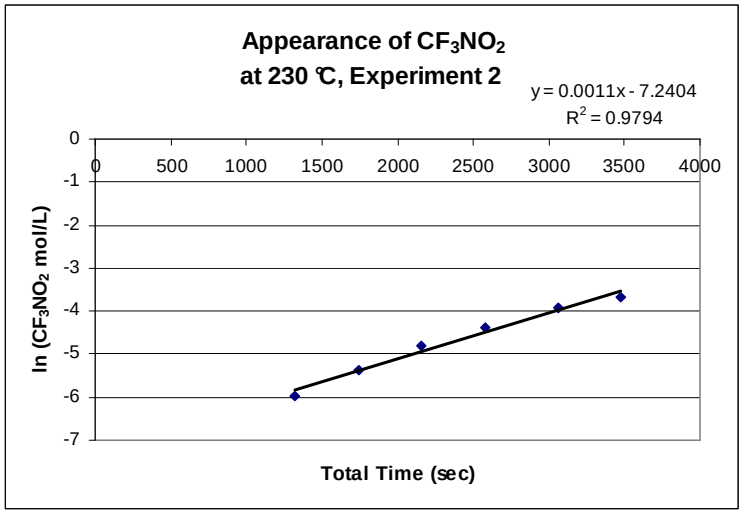

Figure 3.23. Appearance of CF_3NO_2 in 230 °C kinetic experiment 2.

The rate of disappearance for this experiment is 1 x 10^{-4} mol/L * sec.

3.2.7.2.6 Kinetics at 250 °C in Glass NMR Tube

This experiment was set up in a NMR tube with a 10.64% concentration of CF_3NO_2, which was generated previously in the 200 °C Experiment 2. This value was subtracted from all the results shown in Table 3.20.

Table 3.20. Kinetics in Glass at 250 °C Experiment

Reaction	Time (sec)	CF_3I (Mol%)	CF_3I (Mol/L)	CF_3NO_2 (Mol%)	CF_3NO_2 (Mol/L)
0	0	89.4	0.081	10.6	0.010
1	300	87.3	0.079	12.7	0.012
2	600	71.4	0.065	28.6	0.026
3	900	53.8	0.049	46.2	0.042
4	1200	39.8	0.036	60.2	0.055
5	1500	29.4	0.027	70.6	0.064

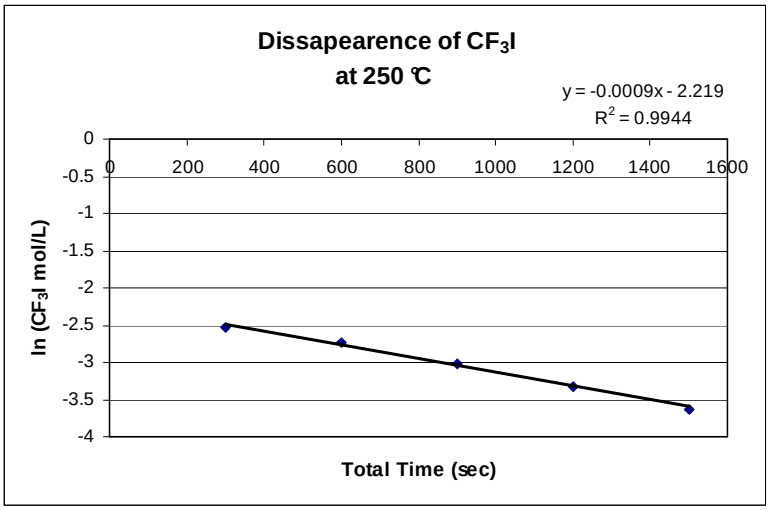

Figure 3.24. Disappearance of CF_3I in 250 °C kinetic experiment 1.

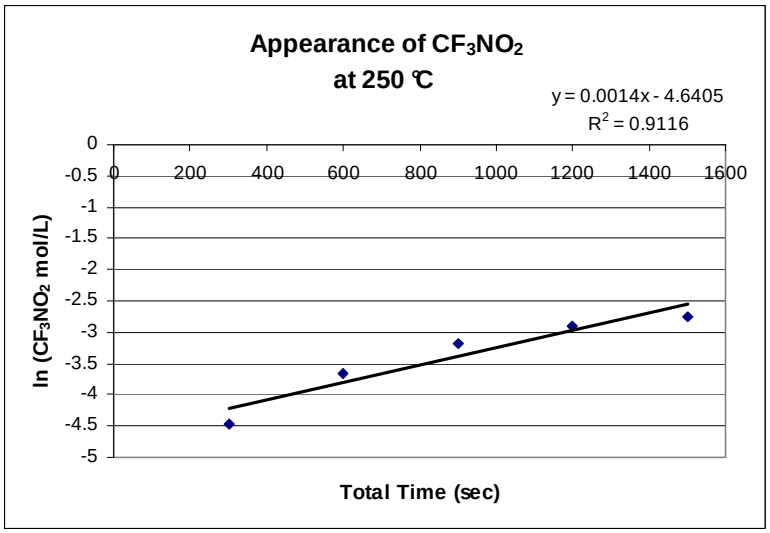

Figure 3.25. Appearance of CF_3NO_2 in 250 °C kinetic experiment 1.

The rate of disappearance of CF_3I for this reaction is 9×10^{-4} mol/L * sec.

3.2.7.2.7 Summary of Glass NMR Kinetic Results

The results of all the kinetic experiments are summarized in Table 3.21. The experiment was set up as close to a pseudo first order reaction as the equipment would allow. The excess of the non-limiting starting reagent, $\cdot NO_2$, was ~3 : 1, not the typical 20 : 1, due to the limits of NMR detection. Most of the data received fits the first order kinetics in the expected manner, linear rate lines, etc. The proposed mechanism does not support CF_3NO_2 appearing faster than the disappearance of CF_3I. So, any of the experiments with a "factor" (rate of appearance CF_3NO_2/rate of disappearance of CF_3I) that is much greater than 1 is suspect, and many of these points were removed from the final Arrhenius plot. Some reasons for this abnormality will be discussed below. The three experiments that have the worst "factor" are both of the 200 °C experiments and the 230 °C Experiment 2. Several of the experiments have "factors" slightly above 1 and these include the 170 °C, 230 °C and the 250 °C experiments, but they were determined to be within the error of the experiment and retained. The cause of this error requires some explaining. In order to get useful data, more kinetic experiments had to be eliminated than expected to get a linear Arrhenius plot.

First, only 8 experiments were performed in this kinetic study. This is not enough experiments to get more than an estimate for the BDE of the reaction. The error for the final calculated value will be somewhere between 5-10 kcal/mol. Each temperature value should be repeated at least five to ten times before the error can be brought down and more definite trends can be seen. Without this larger set of data points, the possible sources of error can have a dramatic effect on the results. The final best fit data matched the literature values, but only 3 of the 8 points were used to calculate this value. When all 8 values were used, the results began to

drift further from the expected results. These experiments must be taken for what they are, an experimental starting point to much larger kinetic experiment.

There are many factors that can cause the rate of the CF_3I disappearance to be slower than the appearance of CF_3NO_2. If enough runs were performed, this should average out many of these errors, and this trend would not be observed. First, the surface area of the NMR tube may be having an effect on the reaction. During the reaction, FNO is generated and will react with the glass, which will consume $\cdot NO_2$ as discussed in Chapter 2. The amount of starting material does vary slightly in each sealed tube, and it is likely that the NMR tubes with more material in the system keeps its pseudo-first order kinetics better than in the tube will less starting material. Also, the fact that there is only a 3 : 1 ratio, not the typical 20 : 1, means that removal of $\cdot NO_2$ by the glass makes these experiments even less pseudo-first order than it already is. The surface condition of the inside of the NMR tube is changing by handling between runs. The NMR tubes are sealed and cut open for use in another run. This changes the length, internal volume and surface area of each tube which has an effect on each subsequent run. The more surface there is, the greater the possibility for a side reaction and an unwanted consumption of $\cdot NO_2$.

Second, the NMR experiment has its own set of issues such as the lack of a lock solvent, the paramagnetic nature of $\cdot NO_2$ and the difference in relaxation rates of CF_3NO_2 and CF_3I which will all have an effect on the baseline noise. The nosier the baseline, the more difficult getting a consistent integration becomes.

The relaxation rate variable can be corrected, if necessary. A T_1 relaxation experiment is easily done on the NMR instrument and will confirm if the molecules have enough time to relax back to their non-excited state during the NMR experiment. If the molecules do not reach their

non-excited state before the next NMR pulse, then the integration will be thrown off. Especially, if one molecule reaches its relaxed state while the other has not. The T_1 relaxation experiment gave the following relaxation time for the two molecules. The CF_3I had a T_1 value of 1.44 ms, while CF_3NO_2 had a T_1 value of 2.88 ms. All of the kinetic experiments had relaxation times of 2 or 6 seconds, giving the molecules plenty of time to reach their relaxed state. This experiment eliminates the relaxation variable as a source of error. Unfortunately, many of the other variables could not be completely eliminated.

The results from the kinetic experiments are shown in Table 3.21, and this information was used to calculate the Arrhenius plots, see Figures 3.26-3.28. From the rate constants, the half-lives of the various kinetic reactions can also be calculated. The formula for the half-life of a first order reaction $t_{1/2} = (\ln 2)/k_1$.

In Figure 3.26, all experiments are plotted, and a linear trend can be observed, but the fit is not as high as desired, $R^2 = 0.87$. The Arrhenius formula for this plot, which fits the expression $k_1 = A \exp(-E_a/RT)$ is shown in Equation 3:

$$k_1 = 1.62 \times 10^{12} \exp(-18277\ K/T)\ cm^3\ mol^{-1}\ s^{-1} \qquad \text{(Eq. 3)}$$

The removal of the experiments at 185 °C, 200 °C experiment 2 and 230 °C experiment 2 produced an Arrhenius plot, Equation 4, with a substantial increase in the $R^2 = 0.96$, and this is summarized in Figure 3.27. These points are removed because the ratio or appearance of CF_3I to CF_3NO_2 is 4 or greater.

$$k_1 = 1.38 \times 10^{14} \exp(-20335\ K/T)\ cm^3\ mol^{-1}\ s^{-1} \qquad \text{(Eq. 4)}$$

Table 3.21. Summary of Kinetic Experiments

Experiment	Disappearance of CF_3I (mol/L * sec)	Appearance of CF_3NO^2 (mol/L * sec) k_1	Factor (CF_3NO_2/CF_3I)	Half Life ($t_{1/2}$) (sec)
170 °C	-1×10^{-6}	2×10^{-6}	0.5	346573
185 °C	-2×10^{-5}	1×10^{-6}	20	693147
200 °C, Experiment 1	-4×10^{-5}	1×10^{-4}	0.4	6931
200 °C, Experiment 2	-1×10^{-5}	2×10^{-4}	0.5	3465
215 °C	-2×10^{-4}	5×10^{-5}	4	13862
230 °C Experiment 1	-5×10^{-4}	6×10^{-4}	0.45	1155
230 °C Experiment 2	-1×10^{-4}	1.1×10^{-3}	0.17	630
250 °C	-9×10^{-4}	1.4×10^{-3}	0.64	495

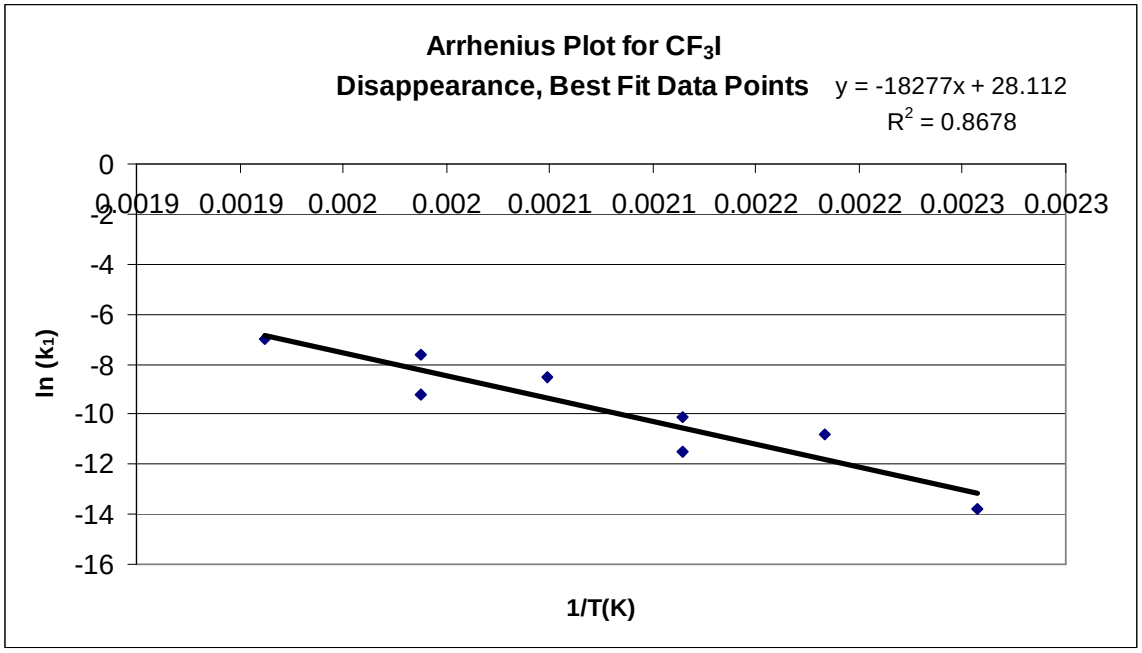

Figure 3.26. Arrhenius plot for all kinetic experiments, CF_3I disappearance.

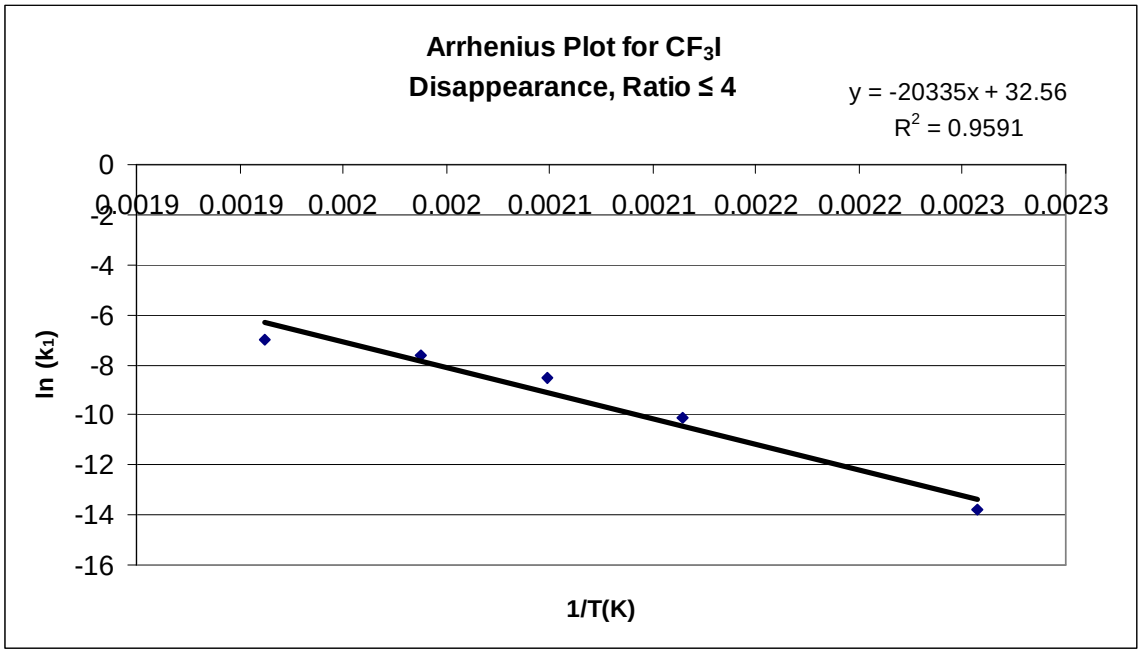

Figure 3.27. Arrhenius plot for best-fit data, CF_3NO_2 appearance.

If all the experiments are removed with the exception of the 170 °C, 200 °C experiment 1 and 230 °C experiment 1 data, an excellent linear line is formed with an $R^2 = 0.995$. These points are the best possible fit from all the experiments, and no other set of points has a linear fit as good as these three points, see Figure 3.28. The points chosen have the closest 1 : 1 ratio of appearance to disappearance of CF_3I : CF_3NO_2. The Arrhenius formula for these points is shown in Equation 5.

$$k_1 = 5.47 \times 10^{16} \exp(-23140\ K/T)\ cm^3\ mol^{-1}\ s^{-1} \qquad \text{(Eq. 5)}$$

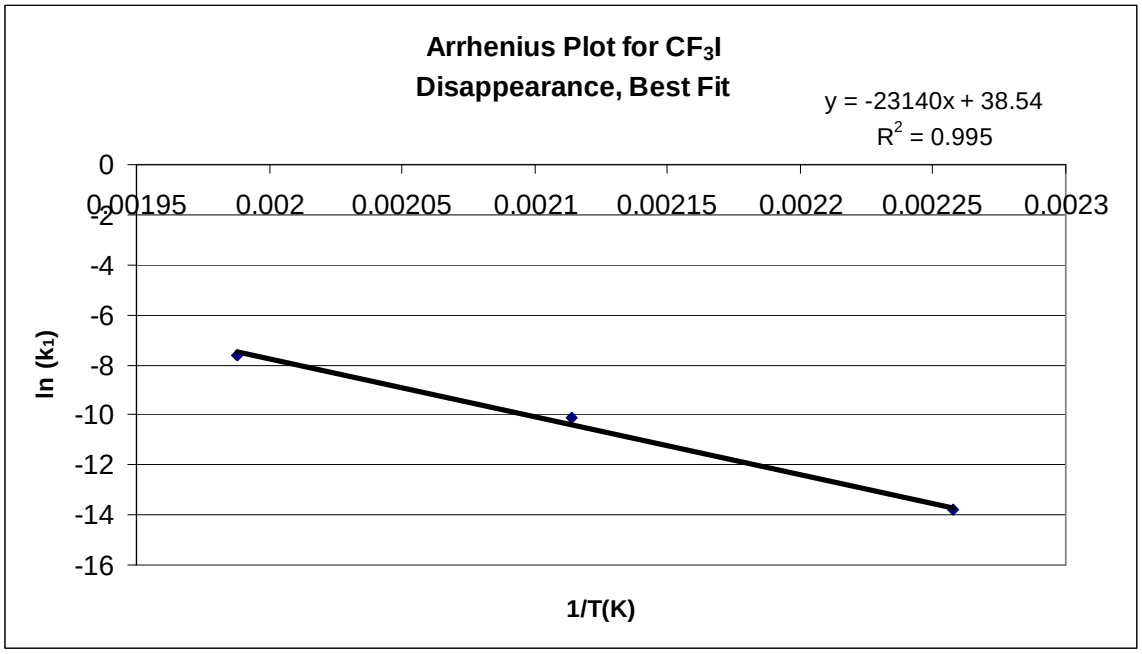

Figure 3.28. Arrhenius plot for best-fit data, 3 experiments, CF_3NO_2 appearance.

The data from the three Arrhenius plots are summarized and compared in Tables 3.22 and 3.23

Table 3.22. Summary of Arrhenius Plots

Experiment	k	ln k	T (K)	1/T (K)
170 °C	x 10^{-6}	-13.815	443	0.00226
185 °C	2 x 10^{-5}	-10.820	458	0.00218
200 °C Experiment 1	4 x 10^{-5}	-10.127	473	0.00211
200 °C Experiment 2	1 x 10^{-5}	-11.513	473	0.00211
215 °C	2 x 10^{-4}	-8.517	488	0.00205
230 °C Experiment 1	5 x 10^{-4}	-7.601	503	0.00199
230 °C Experiment 2	1 x 10^{-4}	-9.210	503	0.00199
250 °C	9 x 10^{-4}	-7.013	523	0.00191

From the Arrhenius plots, two important pieces of information can be determined, the activation energy of the system and if the transition state is similar to the reactants or the product. The key values are calculated in Table 3.23. They are A, which provides insight into the transitions state and E_a, which is the activation energy or bond dissociation energy of the system.

Table 3.23. Summary Table of Arrhenius Plots

Plot	Equation	X = 0 Intercept (ln A)	A	Slope (Ea/R)	E_a (kJ/ mol)	E_a (kcal/ mol)
All Points CF_3NO_2	**y = -18277x + 28.112**	**28.112**	**1.62×10^{12}**	**-18277**	**151.96**	**36.3**
Best Fit CF_3NO_2	**y = -20335x + 32.56**	**32.56**	**1.38×10^{14}**	**-20335**	**169.07**	**40.4**
3 Points	**y = 23.140x + 38.54**	**38.54**	**5.47×10^{16}**	**-23140**	**192.39**	**46.0**

With the three Arrhenius plots determined for the various combinations of experiments, some trends can now be seen. The E_a value determined from the plots corresponds to the dissociation energy of the CF_3I bond because the reaction cannot progress until this bond is broken. The dissociation energy of the CF_3I bond has been determined several different ways, and the results are summarized in Table 24.

The literature finds the experimental value for the bond dissociation energy of CF_3I to be between 47.1 and 56.91 kcal/mol. The first two Arrhenius plots found in this kinetic experiment have a much lower BDE, 36 and 40 kcal/mol, but as the experiments that are erroneous or flawed are removed, a merging towards the accepted value is seen. When the best-fit line is plotted, a BDE of 46 kcal/mol is achieved fitting in nicely with the previous experimental data especially, if the rather large error of the experiment is taken into account. Instead of removing values,

more experiments should have been performed. A large set of experiments would average out many of the errors observed during this experiment, and a convergence towards the expected BDE should be seen.

Table 3.24. Bond Dissociation Energy for CF_3I

BDE of CF_3I (kcal/mol)	A	Experimental Technique	Reference
56.91	Secondary Kinetic Experiment	Shock tube, and laser-schlieren apparatus	3.2
52.6 ± 1.1	$1 \times 10^{13.9}$	Optical density	3.3
53.3			3.4
55.0		Shock tube, I-atom absorbance	3.5
54.01	$1 \times 10^{14.67}$	Shock Wave Study, UV Absorption	3.1
52.6	1×10^{14}		3.30
47.2	$1 \times 10^{15.40}$		3.31
53.0	2.26×10^{19}	NMR spectroscopy and Heat	This Research

The A value gives insight into the transition state of the system. Using the Gorin model of nearly free particles, a weak interaction of particles is about 3 times the initial bond distance, and this corresponds to an A value in the range of $10^{16\pm1}$ s^{-1}.[3.26] The A values found for this reaction were within limit for the two Arrhenius plots with more points, and the best fit plot had an A value of 5.47×10^{16}. This A value is larger and suggests a very reactant-like transition state with a long interaction between molecules. The "soft", electron-dispersed iodine atom can absorb some of the electron density of the CF_3 stabilizing the molecule while it interacts with the $\cdot NO_2$ molecule. The stabilizing effect of the iodine lengthens the bonds formed in the transition state leading to the larger A value observed in this reaction.

3.2.7.3 Conclusions on Kinetic Experiments

The glass NMR thermal kinetic experiments were fairly successful, but more experiments must be run to reduce the error. By eliminating the less accurate data, a better Arrhenius plot to be plotted. Again, this is not the conventional way to run a kinetic experiment, and more data points are always preferred. This experiment laid out the groundwork and eliminated many of the issues involved with the different kinetic experiments so a new experiment can be started quickly and efficiently. The E_a values calculated were within the range of the other kinetic reactions. The A value suggested an elongated transition state.

Ideally, more useable experimental points would have been better, and this may be fixed by changing the experimental approach or just running many more experiments for a better average. The addition of a sealed capillary tube containing a duterated solvent to the reaction before adding the CF_3I and $\cdot NO_2$ gaseous mixture might fix the solvent intensity issue observed in these experiments. A lockable solvent might also allow for a greater ratio of $\cdot NO_2$: CF_3I to be used because the solvent would help to flatten the base line. The biggest concern for this experimental change would be the possible pressure build up of the solvent in the capillary tube. This could be avoided using a high boiling solvent like DMSO. More changes to the experimental procedure could lead to even more success. A sealed autoclave with constant IR monitoring capability has excellent possibilities, and this method would be a derivative of many of the kinetic experiments already performed. A system that could be monitored by GC/FID might also be very effective, assuming the samples could be removed while the system is hot. This would eliminate the very slow warm up and cool down stages seen in the stainless steel experiment. The biggest issue would be the sampling procedure. This kinetic experiment has

laid down the groundwork for any number of experiments that can hopefully begin and expand on the kinetics of the thermal reaction of $\cdot NO_2$ with CF_3I.

3.3 Experimental Section

3.3.1 Instrumentation

The ^{19}F-NMR spectra were recorded on a Bruker 500 MHz NMR spectrometer. All gaseous NMR samples were condensed into a sealable NMR tube (4 mm O.D., Teflon® stopcock) on a vacuum line or sealed in a thick-walled tube (4 mm O.D.). Trichlorofluoromethane, $CFCl_3$, was used as the reference material (0.0 ppm), and chloroform was the primary solvent, 99% by volume. No solvent was used in the pressure experiments.

3.3.2 Starting Materials

3.3.2.1 Trifluoronitromethane, CF_3I

Trifluoronitromethane, CF_3I, was used as received from SynQuest

3.3.2.2 Nitrogen dioxide, $\cdot NO_2$

Nitrogen dioxide, $\cdot NO_2$, was used as received from Matheson Trigas and purified if necessary, as described in Chapter 2.

3.3.3 Thermal Generation of CF_3NO_2

A 2.25-L stainless steel Hoke® cylinder was passivated with 200 torr of SF_4 by heating overnight at 200 °C. The SF_4 was removed, then the cylinder was cooled to -196 °C. This passivation step is not necessary but cuts down on the flakes produced during the runs. To the cooled cylinder, $\cdot NO_2$ was added, 71 g (1.5 mol). The cylinder is warmed between each addition, and the weight is checked. The $\cdot NO_2$ addition is followed by the addition of CF_3I, 215 g (1.10 mol) to the recooled cylinder. This produces a stoichiometric ratio of 1 : 1.41 of CF_3I : $\cdot NO_2$. The cylinder is capped, placed in the oven which is preheated to 200 °C and heated for at least 72 hours. The cylinder is removed, cooled to room temperature and purified according to Method 4 as described in Chapter 4.

3.3.4 Thermal Generation of CF_3NO_2 Using Trifluoroacetic Acid

A clean and dry 150-mL stainless steel cylinder was fitted with a burst disk, 1500 psig. The vessel was flushed with nitrogen, and under a nitrogen flow, an amount of 3.35 g (29.4 mmol) of trifluoroacetic acid was added via pipette. The cylinder was sealed and freeze-pump-thawed three times. Upon warming back to room temperature, the cylinder was cooled to -196 °C, and 0.14 g (0.66 mmol) of trifluoroacetic anhydride was added under a static vacuum to the cylinder to dry the trifluoroacetic acid. The cylinder was allowed to warm to room temperature and sit for several hours. The cylinder was then cooled back to -196 °C, and $\cdot NO_2$ (6.59 g, 143.3 mmol) was added under a static vacuum. Upon warming, the cylinder was placed in an oven preheated to 200 °C for 6 hours. The cylinder is cooled to room temperature

upon removal from the oven and then cooled to -78 °C. Once -78 °C is reached, the cylinder is placed under a dynamic vacuum, and any volatiles are collected in a -196 °C trap. This -196 °C trap collection, 0.22 g, was placed in a clean, dry cylinder and analyzed by ^{19}F-NMR spectroscopy. At this point, no attempts were made to remove the NO_x compounds that were present, but the only fluorinated product present in the sample was CF_3NO_2.

In an attempt to achieve the 30% yield clamed in the literature, the cylinder was put back into the 200 °C oven for ~2 weeks. The cylinder was allowed to cool back to room temperature and then cooled to -78 °C. The cylinder was then placed under a dynamic vacuum, and any volatiles were collected in a -196 °C trap. This purification yielded another 0.97 g of material, which was combined with the previous collection giving a total sample of 1.19 g. The crude material was transferred to a new cylinder containing ~5 g of NaOH and allowed to sit overnight. Upon purification 0.14 g of pure CF_3NO_2 was isolated with a 2.1 %-yield.

3.3.5 Thermal Addition of $\cdot NO_2$ to 2-Iododecafluoro-2-(trifluoromethyl)pentane at 165 °C

A 60-mL stainless steel cylinder was dried in a 200 °C oven overnight and upon cooling back to room temperature, an amount of 5.38 g (12.1 mmol) of 2-nitrodecafluoro-2-(trifluoromethyl)pentane was added via pipette, and the cylinder was then sealed. The cylinder was cooled to -196 °C and freeze-pump-thawed three times on the vacuum line. Under static vacuum, $\cdot NO_2$ (1.89 g, 41.0 mmol) was then added to the cylinder. The capped cylinder was then placed in a 165 °C preheated oven for 69 hours 15 minutes. Upon cooling to room temperature, the cylinder was cooled to -78 °C, and all volatile materials were pumped into a -196 °C trap. The material collected in the -196 °C trap (1.36 g) was then transferred into a

cylinder containing ~5 g of NaOH pellets. After sitting overnight on the NaOH pellets, the cleaned mixture (0.70 g) was transferred to an empty, dry cylinder for further analysis.

The cylinder that was cooled to -78 °C was allowed to warm back to room temperature. Once warmed, all volatile materials were removed under a static vacuum into a -196 °C trap. This crude mixture, 1.35 g, was placed in a cylinder containing NaOH and allowed to sit overnight. The cleaner mixture, 0.56 g, was placed in an empty, dry cylinder for analysis.

Note: 2-Iododecafluoro-2-(trifluoromethyl)pentane is very poisonous and proper handling and safety gear should be worn when handling at all times.

3.3.6 Thermal Addition of $\cdot NO_2$ to 2-Iodoheptafluoropropane at 165 °C

A 60-mL stainless steel cylinder was dried overnight in an oven at 200 °C and upon cooling back to room temperature, 2-iodoheptafluoropropane (2.97 g, 6.70 mmol) was added via pipette to the cylinder, which was sealed. The contents of the cylinder were subjected to three freeze-pump-thaw cycles on a vacuum line. Under static vacuum, 1.55 g (33.7 mmol) of $\cdot NO_2$ was then added to the cylinder. The capped cylinder was then placed in a 165 °C preheated oven for 69 hours 15 minutes. Upon removal from the oven, the cylinder was cooled to -78 °C, and all volatiles were pumped into a -196 °C trap. The crude mixture was transferred into a cylinder containing ~5 g of NaOH pellets. After sitting overnight on the NaOH pellets, the cleaned mixture, 1.19 g, was transferred to an empty, dry cylinder for analysis.

The cylinder that was cooled to -78 °C was allowed to warm back to room temperature, and once warm, all volatile materials were removed under a static vacuum into a -196 °C trap.

This crude mixture was placed in a cylinder containing NaOH and allowed to sit overnight. Upon attempting to collect any material from the NaOH cylinder, no material was present.

3.3.7 Thermal Addition of $\cdot NO_2$ to 2-Iododecafluoro-2-(trifluoromethyl)pentane at 120 °C

A 60-mL Monel cylinder was dried in a 200 °C oven overnight, and upon cooling back to room temperature, 2-iododecafluoro-2-(trifluoromethyl)pentane (2.99 g, 6.70 mmol) was added via pipette, and the cylinder was sealed. This cylinder was then cooled to -196 °C and freeze-pump-thawed three times on the vacuum line. Under static vacuum, $\cdot NO_2$ (0.75 g, 4.69 mmol) was then added to the cylinder. The capped cylinder was then placed in a 120 °C preheated oven for ~5 days. Upon cooling to room temperature, the cylinder was cooled to -196 °C. The cylinder was warmed slowly in an empty dewar, and the contents were collected in a -78 °C trap followed by two -196 °C cylinder. The -196 °C collections were combined producing 0.44 g of material which was transferred into a stainless steel cylinder. The -78 °C sample, 2.44 g was transferred into a clean stainless steel cylinder. The -78 °C sample was transferred into a 250-mL round bottomed flask containing 100 mL of 1 M NaOH aqueous solution. Upon warming, the solution was removed and sealed and allowed to sit overnight. The solution was then acidified using concentrated HCl, and the fluorous layer was removed by pipette and dried over $MgSO_4$. Following filtration, an amount of 2.22 g of a clear colorless liquid consisting of 2-nitro-decafluoro-2-(trifluoromethyl)pentane and decafluoro-2-(trifluoromethyl)-2-pentanol was isolated. No further separation was attempted. According to the NMR spectrum integration, 52% of this mixture was the nitro derivative, while 48% was the alcohol. The %-yield for the generation of 2-nitro-decafluoro-2-(trifluoromethyl)pentane is 47%.

Note: 2-Iododecafluoro-2-(trifluoromethyl)pentane is very poisonous and proper handling and safety gear should be worn when handling at all times.

3.3.8 Thermal Addition of $\cdot NO_2$ to 2-Iodoheptafluoropropane at 50 °C

A 60-mL stainless steel cylinder was dried overnight in an oven at 200 °C. Upon cooling back to room temperature, an amount of 4.47 g (16.0 mmol) of 2-iodoheptafluoropropane was added via pipette, and the cylinder was sealed. The cylinder was freeze-pump-thawed three times on a vacuum line. Under static vacuum, $\cdot NO_2$ (1.24 g, 27.0 mmol) was then added to the cylinder. The capped cylinder was placed in a 50 °C preheated oven for ~17 days. Upon removal from the oven, the cylinder was cooled to -78 °C, and all volatiles were pumped into a -196 °C trap. This crude collection, 0.39 g, was transferred into a cylinder containing ~3 g of NaOH pellets. After sitting overnight over the NaOH pellets, the cleaned mixture, 0.28 g, was transferred to an empty, dry cylinder for analysis. This material was pure 2-nitroheptafluoropropane and the %-yield was 8.1%.

3.3.9 Kinetic Experiments (Example 185 ° C)

A mixture of $\cdot NO_2$ (0.7275 g, 15.82 mmol) and CF_3I (0.9611 g, 4.93 mmol) was added to a 10-mL Hoke® cylinder. This represents a 1 : 3.20 ratio of CF_3I : $\cdot NO_2$. This cylinder was set aside for the additions to multiple thick-walled NMR tubes. All volumes of the six NMR tubes were predetermined by the mass of deionized water needed to fill the NMR tubes and the sealable section of the tube, minus the attachment joint. The average volume was 0.733-mL.

The mass of each tube was also measured, including the joint. For the 185 °C experiment, the mass was 12.393 g. The tube and the cylinder are both attached to the vacuum line, and the entire content of the cylinder was added to the system, giving a pressure between 350-400 torr. The cylinder was heated with hot water and allowed to equilibrate for 5 minutes. The NMR tube was isolated from the rest of the vacuum line and cooled to -196 °C and then the material in the line was transferred back into the cylinder. The NMR tube is flame sealed. Upon cooling, the separated tube and joint are reweighed, and the amount of the CF_3I, $\cdot NO_2$ mixture was determined. The NMR tube had 0.0926 g of the mixture added. The sealed tube was then placed in a preheated 185 °C metal cylinder and reacted for the predetermined period of time. Addition and removal of the tube took no more than 5 seconds of time, and the reaction is repeated as many times as necessary.

3.4 References

3.1 Saito, K.; Yoneda, Y.; Tahara, H.; Kidoguchi, S.; Murakami, I. *Bull. Chem. Soc. Jpn.* **1994**, *57*, 2661-2662.

3.2 Kiefer, J. H.; Sathyanarayana, R. *Int. J. Chem. Kinet.* **1997**, *29*, 705-716.

3.3 Okafo, E. N.; Whittle, E. *Int. J. Chem. Kinet.* **1975**, *Vol 7*, 273-285.

3.4 JANAF Thermochemical Tables, NO. 14., NSRDS-NBS (US GPO, Washington, 1985).

3.5 Kumaran, S. S.; Su, M. C.; Lim, K. P.; Michael, J. V. *Chem. Phys. Lett.* **1995**, *243*, 59-63.

3.6 Yamamoto, T.; Yasuhara, A.; Shiraishi, F.; Kaya, K.; Abe, T. *Chemosphere* **1997**, *35*, 643-654.

3.7 Boschan, R. *J. Org. Chem*. **1960**, *25*, 1450-1451.

3.8 Scribner, R. M. *J. Org. Chem*. **1964**, *29*, 284-286.

3.9 Scribner, R. M. U.S. Patent 3,057,931, 1962.

3.10 Scribner, R. M. *J. Org. Chem*. **1964**, *29*, 279-283.

3.11 Severson, W. A.; Brice, T. J. *J. Am. Chem. Soc*. **1957**, *80*, 2313-2316.

3.12 Brace, N. O. *J. Fluorine Chem*. **1999**, *93*, 1-24.

3.13 Persson, K.; Holmberg, B. *Acta Cryst., Sect. B* **1982**, *B38*, 900-903.

3.14 Lu, N.; Thrasher, J. S. *J. Fluorine Chem*. **2002**, *117*, 181-184.

3.15 http://www.azom.com/details.asp?Articleid=863

3.16 Rossi, M. J.; Barker, J. R.; Golden, D. M. *J. Chem. Phys*. **1989**, *71*, 3722-3727.

3.17 Sugawara, K.; Nakanaga, T.; Takeo, H.; Matsumura, C. *J. Phys. Chem*. **1989**, *93*, 1894-1898.

3.18 Oum, K. W.; Hancock, G. *J. Phys. Chem. A*, **1997**, *101*, 2634-2642.

3.19 Breheny, C.; Hancock, G.; Morrell, C. *Phys. Chem. Chem. Phys*. **2000**, *2*, 5105-5112.

3.20 Vakhtin, A. B. *Int. J. Chem. Kinet*. **1997**, *29*, 203-208.

3.20 Francisco, J. S.; Li, Z. *Chem. Phys. Lett*. **1989**, *162*, 528-534.

3.21 Bevilacqua, T. J.; Hanson, D. R.; Howard, C. J. *J. Phys. Chem*. **1993**, *97*, 3750-3757.

3.22 Sehested, J.; Nielsen, O. J.; Rinaldi, C. A.; Lane, S. I.; Ferrero, J. C. *Int. J. Chem. Kinet*. **1996**, *28*, 579-588.

3.23 Pagsberg, P.; Jodkowski, J. T.; Ratajczak, E.; Sillesen, A. *Chem. Phys. Lett*. **1998**, *286*, 138-144.

3.24 Duan, Y.; Shi, L.; Zhu, M. Han, L. *J. Chem. Eng. Data* **1999**, *44*(3), 501-504.

3.25 Benson, S. W. *Acc. Chem. Res*. **1986**, *19(11)*, 335-342.

3.26 Hidaka, Y.; Kawanami, K.; Kawano, H.; Suga, M. *Chem. Phys. Lett*. **1984**, *103*, 393-396.

3.27 Brouwer, L.; Troe, J. *Chem. Phys. Lett*. **1981**, *82*, 1-4.

3.28 Skorobogatov, G. A. *Kinet. Katal*. **1982**, *23*, 18.

3.29 Danidov, O. B.; Edagin, V. V.; Zadesskii, V. Y.; Yanev, I. L. *Kinet. Katal*. **1975**, *16*, 302.

3.30 Probst, A.; Raab, K.; Ulm, K.; Werner, K. v. *J. Fluorine Chem*. **1987**, *37*, 223.

CHAPTER FOUR

PURIFICATION OF CF_3NO_2

4.1 Introduction

In most industrial reactions, the purification process of a synthesized compound is of paramount importance. If an impure compound is used in food or drugs, the impurity can cause great harm to the human ingesting the impurity, thereby, nullifying any positive effects. A good example of this is thalidomide. It was not free from its harmful enantiomer and caused birth defects during the 1950s and 1960s due to the S-enantiomer in the racemic mixture. Only the R-enantiomer has the desired effects, but the damage had been done. Thalidomide is currently shunned in the United States even though effective purity checks are now in place. The influence of unwanted chemicals on the environment is a much greater issue now than in the past. If the synthesis of a compound produces byproducts that are considered environmentally unfriendly, its production can be banned or severely regulated. Eliminating the generation of these byproducts, by clever chemistry or removing them effectively by a purification processes is greatly desired.

The synthesis of CF_3NO_2 has been discussed in Chapters 2 and 3. The co-products formed in both the photochemical and thermal reactions are COF_2 and FNO, the latter of which decomposes to NO, $\cdot NO_2$, and $(NO)_2SiF_6$ upon reacting with a glass surface.[4.1] These former two byproducts are formed by the spontaneous decay of the O-bonded product, F_3C-ONO.

Along with COF_2, FNO, and ·NO, the excess $·NO_2$ starting material must also be removed in order to produce pure CF_3NO_2.

Nitrogen oxides or NO_x (·NO, $·NO_2$, N_2O_3, etc.) are byproducts of many industrial activities. They are also produced in all internal combustion engines. The NO_x compounds are a key component in the formation of acid rain and ground level ozone. These compounds also affect terrestrial and aquatic ecosystems. They are toxic to humans, particularly asthmatics and are "criteria pollutants" to evaluate air quality.[4.2-4.3] Many different methods have been developed for removing NO_x from industrial waste streams. Some of the more common methods are wet scrubbing, thermal oxidation (incineration), dry scrubbing and bioprocessing.[4.4] The wet scrubbing method was chosen for the purification of product mixtures containing CF_3NO_2. Purification involves bubbling the reaction mixture through an aqueous caustic solution. This procedure is an improvement in terms of cost and ease of operation when compared to the prescribed CsF/AlF_3 treatment.[4.5,4.6]

Aqueous solutions containing NaOH or KOH are a common way for removing NO_x compounds from a gaseous reaction mixture. The concentration of the caustic in the solution can range from 1 mass% up to a saturated solution. The amount of caustic is usually dependent on the type of system being scrubbed. Two main chemical pathways exist for the breakdown of NO_x compounds. The first is the reaction of NO_x with water, Equations 1-3:[4.7-4.8]

$$N_2O_3 + H_2O \rightleftharpoons 2\ HNO_2 \qquad \text{(Eq. 1)}$$

$$2\ ·NO_2 + H_2O \rightarrow HNO_2 + HNO_3 \qquad \text{(Eq. 2)}$$

$$N_2O_4 + H_2O \rightarrow HNO_2 + HNO_3 \qquad \text{(Eq. 3)}$$

These reactions are fast and occur without the addition of caustic to the system. The stable acid HNO_3 begins to build up, while the less stable acid HNO_2 will disproportionate to ·NO and HNO_3/H_2O, Equation 4:[4.7]

$$3\ HNO_2 \rightarrow 2\ \cdot NO + HNO_3 + H_2O \qquad \text{(Eq. 4)}$$

The presence of nitric oxide, ·NO, is problematic due to the very low solubility of ·NO in caustic mixtures.[4.9-4.10] Nitric oxide can be eliminated by adding another scrubber containing an effective oxidizing agent. Solutions containing Na_2SO_3[4.10] and H_2O_2[4.8] are oxidizing agents that have been used for its removal. In the presence of caustic, the undesired disproportionation of HNO_2 into ·NO and HNO_3 can be avoided via formation of the NO_2^- anion, Equations 5-6.

$$HNO_2 + OH^- \rightarrow NO_2^- + H_2O \qquad \text{(Eq. 5)}$$

$$HNO_3 + OH^- \rightarrow NO_3^- + H_2O \qquad \text{(Eq. 6)}$$

This sets up a competition between HNO_3 (major byproduct) and HNO_2 (minor byproduct). The HNO_2 neutralization is a gas-liquid interaction as opposed to HNO_3, which is a liquid-liquid interaction. Therefore, HNO_2 decays at a slower rate than the HNO_3, and if the concentration of caustic is too low, some ·NO may still get through the scrubbing system.[4.8]

In this Chapter, two purification methods of CF_3NO_2 will be discussed and evaluated in terms of time and cost effectiveness. The evolution of a new purification process will also be discussed.

4.2 Results and Discussion

The goal of this project was to evaluate the original purification method developed by Lu, *et al.*[4.5,4.6] during their synthesis of SF_5NO_2, which was then applied to CF_3NO_2, and if necessary, find a method for purifying the CF_3-analog on a much larger scale. The key factors in this discussion are effectiveness, purification time and cost.

4.2.1 Initial Purification Method

The initial purification method developed by Lu is a three-step, "dry process" and was used for quantities of 1 gram or less of the crude CF_3NO_2 mixture. The first step in the purification process involves reacting the crude CF_3NO_2 mixture with cesium fluoride, a fluoride-ion donating Lewis base, in a cylinder for several days. The CsF removes both COF_2 and $\cdot NO_2$ from the crude reaction mixture. The $\cdot NO_2$ is converted into $CsONO_3$ and nitrosyl fluoride, FNO.[4.11] The COF_2 is removed by the CsF by creating a cesium salt, Equations 7-8:

$$CsF + COF_2 \rightarrow Cs^+OCF_3^- \qquad \text{(Eq. 7)}$$

$$CsF + 2\ \cdot NO_2 \rightarrow Cs^+NO_3^- + FNO \qquad \text{(Eq. 8)}$$

The FNO molecule is known to react with stainless steel creating metal salts and ·NO. The newly purified mixture contains FNO, CF_3NO_2 and ·NO, and this mixture is placed over AlF_3, which removes the FNO by forming a salt, Equations 9-10:

$AlF_3 + FNO \rightarrow NO^+AlF_4^-$ (proposed formula)[4.5] (Eq. 9)

$AlF_3 + 3\ FNO \rightarrow (NO^+)_3AlF_6^{3-}$ (alternate salt formation) (Eq. 10)

The final trap-to-trap distillation will remove any $\cdot NO_2$ not removed by the CsF by trapping it as N_2O_4 in the -78 °C trap, the -135 °C trap (Lu)[5] or -155 °C trap (this research) collects pure CF_3NO_2. If any ·NO is present in the mixture, it will collect largely in the -196 °C trap with a minimum amount pumped through the vacuum-pump due to its vapor pressure of ~4 torr at -196 °C.

This method works very well on a small scale, but a number of problems occurred when larger quantities of crude CF_3NO_2 had to be purified.

4.2.2 Scale-up Using the Original Purification Method

The purification method used by N. Lu[4.5-4.6] was quickly discovered not to be feasible for larger amounts of crude CF_3NO_2. One of the first factors investigated was the ability of CsF and AlF_3 to be used with multiple samples and/or larger amounts of crude material. A typical diazo blue light reaction in this project yielded about 5-10 grams of a crude reaction mixture. An initial purification step removed most of the excess $\cdot NO_2$ by trap-to-trap distillation through a -78 °C trap, where it is stopped as the colorless solid N_2O_4. After that purification step, 3-7 g of the enriched CF_3NO_2 product mixture was introduced to the standard CsF and AlF_3 purification steps.

When N. Lu performed the initial purification with CsF, the crude mixture was transferred into a cylinder containing a huge excess of CsF, ~300 g, which was used as received.

To evaluate the efficiency of this reaction, the amount of CsF was reduced to 20-30 g. This CsF was fused and then ground in a jar mill to maximize its surface area and activity. Typically two, and at best three, crude product mixtures could be freed of $\cdot NO_2$ and COF_2 with this activated CsF. This translates to roughly 50% of the CsF being utilized as indicated in Eqs. 6 and 7. Typically two days were required to purify the crude sample, ~10 g starting mass. If larger amounts of CsF were used or smaller quantities of crude material, the time may be shortened. Lu could not detect the limitation in the efficiency of the purification of the product by this heterogeneous reaction because of the huge excess of CsF used.

The purification step using amorphous AlF_3 was more efficient due to the fact that the enriched CF_3NO_2 sample does not contain nearly as large a quantity of byproducts to be scrubbed as when it is reacted with CsF. For the AlF_3 purification step, roughly a 1 : 1 mass ratio of the partially purified product mixture to amorphous AlF_3 is used. This reaction typically requires a reaction time of 12-24 h to reach completion. Neither of the purification steps involving CsF or AlF_3 is economical, and both steps are time consuming, taking at least 36-48 h for the CsF step and a 12-24 h reaction time for AlF_3 to complete the individual purification steps. The time required for this part of the purification does not take into account the time required to generate the required AlF_3, and the fact is there no good way to recycle the AlF_3 once it is used. An economical breakdown of this method will be discussed in Section 4.2.4. Overall, this work-up procedure is fine for 1-2 g quantities, but for larger amounts of CF_3NO_2, a new method must be devised.

4.2.3 New Wet-Scrubbing Purification Method

A new, inexpensive and fast method for purifying crude CF_3NO_2 by bubbling it through a solution of NaOH or KOH was suggested. Caustic solutions of NaOH, KOH or $Ca(OH)_2$ are widely used for removing nitrogen oxides from industrial waste streams, and this turned out to be suitable for the CF_3NO_2 process.

Since it was unknown if CF_3NO_2 would be hydrolyzed by a caustic solution, a simple experiment was set up placing 2 g of pure CF_3NO_2 in a cylinder containing a 20% aqueous NaOH. The cylinder was vigorously shaken for five minute periods over the next several days. The cylinder was then cooled to -78 °C, and the CF_3NO_2 was recovered quantitatively by vacuum transfer. Trifluoroiodomethane, CF_3I, is slightly less inert. Between 1-2% is hydrolyzed upon bubbling through the caustic solution. This was detected by ^{19}F-NMR measurements on the reaction mixtures before and after the aqueous caustic scrubbing. The contact time of the crude sample of CF_3NO_2 with the caustic solution was found to be crucial, as the following search for a mystery contaminant shows.

After bubbling large batches of enriched CF_3NO_2 reaction mixtures through the caustic solution, a royal blue color was observed along with the colorless CF_3NO_2 in the -196 °C collection trap. This blue color was not observed with small samples, $\leq$ 5 g, unless bubbling was faster than 5-10 bubbles a second. A typical flow rate was 1 bubble a second. Several blue compounds were quickly eliminated via analysis by IR-spectroscopy. First, ozone was eliminated because it contains a characteristic O-O bond stretch at 1055 cm^{-1}. Second, oxygen was eliminated by cooling the system to -196 °C and pumping on the mixture. Oxygen has a vapor pressure at -196 °C and would be removed when pumping down the system. This was not

observed. Third, CF_3NO was eliminated by ^{19}F-NMR spectroscopy, as the spectra contained no peaks due to fluorine-containing compounds with the exception of CF_3NO_2 (^{19}F-NMR spectrum, triplet, δ = -73.6 ppm, $^1J_{FC}$ = 298 Hz, $^2J_{FN}$ = 14.6 Hz) and occasionally, CF_3I (^{19}F-NMR spectrum, singlet, δ = -5.0 ppm). ^{14}N-NMR spectroscopy was then performed in order to determine whether it was a nitrogen containing compound that was causing the blue discoloration. No peaks were present in the spectrum with the exception of CF_3NO_2 (^{14}N-NMR spectrum, quartet, δ = 273.1 ppm, $^2J_{FN}$ = 20.5 Hz)[4.5]. Both $\cdot NO_2$ and $\cdot NO$ have extremely broad signals due to their paramagnetic nature and are difficult to detect by NMR, so their presence cannot be determined by this method. These two compounds are also very difficult to characterize by GC/MS due to their high polarity and low molecular weight. As expected, only CF_3NO_2 and in some cases, CF_3I were present in the GC/MS spectrum. However, it was during the GC/MS measurement that the final piece of the puzzle fell into place.

The GC/MS sample was placed in a 3-way sealed glass vessel. Two sides were sealed with a Teflon stopcock while the top was sealed with a rubber septum, which is where the sample was taken with a syringe. After removing one or two samples from that vessel, the color of the gas turned from colorless to orange/brown, the color of $\cdot NO_2$. When this gaseous mixture was collected again at -196 °C, the blue color had disappeared, and only an opaque white solid remained. Nitrogen oxide, $\cdot NO$, quickly oxidizes to nitrogen dioxide, $\cdot NO_2$, in the presence of oxygen, O_2, and this is what may have been occurring when the septum was punctured. The $\cdot NO$ comes from the decay of nitrous acid, HNO_2, in water.[4.7-4.8] The $\cdot NO$ can also come from the decay of $\cdot NO_2$ in the blue light reactor or FNO reacting with the glass surface. Nitrogen oxide, $\cdot NO$, is insoluble in water, and whatever $\cdot NO_2$ that makes it through the bubbler and collects with the $\cdot NO$ in the -196 °C trap will form N_2O_3, a bright royal blue solid. In the gas phase,

dinitrogen trioxide is almost completely dissociated into ·NO and $\cdot NO_2$ molecules. This is the explanation for the color of the gas, as the equilibrium $N_2O_3 \rightleftharpoons \cdot NO + \cdot NO_2$ begins to shift to the right. The lack of blue color forming upon re-cooling again indicates the formation of N_2O_4 as the most likely option. Dinitrogen trioxide, as the impurity, would help explain why none of the spectroscopic methods used to detect the impurity worked. Both ·NO and $\cdot NO_2$ IR absorptions overlap with CF_3NO_2 absorptions in the spectrum when CF_3NO_2 is the dominant analyte (≥75%). Both ·NO and $\cdot NO_2$ are problematic for detection by GC/MS, and as stated before, their signals are too broad due to their paramagnetism to be observed by ^{14}N-NMR spectroscopy.

Several approaches were taken to eliminate the N_2O_3 impurity. The first approach was to cool the mixture to -150 °C and remove all the volatiles. This allows for ·NO to be removed from the system, if it is not complexed with $\cdot NO_2$. These attempts turned out to be very time consuming, and usually requires an entire day and multiple pump downs. The ·NO removal was followed by repeated weight checks of the stainless steel cylinder until a constant weight was reached. After removal of the ·NO by vacuum, removal of any remaining $\cdot NO_2$ was achieved by another scrubbing through aqueous NaOH/KOH. This caustic scrubbing was occasionally followed by the observation of N_2O_3 still being present. This would required yet another freeze-pump-scrub procedure. This method was abandoned for an improved process where the $\cdot NO_2$ was removed first. This was achieved by cooling the collection cylinder with the crude CF_3NO_2 mixture to -196 °C and then allowing the cylinder to slowly warm. This causes the gases to pass through a 30 cm, 1 inch O.D. column of activated charcoal pellets, ~50-60 g, which absorbs $\cdot NO_2$. The unabsorbed ·NO and CF_3NO_2 were collected in a -196 °C trap, transferred back into a cylinder and then cooled to -150 °C, at which temperature the ·NO was removed under vacuum.

This process works well, but activation of the charcoal requires heating the pellets overnight to 200 °C followed by pumping on the pellets overnight with the vacuum pump. Also, larger batches of the crude CF_3NO_2 mixtures (≥ 30 g) usually required an additional pass through the charcoal column. This method is better but still requires a long set-up time and multiple charcoal activations for larger batches. The charcoal pellets can be recycled easily in the same manor in which they were activated.

The best method found for removing traces of dinitrogen trioxide, N_2O_3, is by storing the almost pure CF_3NO_2 over sodium hydroxide pellets for at least 24 hours after the caustic scrubbing is complete. The trace amounts of water present in the CF_3NO_2 mixture allows the $\cdot NO_2$ to react with NaOH to form $NaNO_2$ and $NaNO_3$ (Eqs. 1-5).[4.7-4.8] Any remaining ·NO and any trace water are removed when the cylinder is cooled to -78 °C. The CF_3NO_2 is transferred into a clean cylinder, and the ·NO is pumped away while the water remains behind in the -78 °C cylinder. This method has been used successfully on crude batches weighing 60 g. If larger purification sizes are desired, more NaOH can be used. In general, twice as much mass of NaOH is required to successfully remove all of the $\cdot NO_2$ from the mixture. The purity is determined by the sharpening of the IR spectrum with little to no $\cdot NO_2$ or ·NO impurities being observed.

Several other experiments were performed to see if the purification method could be improved further. The caustic solution was heated to 85-90 °C while the crude mixture was bubbled through the system. The hope was to increase the amount of $\cdot NO_2$ reacting with the scrubber solution and eliminate the N_2O_3 formation. This was not the case, and by visual impression, the mixture that was recovered contained more N_2O_3 than those obtained by the standard room temperature purification. This was confirmed by weighing the sample after the purification. The mass change was minimal after the purification, except the crude mixture now

had the blue N_2O_3 color, not the initial brownish color that is observed before the purification. Pure water was also tested for the scrubbing process. This worked the least well of all the scrubbing solutions, and in this purification, the least pure material was recovered. With no base present, the $\cdot NO_2$ reacts to form $\cdot NO$ and HNO_3. The absence of base from the scrubbing solution allows for even greater amounts of N_2O_3 to be formed, and the deionized water removes the least amount of NO_x byproducts of all scrubber solutions tested. A summary of the different purification methods tried are shown in Table 4.1.

Table 4.1. Selection of Batch Reactions After Various Purification Techniques

Thermal Reaction #	CF_3I (g)	$\cdot NO_2$ (g)	Mass After Passing Through Dry Ice (g)	Mass After 1st Caustic Wash (g)	Mass After Passing Through Activated Charcoal (g)	Mass After Storing Over Solid NaOH Pellets (g)	%-Yield
3	6.28	29.35	4.20	1.60			43
4	12.48	20.67	6.98	3.45			47
9	68	50	69.84	32.08	21.61		54
10	154	65	86.66	41.10	33.57		37
11	150	72	87.01	40.14	29.54		33
12	165	88	88.16	49.10	44.59		46
13	159	76	50.37	44.60	27.34		29
14	151	74	77.48	44.70	37.59		35
16	187	71	103.99	48.9		40.08	36
17	215	71	106.07	63.7		51.02	40

4.2.4 Cost and Time Comparison of Lu Method Versus New NaOH/KOH Wet Scrubbing Method

A new purification method must take into account the time required for the purification along with the minimum amount of material loss and overall cost. The two methods proposed for the purification of CF_3NO_2 vary drastically in both time and cost. However, both methods work giving overall yields of ca. 33% of pure CF_3NO_2. The new wet scrubbing method developed in this study has been found to be superior in both time and cost for the purification of larger quantities of CF_3NO_2 than the initial method developed by Lu for the purification of SF_5NO_2. However, this method was found to work well for purifying CF_3NO_2.

The time required for purifying CF_3NO_2 can be split into two stages, set-up and work-up time. The set-up time includes preparing any compounds or mixtures that are needed in the purification process, and the work-up time is that time actually required to clean up the crude reaction mixture to give pure CF_3NO_2.

In the procedure used by Lu, significant set-up time is required for the preparation of amorphous AlF_3, which is not commercially available. Amorphous aluminum trifluoride, AlF_3, is synthesized by passing a mixture of 20% F_2 in N_2 at ambient temperature slowly over anhydrous, sublimed aluminum trichloride, $AlCl_3$. A batch of 100 g of $AlCl_3$ takes ~2 weeks to convert to ~70 g of AlF_3. This alone is a large commitment of time, and currently no method is known for recycling the AlF_3 once it is spent. The AlF_3 is consumed in approximately a 1 : 1 mass ratio with the crude CF_3NO_2 mixture, meaning a batch of AlF_3 will not last long and a constant generation of more AlF_3 is required, if larger amounts of CF_3NO_2 need to be purified. Lu's method has another time intensive step, namely, the activation of cesium fluoride, CsF.

Proper activation includes the melting of the CsF to remove HF and H_2O followed by grinding overnight in a jar mill. This step may not be necessary as long as a sufficiently large excess of CsF is used, but this is also not cost effective (*vide infra*). The cesium fluoride consumed during the purification step can be regenerated by heating to 150 °C and removing the COF_2 under vacuum. After this step, the cesium salt must be reacted with fluorine gas in small quantities and at elevated temperatures to destroy any $FONO_2$ formed during this step. The resulting CsF must then be melted and reground. The only set-up required for the wet scrubbing is dissolving KOH/NaOH in water and assembly of the wash-bottle train. Sodium hydroxide and potassium hydroxide are relatively inexpensive chemicals that can be purchased on the multi-kilogram scale and do not require any recycling.

The cost comparison will be based on the generation of 10 g of pure CF_3NO_2. The cost of $\cdot NO_2$ and CF_3I will be ignored for this calculation because it will be the same for both reactions. A typical high yield blue light reaction generates 1.4 g of pure CF_3NO_2. In order to generate 10 g of product, at least 7 reactions will be required. Generally, 5 g of crude product is recovered after each of the initial dry ice purifications giving 35 g of crude material from seven reactions. This crude mixture is what is placed over the CsF and followed by storage over AlF_3. All prices, unless noted, are from the Sigma-Aldrich 2007/2008 catalog.

The generation of AlF_3 has two costs, the aluminum chloride, $AlCl_3$ and the elemental fluorine, F_2. Bulk, anhydrous, sublimed $\geq$ 98% pure aluminum chloride costs $42 for 1 kg. Paying the extra for the sublimed material is worth the cost because subliming technical $AlCl_3$ from the iron (III) chloride, $FeCl_3$, impurity, present is another couple of days of process time saved. For the bulk reaction, 100 g (0.750 mol) of $AlCl_3$ will be used costing $4.20. The reaction of $AlCl_3$ with fluorine requires a slight excess, 1.2 equivalents of F_2. This gives

qualitative yields of AlF_3. The amount of fluorine required to fluorinate $AlCl_3$ is 35 g (0.92 mols) which costs ca. $7 (Fisher 07/08). This reaction produces 63 g (~0.75 mol) of aluminum trifluoride, AlF_3, working out to a cost of $0.18 per gram or $15 per mol.

In the first step of Lu's purification method, 35 g of the crude product mixture must be reacted with CsF. This requires a two-fold excess of CsF, meaning at least 70 g of CsF ($1.12/g) will be needed to purify the crude mixture before the AlF_3 purification step, at a cost of $78.50. The CsF removes the majority of the impurities, and usually, 1-2 g of impurities remain leaving 11-12 grams of the enriched CF_3NO_2 mixture. The AlF_3 purification step requires an equal amount of AlF_3 by mass ($0.18/g), at a cost of $2.16. This brings the total cost of chemicals required to purify 10 g of CF_3NO_2 to ~$80, which equates to $0.80/gram or $92/mol.

In contrast, the new wet scrubbing method using sodium hydroxide, NaOH ($0.035/g) is significantly less expensive. The same 35 g of the crude CF_3NO_2 mixture (a maximum of 65 g can be handled at this scale) is bubbled through a 20% caustic solution (200 g NaOH/1 L H_2O) costing 7 dollars. The remaining material is then stored over 20 g of NaOH, which removes any remaining $\cdot NO_2$ or NO, costing another 0.70 dollars for a total purification cost of ~$8. The chemicals for this purification method costs $0.08/g or $10/mol, a ten-fold decrease in cost. This represents a huge saving, especially if the reaction is scaled-up to kg amounts.

4.3 Experimental

4.3.1 Purification of CF_3NO_2

4.3.1.1 Method 1. Initial Purification Method, Lu's Method

The reaction mixture is cooled to -196 °C, warmed slowly and passed through -78 °C and -196 °C traps under dynamic vacuum. The -78 °C trap removes most of the unreacted $\cdot NO_2$ and I_2 present in the crude product. The -196 °C trap collects all of the CF_3NO_2, COF_2, FNO and any unreacted CF_3I. This crude mixture is then placed over activated CsF for several days. This removes any COF_2 by forming the $Cs^+OCF_3^-$ salt and residual traces of $\cdot NO_2$. In general, 2 g of CsF is deactivated by 1 g of crude material. The purified mixture is transferred into another cylinder containing amorphous AlF_3 and allowed to sit for several days. This removes FNO forming the $NO^+AlF_4^-$ (and/or $(NO^+)_3AlF_6^{3-}$) salt. In general, 1 g of AlF_3 is deactivated by 1 g of the crude mixture. The remaining mixture is pumped through a -78 °C trap, followed by a -155 °C trap and finally, a -196 °C trap under dynamic vacuum-line conditions. Pure CF_3NO_2 is collected in the -155 °C trap, and if any CF_3NO is present, it is collected in the -196 °C trap.

4.3.1.2 Method 2. Vacuum Trap-to-Trap Distillation

The reaction mixture is cooled to -196 °C, allowed to warm slowly and passed through -78 °C and -196 °C traps under dynamic vacuum. The -78 °C trap collects most of the unreacted

·NO_2 and I_2 byproduct, and the COF_2, CF_3NO_2, FNO and unreacted CF_3I are stopped in the -196 °C trap. In all cases, the contents of the -196 °C trap are blue/green in color.

4.3.1.3 Method 3. NaOH Purification

This procedure follows the trap-to-trap distillation by bubbling material collected in the -196 °C trap through aqueous NaOH/KOH. Two wash bottles are used with the first containing 2 L of caustic solution and the second, 500 mL of caustic. Successful purifications were made with the concentrations of the caustic solutions ranging from 5-30% KOH by weight. The dip-tube went approximately 3/4 of the depth of the wash bottles. If sample size is small enough, 5 g or less, pure CF_3NO_2 is recovered after a single wash procedure.

4.3.1.4 Method 4. Activated Charcoal Method

This method is necessary for reaction mixtures consisting of ≥ 10 g quantities. This procedure follows the trap-to-trap distillation described in Method 2. The contents of the -196 °C trap are transferred into a stainless steel cylinder and then bubbled through wash bottles as described in Method 3. After these steps, the product mixture consists of CF_3NO_2, N_2O_3 and CF_3I. The cylinder containing the mixture is then cooled to -78 °C. The mixture is allowed to warm slowly to room temperature with the vapor being passed through a tube filled with charcoal before being collected in a -196 °C trap held under dynamic vacuum. The scrubber tube was a 30-cm long, 1-inch O.D. Pyrex® glass tube filled with 40-60 g of activated charcoal pellets. Should any nitric oxide impurity remain after transferring the CF_3NO_2 back to a storage

cylinder, it can be removed by cooling the cylinder to -196 °C and pumping on the cylinder until the mass remains constant. If the sample is large enough, the cylinder may have to be put through several freeze-pump-thaw cycles to remove all of the remaining ·NO.

4.3.1.5 Method 5. Large-Scale Purification, Finalized Method

This method follows purification Method 3, including a trap-to-trap distillation and scrubbing through a caustic solution. The remaining CF_3NO_2/N_2O_3 mixture is then transferred into a 500-mL stainless steel cylinder containing a two-fold excess of NaOH pellets by mass, and the contents of the cylinder are allowed to stand at room temperature for at least 24 hours. Thereafter, the purified CF_3NO_2 is transferred first to a glass bulb and then to a storage cylinder for clean product. If any blue color is observed, then more time over fresh NaOH pellets is required. Once all the color is gone, the purity is finally confirmed by IR spectroscopy.

4.4 References

4.1 Andreades, S. *J. Org. Chem*. **1962**, *27*, 4157-4162.

4.2 Bagheri, S. R.; Jamshidi, E.; Najafabadi, A. *Chem. Eng. Technol*. **2007**, *30*, 250-254.

4.3 EPA Air Pollution Control Cost Manual, *Technical Manual EPS-452/B-02-001*, 6th ed., US Environmental Protection Agency, Research Triangle Park, NC **2001**.

4.4 Jin, Y.; Veiga, M. C.; Kennes, K. *J. Chem. Tech. Biotechnol*. **2005**, *80*, 483-494.

4.5 Lu, N.; Thrasher, J. S. *J. Fluorine Chem*. **2002**, *117*, 181-184.

4.6 Lu, N.; Kumar, H.P.S.; Fye, J.L.; Banks, J.S.; Thrasher, J.S.; Willner, H.; Oberhammer, H. *Angew. Chem. Int. Ed*. **2006**, *45*, 938-940.

4.7 Thomas, D.; Vanderschuren, J. *Sep. and Pur. Tech*. **2000**, *18*, 37-45.

4.8 Paiva, J. L.; Kachan, G. C. *Chem. Eng. Proc*. **2004**, *43*, 941-948.

4.9 Thomas, D.; Vanderschuren, J. *Chem. Eng. Technol*. **2000**, *23*, 449-455.

4.10 Chang, M. B.; Lee, H. M.; Wu, F.; Lai, C. R. *J. Air Waste Manage. Assoc*. **2004**, *54*, 941-949.

4.11 Ratcliffe, C. T.; Shreeve, J. M. *Chem. Commun*. **1966**, 674.

CHAPTER FIVE

USING AN ACCELERATING RATE CALORIMETER (ARC) TO DETERMINE THE SELF HEATING RATES OF THE THERMAL DECOMPOSITION OF CF_3NO_2

5.1 Introduction

The **A**ccelerating **R**ate **C**alorimeter (ARC) is a device used to evaluate compounds suspected to undergo runaway, self-heating reactions. It has become popular in the industrial workplace, where it is used to determine the safety of chemicals during transport, storage and chemical reactions. The ARC performs its measurements under near perfect adiabatic conditions. In the ARC, a small test-sample is heated, and in case it undergoes exothermal decomposition, the ARC will record the time-temperature-pressure relationships. Townsend, *et al*. developed the instrument in the late 1970s and early 1980s.[5.1-5.3] This development included operation procedures and data analysis of the early ARCs, which were quickly adopted by industry, where the instrument was further developed.[5.1-5.7]

The ARC is most commonly used with non-air-sensitive solids and liquids. The original ARC design did not allow for the use of gases. In order to work with gases, the sample container, also called a bomb, must be connected to a vacuum system and given the opportunity to cool down to a temperature that will condense the gas. This cooling allows for gases to be condensed into the bomb and moved. While the sample is at -196 °C, it can become

contaminated by water, oxygen, carbon dioxide or any other gases present in the atmosphere during movement of the bomb between the ARC and the vacuum line. Any one of these impurities can influence the very sensitive ARC measurements. Also, if the sample contains a volatile toxic material, the operator is at risk for unnecessary exposure. In the Thrasher group, the ARC was modified to solve this problem by adding a small stainless vacuum system to the top of the bomb outlet.[5.8] A valve keeps the volume of the system practically unchanged, but gases can now be added to, or removed from, the system. This vacuum line addition allows other procedures such as leak checking, degassing, sample drying, other pretreatments and reacting the material under inert gases such as nitrogen/argon or reactive ones such as oxygen.[5.8] This vacuum line modification has allowed the Thrasher group to study trifluoronitromethane, CF_3NO_2, with the ARC. Very little work has been done on the energetics of gases in an ARC for the reasons stated above. Most experiments involved with the thermal decomposition of gases are experiments in shock tubes or were performed by studying the decay products after heating in a sealed vessel.[5.9] With the aforementioned changes, the ARC is well suited for investigating the thermal behavior of gases and because little is known about CF_3NO_2, at elevated temperatures, it was a good candidate to investigate. Trifluoronitromethane has many proposed uses, and one of the most promising is as a dielectric gas.[5.10] Dielectric gases are inevitably exposed to high temperatures, for example, in the case of electric arc formation. Therefore, determining its behavior at high temperatures is well worth studying.

Interpretation of an ARC spectrum is sometimes more of an art than a science. Runaway reactions are easily identified and measured, but there are many subtle events that can be interpreted many different ways. An event can be anything that deviates from a typical heat-wait-search spectrum, shown in Figure 5.1. For comparison, a standard heat-wait-search

experiment is always performed before a set of experiments. The main characteristic of the heat-wait-search mode is a consistent stepwise progression in both the pressure and temperature. Deviations in the heat-wait-search mode are caused by exotherms or endotherms in the reaction vessel. Due to the sensitivity of the ARC (0.010 °C/min), a small exotherm may appear as a low angle upward slope during the search period. Endotherms are not actively measured by the ARC but can be observed. An endotherm is indicated by a drop in temperature which prolongs the search mode until the set temperature is again constant. Once constant, the next heat-up phase will begin. When an endotherm occurs, the program tries immediately to keep the pre-endotherm temperature constant while the endotherm, for example a phase-transition, is still ongoing. For this reason, the magnitude of the endotherm event cannot be measured by the ARC due to the heat added to the system by the ARC. At this point, an energy totalizer has not been built into the ARC system that could give information on the extent of an endotherm. The primary purpose of the ARC is to detect runaway exotherms which are detected by sharp increases, generally, in both the pressure and the temperature. The steeper the increases of the temperature and the pressure, the more dangerous the investigated compound or mixture of compounds. Often the minor events are overlooked or ignored because the goal of most ARC experiments is to determine if a compound will undergo a runaway reaction, not the minor events that lead to that runaway reaction.

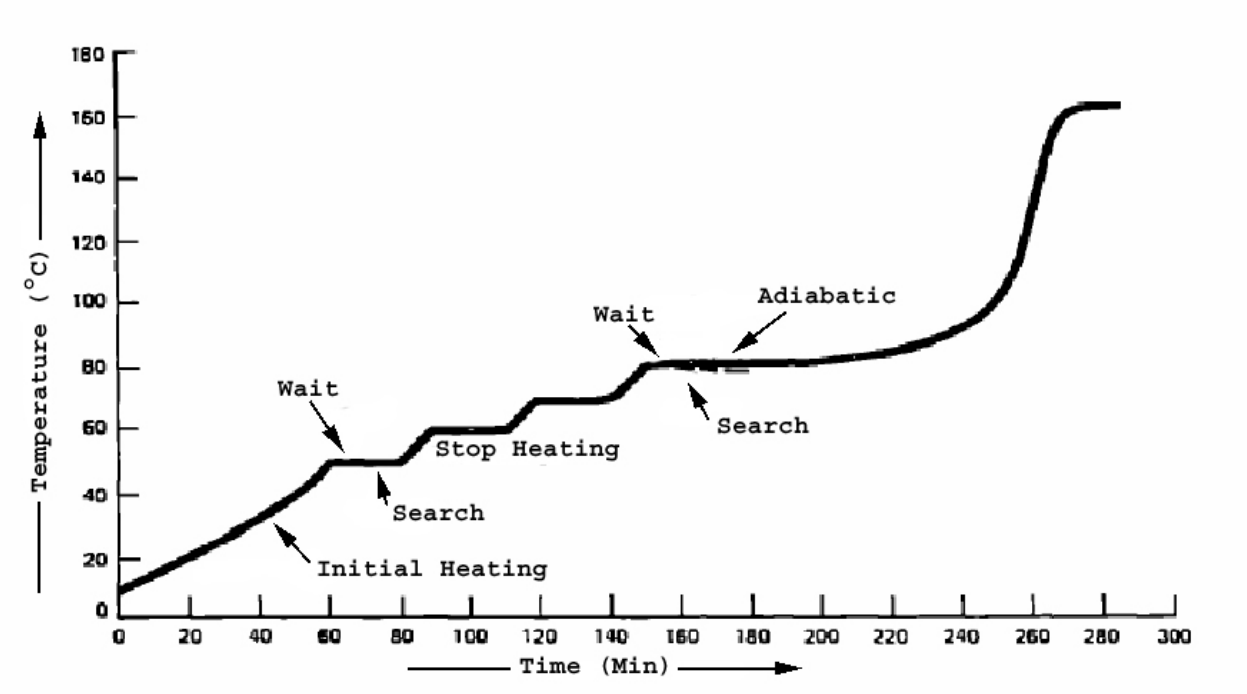

Figure 5.1. Typical heat-wait-search mode of an ARC

To date, no established set of rules are universally accepted to determine if an ARC reaction can be designated a runaway reaction. In most cases, the slope of the heat and pressure lines are examined, and the steeper the line, the more severe the reaction and the higher the potential for a runaway reaction. Recently, some effort has been put into comparing ARC data with standards set down by the United Nations for runaway reaction.[5.11-5.14] Bodman, *et al.* has worked on establishing ARC conditions that model the UN standards as shown in Table 5.1.[5.15] Using these criteria, the decomposition temperature of CF_3NO_2.

Table 5.1. Explosivity and predictive ARC breakpoints[5.15]

Explosivity Rank	Severest Class 1 property	Correspondence to UN classification	Preliminary breakpoints based on ARC dP/dt_{max} (Mpsi/min), T_p (°C)
A	Detonates (positive result in UN Gap, or BAM 50/60 or TNO 50/70 in UN Gap unavailable	Potentially Class 1	$dP/dt_{max} \geq 2.25$
B	Heating under confinement: violent (Koenen limiting diameter ≥ 2 mm), and/or Deflagration: rapidly (pressure in Time/Pressure ≥ 2070 kPa in <30 ms	Potentially Class 1 but not detonable	$0.25 \leq dP/dt_{max} < 2.25$ and $dP/dt_{max} \geq 0.04T_p - 5$
C	Heating under confinement: medium or low (Koenen limiting diameter ≤ 1.5 mm), and/or Deflagration: slowly (pressure in Time/Pressure ≥ 2070 Kpa in ≥ 30 ms)	Not Class 1	$0.25 \leq dP/dt_{max} < 2.25$ and $dP/dt_{max} < 0.04T_p - 5$
D	No effect of heating under confinement, and does not deflagrate (pressure rise in Time/Pressure < 2070 kPa)	No explosive properties with respect to transport classification	$dP/dt_{max} < 0.25$

5.2 Results and Discussion

The ARC run of CF_3NO_2 has three major points of interest. Areas of interest are indicated by a deviation from the normal heat-wait-search mode that the ARC routinely follows. In the ARC runs of CF_3NO_2, both low- and high-slope events were observed. In the ARC study of CF_3NO_2, three events were observed. Two are small slope exotherms, and one is a long exotherm with a very steep upward slope near the end of the run, as shown in Figures 5.2 and 5.3.

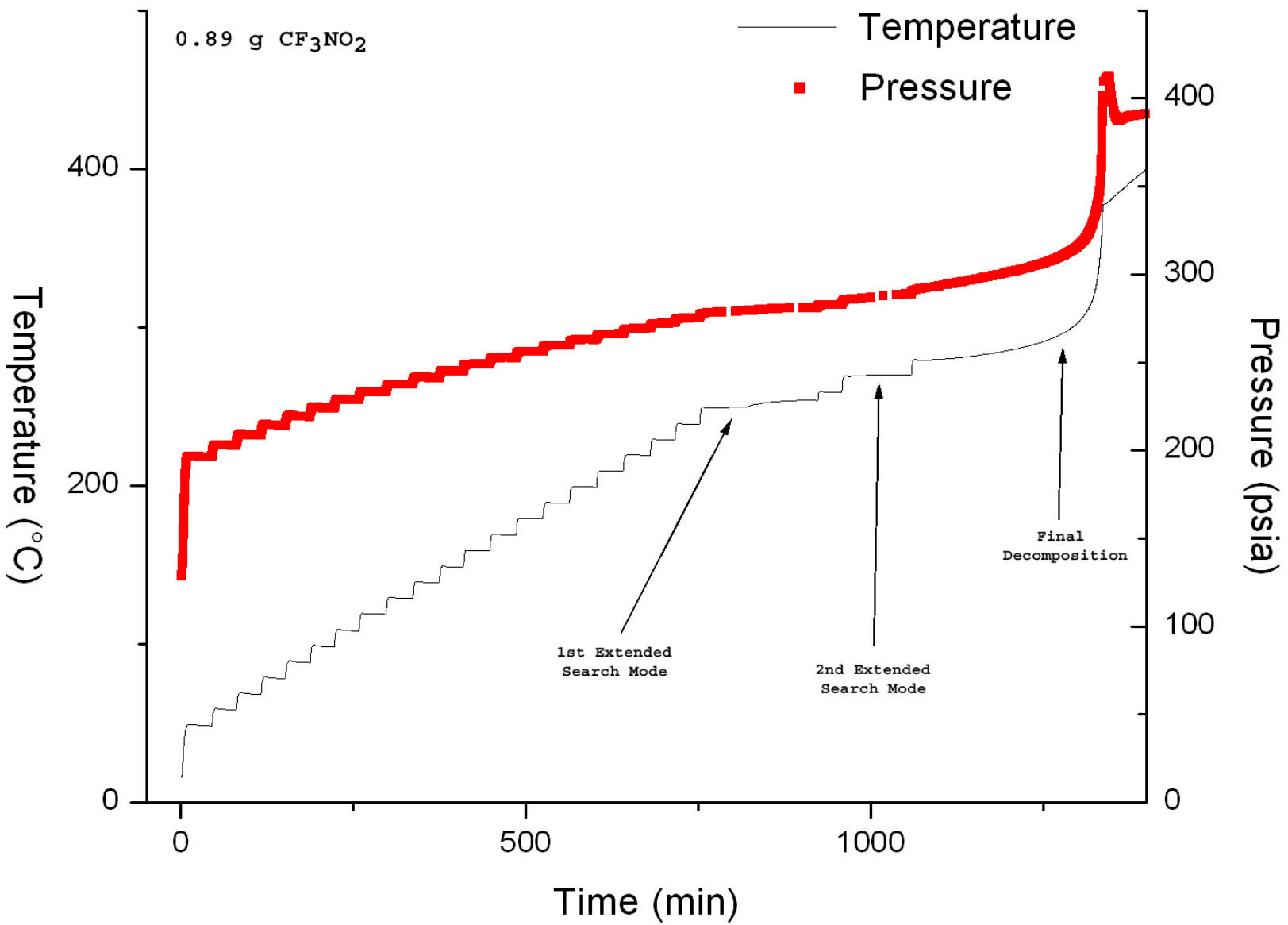

Figure 5.2. ARC of CF_3NO_2 heated to 400 °C

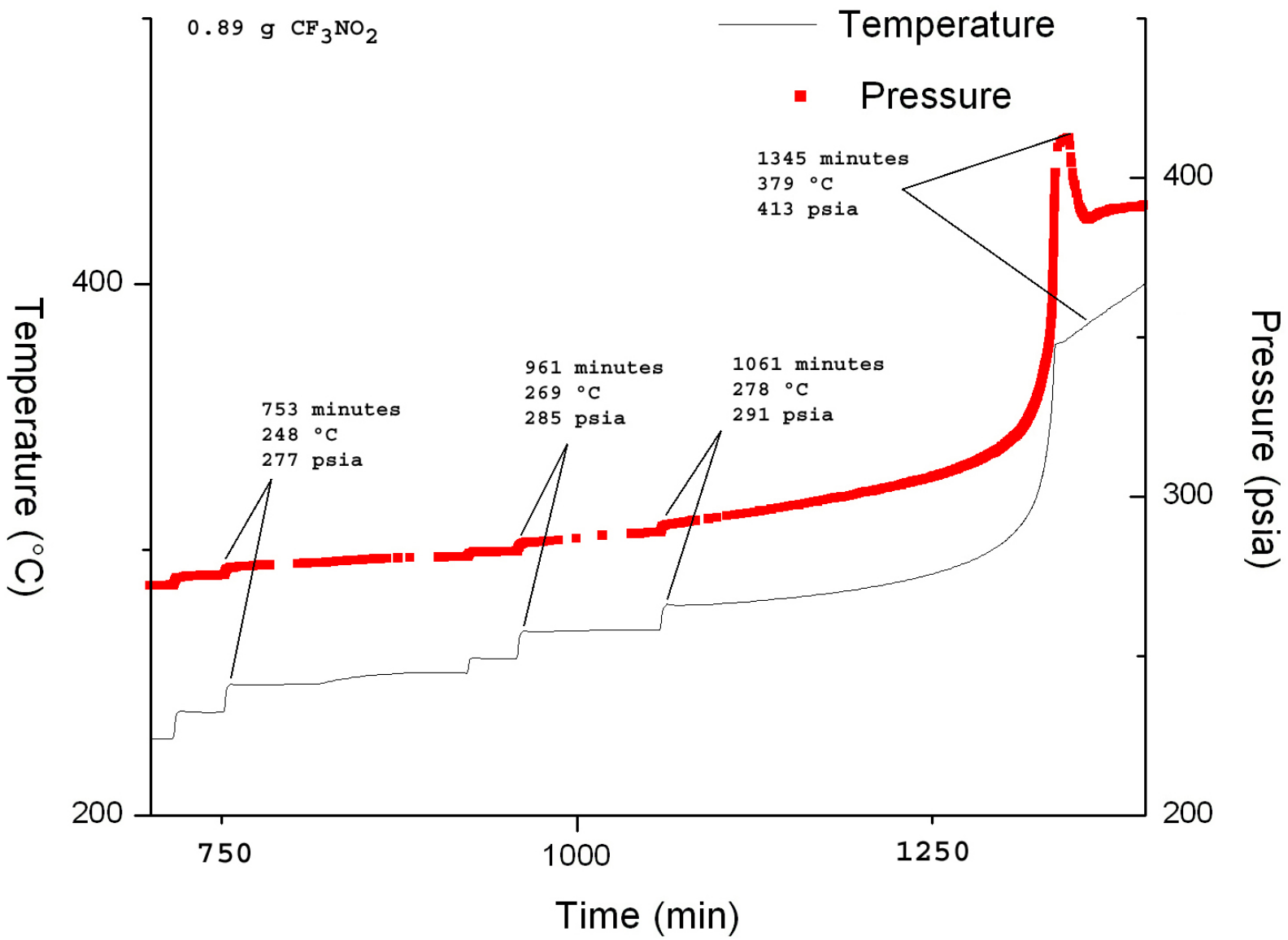

Figure 5.3. ARC of CF_3NO_2 heated to 400 °C, blowup of exotherm

The first exotherm starts at minute 753 (248 °C, 277 psia) and ends 169 minutes later (254 °C, 281 psia). The second exotherm begins at minute 962 (269 °C, 285 psia) and ends 96 minutes later (270 °C, 288 psia). The next significant event is at the end of the heating cycle where CF_3NO_2 decays. This event can be split into two parts, the low-slope and high-slope portion, even though it is one long event. The third decay begins at minute 1063 (279 °C, 291 psia) and continues for 283 minutes, finally, reaching 379 °C, 413 psia. The third thermal decay of trifluoronitromethane really begins its significant exothermic decomposition at 1295 minutes (300 °C, 314 psia). From this point to the end of the exotherm, a 51 minute period, the temperature rose 79 °C and 99 psia. This is a definite, observable decay, but neither the heat nor the pressure increase is great enough to consider CF_3NO_2 an explosive compound. The self heating rate of the decay never got higher than 30 °C/min. The CF_3NO_2 decays primarily into C_2F_6, $\cdot NO_2$ and $\cdot NO$. Other minor products were observed by ^{19}F-NMR spectroscopy, but their identities and quantities were not determined.

5.3 Conclusions

This ARC investigation shows that CF_3NO_2 can reach temperatures close to 300 °C before any significant decay begins. This demonstrates the good thermal stability of CF_3NO_2. This is an encouraging finding if CF_3NO_2 is to be a possible replacement for SF_6 as a dielectric gas in some applications.[5.10] Trifluoronitromethane does not have as high a thermal stability as SF_6, which is stable up to 530 °C.[5.16,5.17] Even though trifluoronitromethane is not as thermally stable as SF_6, for applications under 275 °C, it could be an excellent replacement. A major shortcoming of potentially using CF_3NO_2 as a substitute dielectric gas for SF_6, might be the

decay products of CF_3NO_2. The creation of strong oxidizing molecules like $\cdot NO_2$ and $\cdot NO$ would presumably be detrimental to many of the materials a dielectric gas is trying to protect. The application of CF_3NO_2 as a dielectric gas must be chosen wisely where oxidation will not be a concern. Another solution is using small amounts of CF_3NO_2 in a mixture with other inexpensive dielectric gases, as proposed by Wootton.[5.10] In his patent, CF_3NO_2 is proposed to reduce the carbonization of various halogenated hydrocarbons in mixtures containing 10-50 mol% of CF_3NO_2. The reduced amount of CF_3NO_2 would cut down on the harmful oxidizers that would be formed if decay happens.

5.4 Experimental

5.4.1 Preparation of CF_3NO_2

Trifluoronitromethane, CF_3NO_2, was prepared according to the method discussed in Chapter 3 and was purified, by wet scrubbing, using Method 4 described in Chapter 4. The purity was verified by IR and ^{19}F-NMR spectroscopy.

5.4.2 Preparation of the ARC and Its Settings

An 8.5-mL, 1-inch diameter, ¼-inch O.D. neck, titanium bomb was prepared by washing with acetone followed by deionized water and then heating in an oven overnight at 200 °C. The bomb was attached to the ARC by Swagelok® fittings and leak checked by evacuating the system and allowing it to sit for 15 minutes. If no change was observed, 500 psia of nitrogen was added,

and leaks were looked for using soapy water. A sample of CF_3NO_2, 0.89 g (7.7 mmol), was vacuum-transferred into a bomb that was cooled to -196 °C. The vacuum system was sealed, and the bomb was allowed to warm to room temperature. At 16 °C, the bomb was wiped free of condensed water, and the safety-shell was closed. The initial pressure inside the system at 20 °C was 128 psia. The settings for the ARC are summarized in Table 5.2.

Table 5.2. ARC Settings for the CF_3NO_2 Experiment

Heating Rate	10.00 °C/min
Start Temperature	50 °C
End Temperature	400 °C
Slope Sensitivity	0.010 °C/min
Heat Temperature Step	10 °C
Logging Data Step	0.50 °C
Calibration Temperature Step	0.20 °C
Burst Temperature Difference	150 °C
Cool Temperature	35 °C
Temperature Rate Stop	1000 °C/min
Pressure Rate Stop	2350 psia
Wait Time	10 min

5.5 References

5.1 Townsend, D. I. *Chem. Eng. Prog*. **1977**, *73*, 80.

5.2 Townsend, D. I. *Thermochim. Acta* **1980**, *37*, 1.

5.3 Townsend, D. I. *Inst. Chem. Eng. Symp. Ser*. **1981**, *68*, 3/Q:1.

5.4 Smith, D. W.; Taylor, M. C.; Young, R.; Stephenes, T. *Am. Lab. (Fairfield, Conn.)* **1980**, *12*, 51.

5.5 Tou, J. C.; Whiting, L. F.; Townsend, D. I. *Proc. Int. Conf. Therm. Anal*. **1980**, *1*, 177.

5.6 Tou, J. C.; Whiting, L. F. *Thermochim. Acta* **1981**, *48*, 21.

5.7 Hankin, S. H. *Thermochim. Acta* **1985**, *84*, 309.

5.8 Sun, L.; Waterfeld, A.; Thrasher, J. S. *J. Fluorine Chem*. **2006**, *127*, 1436.

5.9 Michael, J. V.; Kumaran, S. S. *Combust. Sci. Technol*. **1998**, *134*, 31.

5.10 Wootton, R. E. U. S. Patent 4,275,260, 1981.

5.11 *Recommendations on the Transport of Dangerous Goods*; Manual of Tests and Criteria, 3rd ed.; United Nations, 1999, pp. 27-47.

5.12 *Recommendations on the Transport of Dangerous Goods*; Manual of Tests and Criteria, 3rd ed.; United Nations, 1999, pp. 397-401.

5.13 *Recommendation on the Transport of Dangerous Goods*; Tests and Criteria, 2nd ed.; United Nations, 1990, pp. 10-42.

5.14 United Nations Document ST/SG.AC.10/2001/31, 2000.

5.15 Bodman, G. T.; Chervin, S. *J. Haz. Mat.* **2004**, *115*, 101.

5.16 Braker, W.; Mossman, A. L. *Matheson Gas Data Book*, 5th and 6th ed.; East Rutherford, NJ, and Secaucs, NJ: 1979 and 1980.

5.17 Viggiano, A. A.; Miller, T. M.; Friedman, J. F.; Troe, J. *J. Chem. Phys*. **2007**, *127*, 244305.

CHAPTER SIX

CONCLUSIONS AND FUTURE WORK

6.1 Conclusions

The first goal of this project was to scale up the photochemical method developed by Lu and Thrasher for the generation of CF_3NO_2 to 5-10 g a batch. Due to the batch nature of the process and the size limitations of both the reaction vessel (ca. 16-L capacity) and the blue light reaction chamber, this was reasonable for the photochemical method. However, due to the equilibrium content of N_2O_4 versus $\cdot NO_2$ at the elevated pressures required, this goal could not be achieved, and alternate methods for the generation of CF_3NO_2 were tested. Once a new method was found, namely a thermal process that could generate CF_3NO_2 in 10-60 g per batch, a new, less expensive purification method was needed due to the expensive multi-step method previously used by Lu. The kinetics of this new thermal route was then measured experimentally. The optimum conditions for the thermal reaction are: a mole ratio of 1.1 : 1 for $\cdot NO_2$: CF_3I, a reaction temperature of 200 °C, a reaction time of at least 12 hours and a pressure that the reaction cylinder can hold safely. Using an accelerating rate calorimetry (ARC), the thermal decomposition point of CF_3NO_2 was found to be between 270-290 °C, which helped to validate the proposed stability of the CF_3NO_2 molecule. The thermal method of preparing other perfluoronitroalkanes was then expanded to decafluoro-4-trifluoromethyl-4-iodopentane, a mixture of C_6-C_{12} 1-iodoperfluoroalkanes and 2-iodoheptafluoropropane.

While the photochemical method is an excellent method for generating 1-3 g quantities of CF_3NO_2, attempts to scale-up the photochemical reaction by increasing the total pressure above 0.3 atm resulted in only mixtures of CF_3NO_2 and CF_3I. The CF_3NO_2 and CF_3I are difficult to separate due to the closeness of their boiling points and the similarity of their inertness. The lack of the complete consumption of the CF_3I in the photochemical process can be attributed to the equilibrium between $2 \cdot NO_2 \rightleftharpoons N_2O_4$. When the pressure in the system gets too high, N_2O_4 becomes the dominant species. The only way to overcome this equilibrium is to either reduce the pressure of the system to under 0.3 atm and raise the temperature to 55-70 °C. The existing blue light apparatus cannot reach temperatures high enough to push the equilibrium towards $\cdot NO_2$ and convert all the CF_3I to CF_3NO_2 (or COF_2 and FNO), if the pressure in the reaction vessel is above 0.3 atm. The percent yield for the photochemical method never exceeded 33% based on CF_3I.

The C-I bond in trifluoroiodomethane can be split by photoactivation as well as thermally. By heating a mixture of CF_3I and $\cdot NO_2$ in a stainless steel cylinder to 200 °C for 36-48 hours, all CF_3I was consumed with yields of CF_3NO_2 ranging between 37 and 54%. The high temperature pushes the $\cdot NO_2/N_2O_4$ equilibrium towards the reactive $\cdot NO_2$ radical, thereby allowing the reaction to go to completion. Both the photochemical and thermal activation produce radicals, but the photochemical method never exceeds a yield of 33% due to the twice as likely CF_3ONO formation. This O-bonded product irreversibly decays into COF_2 and FNO. The better than 33% yield for the thermal method is most likely due to the fast dissociation of the CF_3ONO molecule back into $\cdot CF_3$ and $\cdot NO_2$. This accounts for the modest increase in the percent yield for the thermal method. The dissociation of CF_3ONO into $\cdot CF_3$ and $\cdot NO_2$ radicals apparently does not occur in the blue light process, which may limit the yield to 33%.

The major byproducts of both methods are $\cdot NO_2$, $\cdot NO$, N_2O_3, I_2, COF_2, and FNO. Lu used a dry method that relied on reacting $\cdot NO_2$ and COF_2 with CsF and FNO with AlF_3 which formed nonvolatile salts that could easily be separated from the CF_3NO_2. This process was replaced by wet scrubbing through 10-30% aqueous KOH/NaOH solutions and storing the collected CF_3NO_2 material over NaOH pellets to remove any residual N_2O_3 that collected with the CF_3NO_2 after the scrubbing. This method is ca. $1/10^{th}$ the cost of the method used by Lu, and it is far less time and equipment intensive.

The kinetics of the thermal reaction were investigated by NMR spectroscopy in sealed, high-pressure NMR tubes at the temperatures of 170, 185, 200, 215, 250, and 250 °C. The rate constant was found to be:

$$k_1 = 5.47 \times 10^{16} \exp(-23140\ K/T)\ cm^3\ mol^{-1}\ s^{-1}$$

An Arrhenius plot gives an activation energy (E_a) of 46 kcal/mol, which is on the low end of the literature data.

The thermal decay of CF_3NO_2 was studied with an accelerating rate calorimeter (ARC). This study revealed that the molecule begins to decompose around 270 °C and decays more rapidly at or near 290 to 300 °C. The major decay products are $\cdot NO_2$, $\cdot NO$, and C_2F_6, as determined by ^{19}F-NMR and IR spectroscopy.

The thermal synthesis of nitroperfluoroalkanes was expanded to higher perfluoroalkyliodides. The addition of $\cdot NO_2$ to other perfluoroalkyl radicals had only limited success. The $\cdot NO_2$ group was added to some primary C_6-C_{12} perfluoroalkyliodides albeit with some shortening of the carbon chain occurring. The addition to secondary and tertiary iodides was more problematic but the addition of $\cdot NO_2$ was successful once the correct temperature range was found. Full characterization and isolation of all the compounds has not been achieved.

6.2 Future Work

Work on the synthesis of secondary and tertiary perfluoroalkyl nitro compounds is still required. All the compounds were successfully made, but pure and fully characterized products were not obtained for all of the species. Isolating and characterizing these compounds should be easily done now that the synthetic route has been determined. There are very few known examples of secondary and tertiary nitroperfluoroalkanes, and this thermal method may be useful for making more members of this interesting class of compounds.

The studies of these batch reactions, both photochemical and thermal, have been taken about as far as they can go. The next logical step would be to develop a continual flow process for producing CF_3NO_2, which would hopefully help eliminate some of the problems associate with the high pressures of the batch reactions. Furthermore, if a catalyst could be identified to decrease the temperature of C-I bond dissociation, the synthesis of nitroperfluoroalkanes could be much improved. A decrease in both the temperature and pressure requirements that might be afforded in a flow system would be very desirable for an industrial setting.